SEISMIC PERFORMANCE OF MULTI-SPAN RC BRIDGE WITH IRREGULAR COLUMN HEIGHTS

by

Samy Muhammad Reza

A THESIS SUBMITTED IN PARTIAL FULFILLMENT
OF THE REQUIREMENTS FOR THE DEGREE OF

MASTER OF APPLIED SCIENCE

in

The College of Graduate Studies
(Civil Engineering)

THE UNIVERSITY OF BRITISH COLUMBIA
(Okanagan)

FEBRUARY 2012

ABSTRACT

Bridges are essential elements in modern transportation network and play a significant role in a country's economy. However, it has always been a major challenge to keep bridges safe and serviceable. Modern bridge design codes include seismic detailing in order to ensure ductile behavior, which was absent in the pre-1970 codes that made older bridges vulnerable during earthquakes. The main parameters effecting the performance of bridge (tie spacing, concrete and steel properties, amount of reinforcement) varies significantly from old to modern bridges. The presence of irregularity in column heights is one of the common causes of seismic vulnerability and the non-uniform column height is the most common form of irregularity. In this study, a four span RC box-girder bridge has been considered for different column height configurations. Here, a detailed parametric study has been performed to understand the effects of various factors on the limit states of the individual bridge columns using factorial analysis. Static pushover analyses, incremental dynamic analyses and fragility analyses of bridges with irregular column heights have been conducted to identify the seismic vulnerability of bridges in the longitudinal direction due to irregularity in column height. This study also investigated the difference of conventional force-based approach and displacement-based approach in designing a bridge with irregular column heights. Canadian Highway Bridge Design Code (CHBDC) and AASHTO 2007, like other traditional design codes follow force-based design (FBD) method, which is focused at the target force resistance capacity of the structure. On the other hand, displacement-based design approach focuses on a target maximum displacement of the bridge during the earthquake in a specific zone. Seismic performances of the bridges designed in two different methods have been compared by non-linear dynamic analyses in the longitudinal direction in terms of maximum and residual displacements and energy dissipation capacity.

TABLE OF CONTENTS

LIST OF TABLES

LIST OF FIGURES

LIST OF NOTATIONS

As	Amount of Longitudinal steel
b	Section width
b_c	Width of core section
d	Effective depth of column section
d_c	Depth of core section
$DDBD$	Direct displacement-based design
DPO	Dynamic pushover
E_c	Elastic modulus of concrete
EDP	Engineering demand parameter
f'_c	Compressive strength of concrete
f'_{cc}	Confined compressive strength of concrete
f'_l	Effective lateral stress of confined concrete
FBD	Force-based Design
f_y	Yield strength of steel
H	Height of column
h_p	Plastic hinge lenght
I_c	Cracked moment of inertia
IDA	Incremental dynamic analysis
IM	Intensity measures
K	Elastic lateral stiffness of column
K_e	Effective lateral stiffness of column
M_c	Cracking moment
M_y	Yield moment
$NTHA$	Non-linear time history analysis
PGA	Peak ground acceleration
PGV	Peak ground velocity
$PSDM$	Probabilistic seismic demand model
R_ξ	Spectral reduction factor
s	Tie spacing

s'	Clear spacing of transverse reinforcement
SPO	Static pushover
T	Time period of structure
T_e	Effective time period of structure
V	Total design base shear
V_c	Base shear at first cracking
V_i	Design base shear of individual column
V_{shear}	Shear capacity
V_y	Base shear at first yileding
W_e	Effective weight
w_i	Clear distance of ith longitudinal bar
$\beta_{EDP|IM}$	Dispersion of demand
Δ_c	Lateral displacement at first cracking
Δ_{crush}	Displacement at first concrete crushing
Δ_d	Target diplacement
Δ_p	Plastic displacement
Δ_y	Yield displacement
Δ_y	Yield displacement
μ	Ductiltiy
ξ_{eq}	Equivalent viscous damping ratio
ξ_{sys}	System viscous damping ratio
φ_c	Cracking curvature
φ_u	Curvature at first concrete crushing
φ_y	Yield curvature

ACKNOWLEDGEMENTS

This is only the mercy of almighty Allah Robbul Izzat that I exist. May the honour and peace of the messenger of Allah (peace be upon him) increase intensely.

I express my sincere gratitude to both of my supervisors, Dr. M. Shahria Alam and Dr. Solomon Tesfamariam. They have been instrumental with knowledge, support, placement, mentoring that made my graduate experience at UBC so impeccably productive and rewarding, at any rate. Overall, I attribute my positive experience at the graduate school here at UBC to them.

Meanwhile, UBC Okanagan campus, being a unique and generous institution, provided an excellent educational refuge, and that deeply reckoned, in a compelling manner. I really enjoyed the life in here. I also would like to acknowledge Natural Sciences and Engineering Research Council of Canada (NSERC)'s support in this rejuvenating and fulfilling journey.

I have had the opportunity to get in touch with an excellent and enthusiastic group of graduate students in the research group who offered technical knowledge and lively discussions. I offer much appreciation to my thoughtful and considerate friends, Muntasir Billah, Nurul Alam, Rafiqul Haque.

Most importantly, I would like to pay my innermost respect to my parents, whom I feel to be the key source of inspiration for all my achievements.

DEDICATED TO MY MENTORS

CHAPTER 1: INTRODUCTION AND THESIS ORGANIZATION

1.1 GENERAL

Bridges play a vital role in a country's economic development and bridges are an essential part of the transportation system. They ensure smooth transportation by establishing links between cities and even between countries. The failure of bridges during an earthquake not only costs human lives but also causes a catastrophe to the transport network and the economy. In recent years several earthquakes caused significant damage to many bridges. The bridges in North America are also at high seismic risk, especially which were designed and constructed before 1970.

There are more than 3000 highway bridges in British Columbia and many of them were constructed before 1970. Since the earthquakes are getting more frequent these days, it is of prime importance to identify the seismically vulnerable bridges in order to take necessary retrofitting action in order to prevent the bridge collapses during probable seismic events. However, the identification of the seismically vulnerable bridges through numerical analyses is a time consuming and expensive task. Most of the old RC bridges were not seismically detailed, whereas, modern codes ensures ductile detailing. Moreover, the presence of irregularity makes bridges more vulnerable to seismic events. There is a strong need to evolve a quicker and cost effective method to identify the seismically vulnerable bridges by classifying them in terms of their material properties, confinement in columns and the presence of irregularity.

It is also necessary to improve and optimize the current design methods for bridges with irregular column heights. Force-based and displacement-based designs have dissimilarities for designing bridges with irregular column heights. Efforts are needed in order to assess their seismic performance and improve the design methods.

1.2 OBJECTIVE OF THE STUDY

The key objectives of the current research include:

1. Determine the effects of different parameters on the limit states of reinforced concrete (RC) bridge column and propose empirical equations for limit states in order to direct determination of limit states of the columns of existing bridges instantly.

2. Determine the effects of irregularity in column heights and spacing of lateral reinforcement in columns on the seismic performance of the RC bridge.

3. Compare the seismic performance of RC bridges with irregular column heights, which are seismically designed for Vancouver region using two different methods, namely: displacement-based approach and force-based approach.

1.3 SCOPE OF THE RESEARCH

In order to achieve the goals of the study, the properties of the old and modern RC bridge piers were obtained from the literature review. This study presents the state-of-the-art of material properties and detailing of old and modern bridge piers as well as the seismic design practice of bridge piers. The procedures to achieve the stated objectives are as follows:

1. Finite element models of 1.5 m X 3 m columns of varying heights (7 m, 14 m and 21 m) with different material properties, confinements and amounts of longitudinal steel have

been generated in SeismoStruct (2010). Limit states of cracking, first rebar yielding and first concrete crushing have been determined using non-linear pushover analyses; 3^4 factorial analyses have been conducted with 243 combinations in order to observe the effect of different parameters on the limit states.

2. Box girder bridges with four equal spans of 50 m have been modeled in SeismoStruct (2010) for different regular and irregular combinations of heights (7 m, 14 m and 21 m) of columns. Limit states of these bridges have been determined using pushover analyses. Effects of irregularity in column height and confinement on the seismic performance of bridge have been determined using fragility analyses.

3. A box girder bridge with irregular column height combination of 7 m, 14 m and 21 m has been designed as per force-based and displacement-based approach. Non-linear time history analyses have been conducted in order to compare the two different methods.

1.4 THESIS ORGANIZATION

This thesis is arranged in six chapters. In the current chapter a short preface and the objectives and scope are presented. The content of the dissertation is organized into the following chapters:

Chapter 2 presents the literature review on the comparison of material and geometric properties of the old and new bridge columns. This study presents the seismic vulnerability of bridges due to irregular columns heights and poor detailing. The design methodologies of force-based approach and displacement-approach have also been described.

Chapter 3 presents the investigation of the effect of different parameters on the limit states of the bridge pier. The formability of generalized functions of limit states and ductility has also been checked.

Chapter 4 investigates the limit states of the bridges with regular and irregular column height configurations and varying tie spacing. This study also evaluates the effect of column height irregularity and tie spacing on the seismic performance of bridges through static pushover and incremental dynamic time history analyses by developing the fragility curves.

Chapter 5 presents the design of a bridge with irregular column heights in conventional force-based and displacement-based approach. Seismic performance of the bridges designed in two different approaches has been evaluated by non-linear time history analyses.

Finally, **Chapter 6** presents the key conclusions attained from this research. Few specific recommendations for future research have also been suggested.

CHAPTER 2: LITERATURE REVIEW

2.1 GENERAL

This chapter comprises the previous works outlining the comparison or old and new RC bridge columns and different factors affecting their performances. The role of the presence of irregularity and poor detailing on the collapse of bridges during earthquakes has been discussed. This study also includes the key features of the traditional and displacement-based seismic design.

2.2 COMPARISON OF OLD AND MODERN BRIDGE COLUMNS

2.2.1 Material Properties

The concrete and steel properties have improved over time. Concrete with comparatively higher compressive strength is used in modern bridges whereas in older bridges concrete compressive strength was as low as 28 MPa. Nowadays concrete compressive strength of 69 MPa in bridges is not uncommon (ACI 363R-92, HPC Bridge Vies 2010). Yield strength of steel can also vary from 276 MPa to 500 MPa between older and modern bridges (Ranf et al. 2006, Alam et al. 2009).

2.2.2 Detailing of Bridge Column

Bridges constructed before 1970 were not designed and detailed according to seismic provisions. Modern code specifies for proper reinforcement detailing with closer transverse reinforcement. Poorly detailed RC columns are susceptible to loss of axial load carrying capacity at drift levels lower than expected during a design level seismic event (Boys et al. 2008). Tie

spacing of 300 mm was commonly used in bridge columns before 1970. Ruth and Zhang (1999) conducted a survey of 33 bridges designed from 1957 to 1969 and found that all bridge columns had a tie spacing of 300 mm. Moustafa et al (2011) presented the modern design of an existing bridge pier in Southern California, which was built before 1970, with a pitch of the spiral reinforcement of 100 mm. This pier design according to modern code (California Department of Transportation design standards 1999) resulted in a pitch of 56 mm, which is much smaller than the previous one.

The maximum tie bar spacing allowed in CSA Standard S6-1974 was 16 longitudinal bar diameter, 48 tie bar diameter or the least dimension of the column, however, in CSA Standard 1978 was 300 mm or the least dimension of the member and tie should cover every alternate bar. According to CHBDC 2010 the maximum tie spacing is the smallest of six times the longitudinal bar diameter or 0.25 times the minimum component dimension or 150 mm and tie should cover every longitudinal bar. Therefore, Canadian code of 2010 allows lower tie spacing than that of 1974 and 1978.

2.3 FACTORS AFFECTING THE PROPERTIES OF RC COLUMN

A number of studies have been conducted in order to show the effect of different factors on the performance of RC bridge column.

2.3.1 Effect of Material Properties

Park and Paulay (1975) discussed the positive or negative effect of the amount of longitudinal steel content, steel yield strength and compressive strength of concrete on the yield point, crushing point and corresponding ductility of the RC column. The improvement of these

factors has positive effect on the yield and crushing limit states. However, the relative effects of the change of the factors were not discussed.

2.3.2 Effect of Detailing

Several experimental and analytical studies have been conducted in order to observe the effect of confinement on the performance of columns under monotonic and cyclic axial loads (Mander et al.1988 (a and b); Sheikh and Uzumeri 1982; Calderone et al. 2000, Razvi and Saatcioglu 1994, Papanikolaou and Kappos 2009). The previous studies indicate that the shear resistance and flexural behaviour improved with the increased confinement.

2.3.3 Geometric Properties

Mo and Nien (2002) concluded that, ductility increases with the increase of axial load. Reduction in displacement ductility and increase of tendency of shear failure rather than flexural failure occur with the decrease in aspect ratio (column height to effective depth ratio) (Stone and Cheok 1989, McDaniel 1997). Zhu et. al. (2007) concluded that column specimens having aspect ratio less than 2.0 fails in shear or flexure-shear, and fails in flexure if the aspect ratio is greater than 4.0.

2.4 FACTORIAL DESIGN

Like many engineering systems, there are several influencing factors that affect the performance of a bridge column under lateral loads, for example earthquake load. The effect analysis will give misleading results if a single factor is varied at a time, because it will not reflect the interaction with other factors. All the factors need to be varied together in order to examine the effect of various factors including interaction among the factors (Montgomery 2001, Box et al. 1978). Factorial design is a good technique for conducting effect analysis. Padgett and

DesRoches (2006) used two level fractional factorial analyses in order to investigate the most important parameter of the seismic performance of retrofitted bridges, however, the system non-linearity was not considered. Here, the main effects of steel strength, mass, damping ratio, hinge gap and elastomeric bearing stiffness on the ductility and bearing deformation for different retrofitting options have been observed. The positive and negative effects have been determined to identify the important factors.

2.5 SEISMIC VULNERABILITY OF BRIDGES

2.5.1 Irregularity

The presence of unequal span length, skew bent or non-uniform height of columns makes bridge structures irregular. Bridges with unequal span lengths have closely spaced natural periods and will face dynamic amplification, if any of these natural periods matches with the natural period of a vehicle (Senthilvasan et al. 2002). Deck displacement in the transverse direction due to seismic force has been found more for skewed bridges compared to straight bridge (Sevgili and Caner 2009).

However, the most common form of irregularity occurs in the non-uniform height of columns of a bridge over a basin (Chen and Duan 2000). If the same section size and reinforcement is provided to the columns of different heights, larger ductility demand will be induced to the shorter columns (Priestley et al. 1996). Bridges with irregular column heights are seismically vulnerable, for example, the shorter columns of Bull Creek Canyon Channel Bridge were damaged in the 1994 Northridge earthquake. This failure was caused by the effects of both irregular column heights and inadequate confinement (Chen and Duan 2000).

Several works have been done regarding bridges with irregular column heights. Kappos et. al. (2002) investigated the effects of soil-structure interaction and irregular heights of hollow column on the dynamic behaviour and seismic response of a four span box-girder bridge. The effect of column height irregularity was found more critical than the effect of inclusion of SSI in the analyses on the bridge dynamic properties and seismic response. Inclusion of SSI effect resulted lower response of structure to ground motion excitation compared to the fixed end analyses. Since, poorly detailed RC columns have lower performance in seismic events (Boys et al. 2008); the effect of ductility capacity of columns should be investigated for bridges with irregular column heights. Saatcioglu and Razvi (2002) developed the design expressions for confinement steel requirement for earthquake resistant concrete columns.

2.5.2 Poor Detailing

Poor detailing of the bridge columns has been identified by researchers as one of the most common deficiencies causing the failure of bridges in the past earthquakes (Mitchell et al. 1994). Specifically, bridges which were constructed and designed before 1970s were not seismically detailed (Ruth and Zhang 1999). The failure of columns of an overpass during San Fernando earthquake in 1971 is an example of bridge column failure due to lack of transverse reinforcement (Chen and Duan 2000).

2.6 SEISMIC DESIGN OF RC BRIDGE COLUMN

2.6.1 Force-Based Design (FBD)

Seismic design in traditional codes is generally force based. Sebai (2009) demonstrated the difference in seismic design of bridges in different codes for Montreal, Toronto and Vancouver. The seismic design and detailing criteria in Eurocode 8 slightly differs from those of CHBDC

2010 and AASHTO 2007 due to the difference in response modificaiton factor. For example, the ductility related response modiciation factor for a single ductile column is 3.0 in CHBDC and AASHTO, whereas, this is 3.5 in Eurocode.

2.6.1.1 Calculation of FBD

The seismic design loads in CHBDC and AASHTO are identical (Sebai 2009). The basic steps of the FBD are:

- Estimation of lateral stiffness of structure

- Estimation of natural period of structure

- Estimation of elastic spectral force

- Selection of force-reduction factor

- Estimation of seismic force

- Displacement and member adequacy check

The seismic base shear according to NBCC 2005 and NBCC 2010 is determine as

$$V = S(T_a)M_v I_E W / R_d R_o \qquad [2\text{-}1]$$

Where, $S(Ta)$ is the spectral acceleration, M_v is a factor to account for higher mode effects on the base shear, the ductility-related factor R_d and the over strength-related factor R_o, I_E is the importance factor, and W is the weight of the structure.

2.6.1.2 Code evolution

Modern codes (AASHTO, CHBDC), based on FBD, have come to this point through different changes and improvements in seismic base shear calculation and detailing over the years in order to ensure safe, ductile and economic design. Previous codes (NRCC 1941, NRCC 1953, NRCC 1960, NRCC 1965) used seismic force coefficients which were not related to the dynamic properties of the structure and thus resulting inaccurate seismic base shear calculation. The codes (NRCC 1970, NRCC 1975, NRCC 1977, NRCC 1980, NRCC 1985, NRCC 1990, NRCC 1995, NRCC 2005, CHBDC 2006, NRCC 2010, CHBDC 2010) gradually improved in seismic base shear calculation by taking time period into account, developing rational importance factor, response modification factor, site coefficient and response spectra. Modern codes also developed better seismic detailing in order to ensure ductile structures.

2.6.1.3 Limitations of FBD

Priestley et al. (2007) addressed several problems associated with the force-based design. The main limitation in this method is that the natural period of the structure is determined from the initial stiffness of the member. However, the stiffness of a structure changes with its deformation. Another limitation is its force-reduction factor that is introduced to scale down the elastic seismic force, which is based on ductility capacity for a given structure type. Here, displacement ductility factor is equal to the force-reduction factor, which is not true for an inelastic system. Traditional force-based methods ignore the fact that the displacement is more important than the strength for inelastic systems. Thirdly, design seismic force is applied to the structures with initial stiffness, which indicates that the elements of the structure will be

subjected to yield point at a time. In reality, seismic force is distributed to the members according to the deformed shape of the structure. Therefore, this assumption is not accurate.

2.6.2 Displacement-Based Design (DBD)

2.6.2.1 Methods of DBD

In order to overcome the limitations of FBD, displacement is set as the main criterion for design rather than force (Priestley et al. 2007). Extensive research has been conducted in the effort of developing improved seismic design criteria by using displacement as the main seismic criteria rather than force after the Loma Prieta earthquake in 1989 (Priestley 1993; Caltrans, 2004; ATC, 2003). The main focus is to enhance ductility. There are different approaches of displacement-based design, such as Direct Displacement-Based Design (Priestley 1993), Equal Displacement Approximation (Veletsos and Newmark, 1960), Seismic Design Criteria (Caltran, 2004) and Substitute Structure Method (Shibata and Sozen 1976). Direct Displacement-Based Design (DDBD) has been found to be the most effective among the available displacement-based design methods for design of bridges and other structures (Kowalsky 1995; Calvi and Kingsley 1995; Kowalsky 2002; Ortiz 2006; Suarez and Kowalsky 2006). Priestley et al. (2007) described different stages of modern direct displacement-based design. Bardakis and Fardis (2010) found that the displacement-based design is more cost effective and rational than Eurocode 8.

2.6.2.2 Direct displacement-based design (DDBD)

The key difference between the DDBD and FBD is that in the case of DDBD effective time period and lateral stiffness is derived from the target displacement in order to calculate seismic base shear whereas in the case of FBD seismic base shear is calculated from the elastic

time period and stiffness without considering the hysteretic damping of the structure. The steps of DDBD include:

- Determine target displacement from yield displacement and required ductility

- Determine damping of the structure (material damping + hysteretic damping) from ductility. However, in the case of FBD only material damping is considered

- Determine the effective time period (T_e) of the structure from displacement spectra, whereas, elastic time period of structure is taken

- Determine the effective lateral stiffness (K_e) of the structure from weight and T_e

- Determine the seismic base shear of the structure

The required spacing of lateral reinforcement is limited by an allowable maximum value in the FBD codes, which rule is not present in DDBD. This study also examines the performance of a DDBD bridge which is restrained by the maximum allowable tie spacing and compares with the original DDBD bridge.

CHAPTER 3: LATERAL LOAD RESISTANCE OF BRIDGE PIERS UNDER FLEXURE AND SHEAR USING FACTORIAL ANALYSIS

3.1 GENERAL

Modern bridge design codes include seismic detailing in order to ensure their ductile behaviour, which was absent in the codes before 1970 that make the older bridges vulnerable during earthquakes. Moreover, there have been significant improvements in the material performance along with its quality control in modern bridge construction. Tie spacing, concrete and steel properties, amount of reinforcement and column height are the main factors which affect the performance of the bridge columns under lateral loads for a constant axial load level. Besides, these parameters differ significantly from old to modern bridges. In this study, nonlinear pushover analyses have been conducted in order to determine the effect of different factors on the limit states of bridge columns. A detailed parametric study has been performed to understand the effect of change of various factors on the limit states, which has been assessed through factorial analysis. The results obtained from the analysis have also been analytically verified.

3.2 SHEAR CAPACITY OF COLUMNS

Table 3-1 shows the aspect ratio and slenderness ratio of the bridge columns considered in this study. The 7 m columns considered in this study has the aspect ratio (column height to effective depth ratio) is 4.83, which is slightly over four; therefore, flexure-shear failures are expected (Zhu et al. 2007). The 14 m and 21 m columns have aspect ratios well above four, therefore, flexural failures are expected. According to Hassoun (1998), the effect of slenderness

is negligible for slenderness ratio less than 22, therefore, the 21 m column is expected to show long column effect. In this study, the 7 m, 14 m and 21 m represent the shear dominated, flexure dominated and long columns respectively. The shear capacities of the columns have been determined using the Modified Compression Field Theory (Vecchio and Collins 1986). This method is very accurate and can predict the experimentally determined shear failure within 1% error (Bentz et al. 2006). The shear capacity corresponds to certain displacement, which can be found from the pushover curve. Columns, with shear capacity greater than the crushing base shear, are flexure dominated. Ductility of the flexure dominated column is greater than one. If the shear capacity of the column is in between the yield and crushing base shear, the columns is shear dominated with ductility greater than one. However, if the shear capacity is less than the yielding of the column, the column will face shear failure before reaching the flexural yielding. This type of column cannot reach the theoretical yield displacement. The ductility of this column can be determined with respect to the virtual yield point, which will be less than one. In this study, this ductility is defined as virtual ductility. Figure 3-1 shows the concept of column classification method used in this study. Three column types have been defined: flexure dominated, shear dominated with ductility greater than one and shear dominated with virtual ductility.

Table 3-1. Slenderness ratio of the columns.

Column height (m)	H/d	kH/r
7	4.83	7.75
14	9.65	15.5
21	14.48	23.4
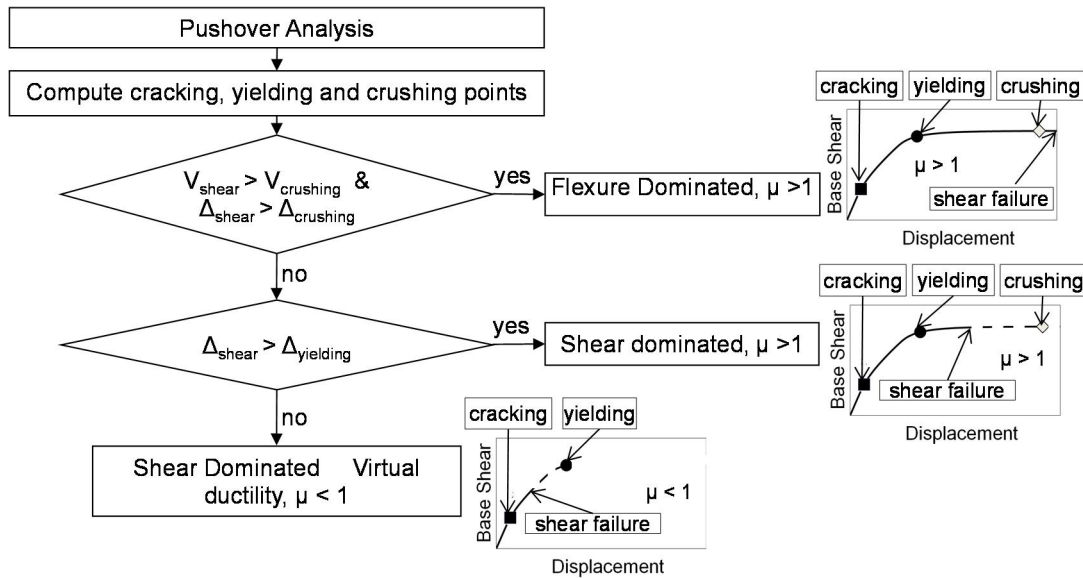
Figure 3-1. Flow chart of column classification.

3.3 MODELING OF THE BRIDGE COLUMN

The range of material properties, longitudinal reinforcement ratio and tie spacing considered in this study is given in Table 3-2. Bridge columns of size 1500 mm x 3000 mm with 92 longitudinal bars have been considered irrespective of the height of columns as shown in Figure 3-2(a). The bar area has been adjusted in order to consider 2, 3 and 4% longitudinal reinforcement ratio. 16 mm tie bar is used at every alternate longitudinal bar as shown in Figure 3-2(b). The column is fixed at the bottom and rotationally restrained at top. It has a constant vertical load of 27000 kN. Therefore, the range of the ratio of vertical load to design axial load is from 15.5% (for 60 MPa concrete, 500 MPa steel and 4% longitudinal steel) to 22.4% (for 25 MPa concrete, 300 MPa steel and 2% longitudinal steel). Confinement factor has been calculated according to Park et al. (1982). Columns have been modeled in SeismoStruct (2010). This software is based on the fibre modeling approach. Inelastic displacement-based frame element has been used for modeling the columns in order to consider material nonlinearity. The cross-

section has been divided into a number of fibres. The uniaxial response of the individual fibre is obtained from the nonlinear stress-strain behavior of the material. These responses of the fibres are integrated in order to get the sectional stress-strain state of the column along the cross-sectional area and length of the member. However, this model does not take shear deformation into account. The 25 MPa and 40 MPa concrete have been modeled using the nonlinear constant confinement concrete model. This model was initiated by Madas (1993) following the constitutive relationship proposed by Mander et al. (1988a) and the cyclic rules proposed by Martinez-Rueda and Elnashai (1997). The 60 MPa concrete has been modeled with nonlinear constant confinement for high-strength concrete model. This model was developed and initiated by Kappos and Konstantinidis (1999) following the constitutive relationship proposed by Nagashima et al. (1992). The confinement effects have been modified by Sheikh and Uzumeri (1982) factor. Steel has been modeled using the model of Monti and Nuti (1992). An additional memory rule (Fragiadakis et al. 2008) has been introduced, for higher numerical stability under transient seismic loading.

Table 3-2. Levels of the factors.

Factors	Low (-1)	Medium (0)	High (+1)
Compressive strength of concrete, f'_c	25 MPa	40 MPa	60 MPa
Yield strength of steel, f_y	300 MPa	400 MPa	500 MPa
Longitudinal steel reinforcement ratio, A_s	2%	3%	4%
Tie spacing, s	75 mm	150 mm	300 mm
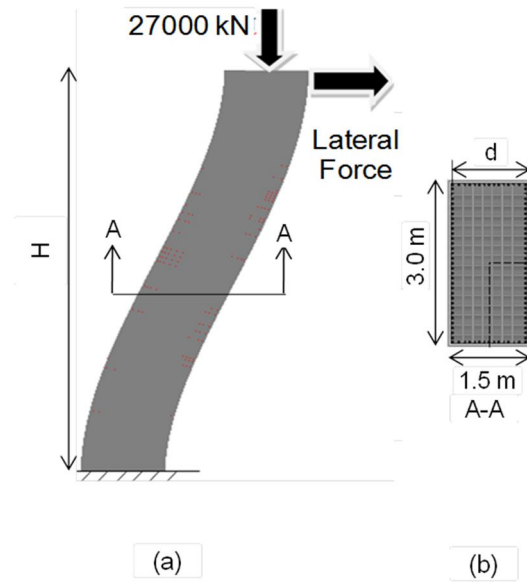
Figure 3-2. (a) Pushover deformation shape of a column, (b) cross section of column.

This model has been verified with a test result of 400x400 mm Type 1 square column for cyclic loading (Takemura and Kawashima, 1997). The effective height of the column was 1245 mm. The compressive strength of concrete and yield strength of the longitudinal reinforcement were 35.9 MPa and 363 MPa respectively. Twenty-13D (13 mm diameter) longitudinal reinforcements were used in the column as shown in Figure 3-3. Tie bar of 6 mm diameter with 368 MPa steel was provided at 70 mm c/c. The applied axial load was 157 kN. The column was free headed and flexure dominated in the cyclic loading test. The base shear vs. displacement graphs for numerical model and test result closely matches, as shown in Figure 3-3. The cracking, yielding and crushing points are identified in the result of numerical analysis. The numerical model stopped analysis, after reaching the first concrete crushing due to convergence error. However, the data beyond the crushing point is not of interest in this study. Therefore, the test data have been considered up to the same phase as the termination of numerical analysis. The differences between the test result and numerical analysis in predicting maximum base shear

and energy dissipation are 0.01% and 14.97%, respectively (Table 3-3), which is acceptable. SeismoStruct has also been validated with shake table test results of RC columns and RC frames in Alam et al. (2008) and Alam et al. (2009) respectively.

3.4 PUSHOVER ANALYSIS AND FLEXURAL LIMIT STATES

The performance of bridge columns can be identified by strain limits. Circular reinforced concrete bridge columns have been investigated in order to establish the curvature relationships for limit states, where simple relationships with curvature and displacement ductility, drift ratio and viscous damping with serviceability and damage control limit state have been established by Kowalsky (2000). Three limit states are considered in this study: first cracking (V_c, Δ_c), first yielding (V_y, Δ_y) and first crushing (V_{crush}, Δ_{crush}) where V and Δ refers to lateral force and lateral displacement, respectively. Pushover analyses have been conducted by applying lateral load parallel to the shorter dimension of the column. Cracking strain of concrete and yield strain of steel in tension have been assumed to be 0.000133 and 0.025, respectively. Crushing strain of unconfined concrete varies from 0.0025 to 0.006 (MacGregor and Wight, 2005). According to Paulay and Priestley (1992), crushing strain for confined concrete is much higher and it ranges from 0.015 to 0.05. In the present study, crushing strain of confined concrete is taken as 0.015.

Table 3-3. Comparison of the cyclic test result of numerical model with experimental result.

	Test	Numerical Model	Difference %
Maximum base shear (kN)	153.66	153.65	0.0065
Energy Dissipation (kN-m)	6.28	7.22	14.968
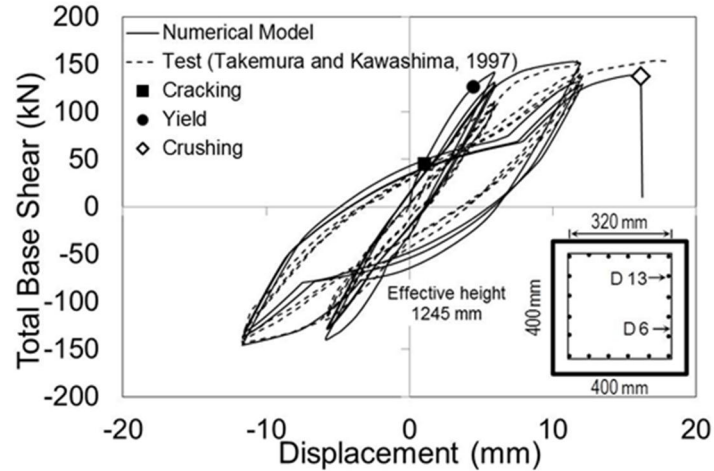
Figure 3-3. Verification of numerical model with test result.

3.5 FACTORIAL ANALYSIS FOR DIFFERENT COLUMN PROPERTIES

Compressive strength of concrete, yield strength of steel, longitudinal steel reinforcement ratio and tie spacing have been taken as the factors affecting the first cracking, yielding and crushing of 7 m, 14 m and 21 m height columns. The full factorial design of 3^4 with no confounding patterns has been conducted to account for the effect of these factors and their interactions. The three levels of these four factors are presented in Table 3-2. The effects estimated from these factorial analyses are valid for the ranges of factors mentioned in this table.

Figure 3-4 shows two typical pushover curves of 7 m column. Case -1-1-1-1 indicates the f'_c, f_y, A_s and s to be 25 MPa, 300 MPa, 2% and 75 mm, respectively. Case +1+1+1+1 indicates the f'_c, f_y, A_s and s to be 60 MPa, 500 MPa, 4% and 300 mm respectively. First cracking, yielding and crushing points are marked on these pushover curves as the performance indicators. Each of these performance indicators has two criteria: base shear and displacement. Full factorial analyses of 3^4 have been conducted for these criteria.
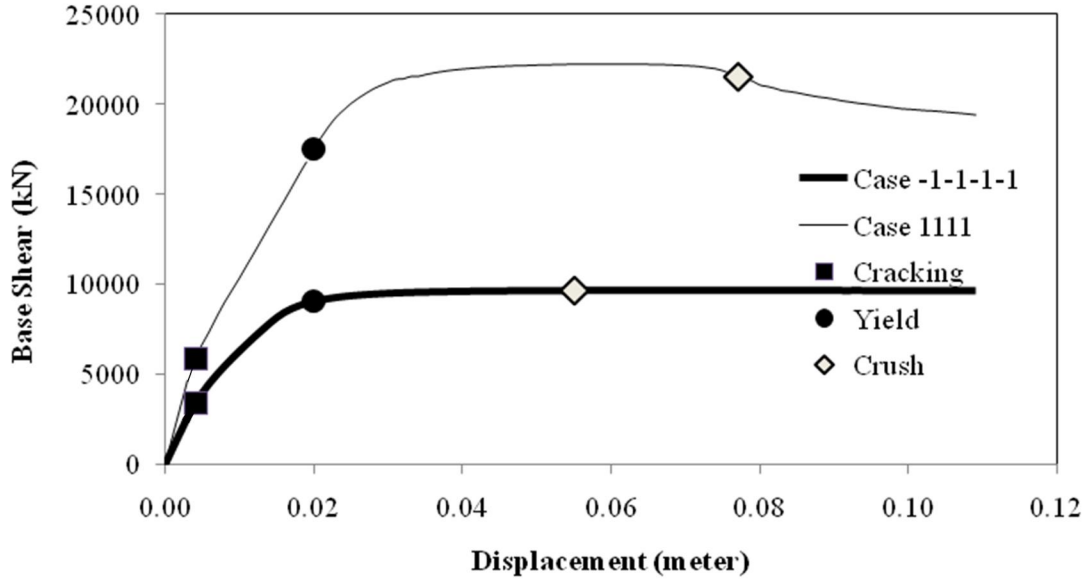
Figure 3-4. Typical pushover curves for 7m column for combinations of the four factors with low levels and high levels.

3.5.1 First Cracking

3.5.1.1 Analytical effect of factors at first cracking

The analytical solution for base shear (V_c) at first cracking is given as

$$\varphi_c = 2 \frac{\varepsilon_{crack}}{b} \qquad (3\text{-}1)$$

$$M_c = \varphi_c\, E_c\, I_c \qquad (3\text{-}2)$$

$$V_c = 2 \frac{M_c}{H} \qquad (3\text{-}3)$$

Where, ε_{crack} is the concrete tensile strain at cracking, φ_c is, the curvature at cracking, b is the section width, I_c is the cracked moment of inertia, varies with the amount of longitudinal reinforcement of steel and E_c is the elastic modulus of concrete, which is proportional to the

21

square root of compressive strength of concrete. Therefore, the change in compressive strength of concrete and longitudinal reinforcement affects the base shear capacity of column of specific height. Column base shear capacity at first cracking is inversely proportional to the height of the column. The lateral deformation at first cracking can be expressed as

$$\Delta_c = \frac{\varphi_c H^2}{6} \qquad\qquad (3\text{-}4)$$

The lateral displacement of the column top is proportional to the square of the length of column.

3.5.1.2 Factorial design at first cracking

The results obtained from the pushover analyses were compiled in Appendix. Figure 3-5(a) shows the cracking base shear for different column heights where the variation of cracking base shear is higher in shorter columns compared to longer columns. Column acts elastically before cracking. Figure 3-5(b) shows the contribution of the four factors and their interactions on the base shear at cracking for different column heights. The results show that the compressive strength, longitudinal reinforcement and tie spacing have significant effect on the base shear at first cracking for 7m height column. The contribution of the interactions between the factors in the change of first cracking is less than 10%. For the 14 m and 21 m column, compressive strength of concrete and longitudinal steel are the controlling factors. f'_c has more contribution among these two, which is about 80%. The effect of confinement of concrete on cracking base shear decreases with the increase in length of the column due to the increase of flexural dominance and decrease of shear dominance. These factors have no significant effect on the cracking displacement.
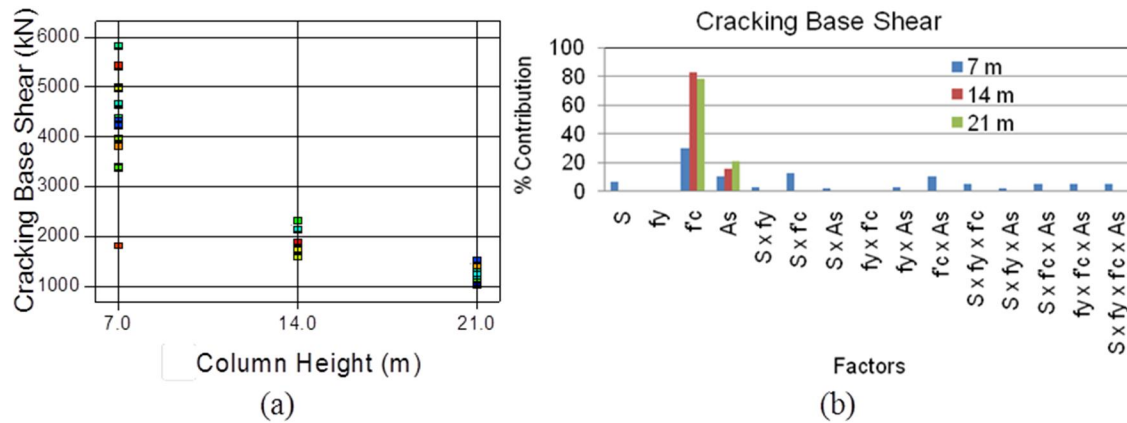
Figure 3-5. (a) Range of cracking base shear for different heights of columns, (b) contribution percentage of factors on the change of cracking base shear.

The effect of compressive strength of concrete is most significant and the amount of the longitudinal steel has the second largest effect on cracking base shear for each column height. These two factors have positive effect, which means, cracking base shear increases with the increase of these two factors separately. However, no interaction is prominent (Figure 3-5(a)). Tie spacing along with the interaction between f_c' and tie spacing has little effect (5%) only for 7 m column as shown in Figure 3-5(b). The effect of column height has been found significant (89%) in combined analysis for all three column heights (Figure 3-6(b)). Although, the percent contribution of f'_c is more in the variation of the cracking base shear for 14 and 21 m column, the total change in cracking base shear with the change in f'_c is more in 7 m column, since the variation of cracking base shear is more in shorter column as shown in Figure 3-6(b). The variation of cracking base shear is less for the change in longitudinal steel ratio as shown in Figure 3-6(c).
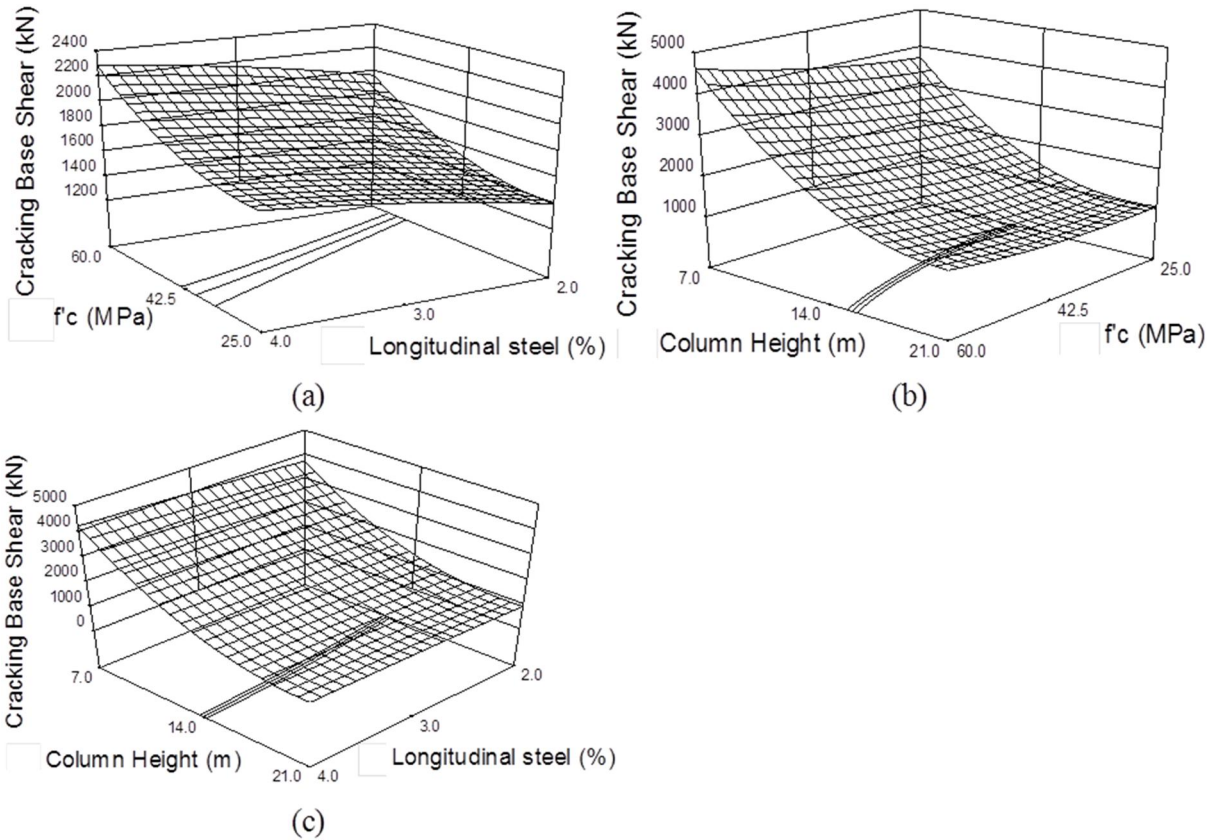
Figure 3-6. Effect of (a) f'_c and amount of longitudinal steel, (b) column height and f'_c, (c) column height and longitudinal steel of concrete on the cracking base shear.

Figure 3-7(a) illustrates the range of cracking displacement for columns of different heights. The results indicate that the variation of cracking displacement is more in longer column (0.001 m in 7 m column and 0.007 m in 21 m column), and longitudinal reinforcement ratio and concrete compressive strength are the main contributing factors on the change of cracking displacement as shown in Figure 3-7(b). However, the change in cracking displacement with the change of these factors is not significant as shown in Figure 3-8.
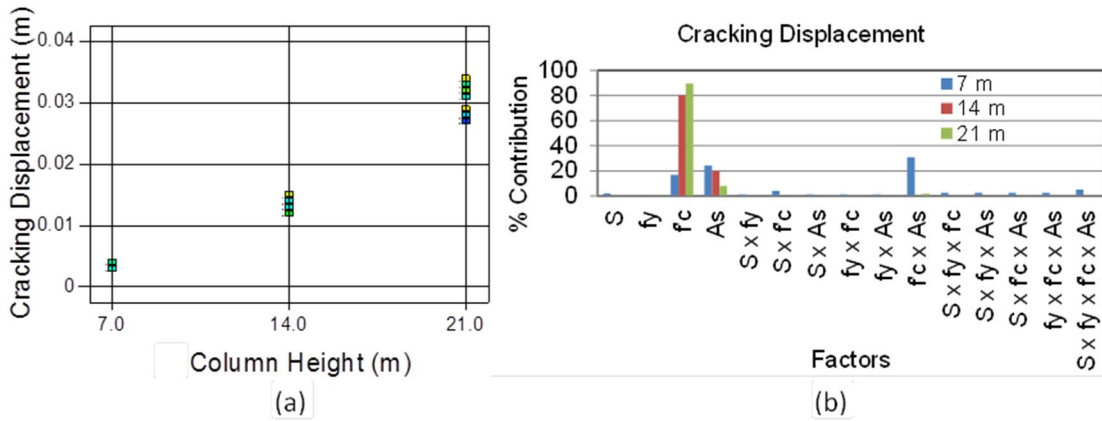
Figure 3-7. (a) Range of cracking displacement for different heights of columns, (b) contribution percentage of factors on the change of cracking displacement.
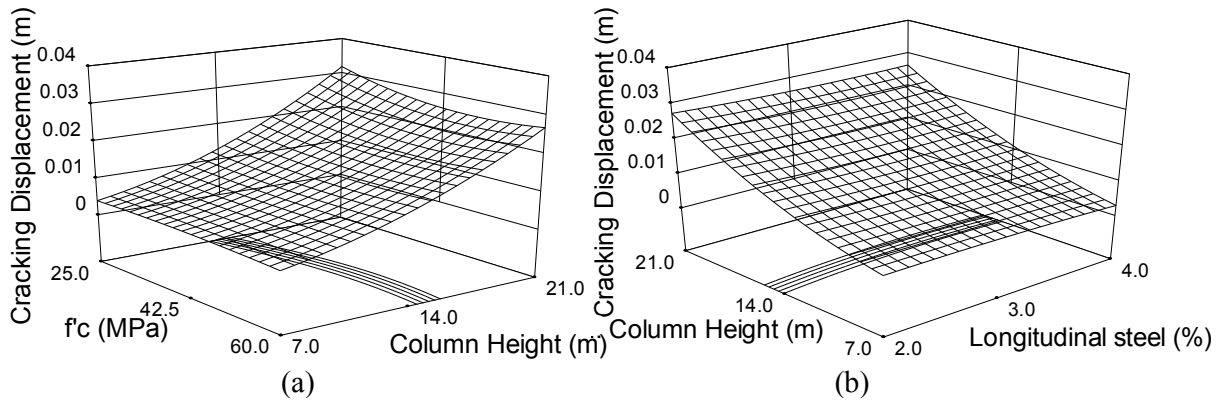
Figure 3-8. Effect of (a) column height and f'_c, (b) column height and longitudinal steel ratio on cracking displacement.

3.5.2 First Yielding

3.5.2.1 Analytical effect of factors at first yielding

The analytical solution for the base shear at first yielding can be expressed as

$$V_y = 2 \frac{M_y}{H} \tag{3-5}$$

Where, M_y is the moment capacity at first yield

$$M_y = A_s f_y (d - a/2) \tag{3-6}$$

A_s and f_y are the amount of longitudinal reinforcement and yield strength of steel, respectively. The depth of equivalent rectangular stress block, a, is a function of amount of longitudinal steel, yield strength of steel and compressive strength of concrete as shown in equation 3-7.

$$a = 0.85 \, \frac{A_s f_y}{f'_c} \tag{3-7}$$

Therefore, the base shear at yield is a function of A_s, f_y, d and f'_c. Since, the value of a is much smaller than d, the amount of longitudinal reinforcement and yield strength of the steel are the main controlling factor for the yield base shear. The concrete compressive strength, f'_c has also a little effect on V_y, as, it affects a.

The expression for the yield displacement is

$$\Delta_y = \frac{\varphi_y H^2}{6} \tag{3-8}$$

Where, φ_y is the curvature at first yield as shown in equation 3-9.

$$\varphi_y = \frac{M_y}{E_c I_{cracked}} \tag{3-9}$$

From the previous discussion, A_s and f_y mainly affect M_y. $I_{cracked}$ depends on amount of longitudinal reinforcement whereas E_c is proportional to the square root of compressive strength of concrete. A_s has contribution in both the numerator and the denominator of (3-9), which causes the decrease in the effect of A_s on Δ_y. The change in Δ_y mainly depends on f_y and f'_c.

3.5.2.2 Factorial design at first yielding

It can be observed from Figure 3-9(a) that yield base shear varies over a wider the range as the column height decreases. Yield strength of steel and reinforcement area play major roles on base shear for yielding as shown in Figure 3-9(b). No interaction is prominent here. The increase in column height from 7m to 21m does not affect the contribution of factors in the change in base shear for yielding whereas the amount of longitudinal reinforcement has 70% contribution. Similar to the cracking base shear, yield base shear is more dispersed for shorter columns with the changes in parameters [Figure 3-9(b)]. The effects of longitudinal steel ratio and f_y are positive and almost linear in the change of yield base shear as shown in Figure 3-10(a). The effects of these two factors are more prominent in shorter column as shown in Figures 3-10(b)-3-10(c). Tie spacing has almost no effect on the yield base shear as shown in Figure 3.10(d). Yield base shear increases with the increase of f'_c; however, Figures 3-10(d)-3-10(f) show that its effect is less than the other factors.

(a)   (b)
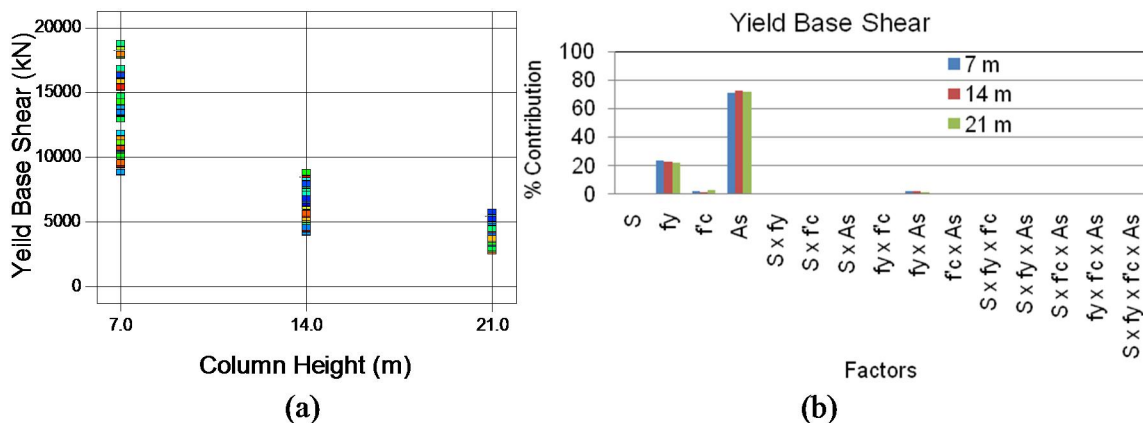
Figure 3-9. (a) Range of yield base shear for different heights of columns, (b) contribution percentage of factors on the change of yielding base shear.
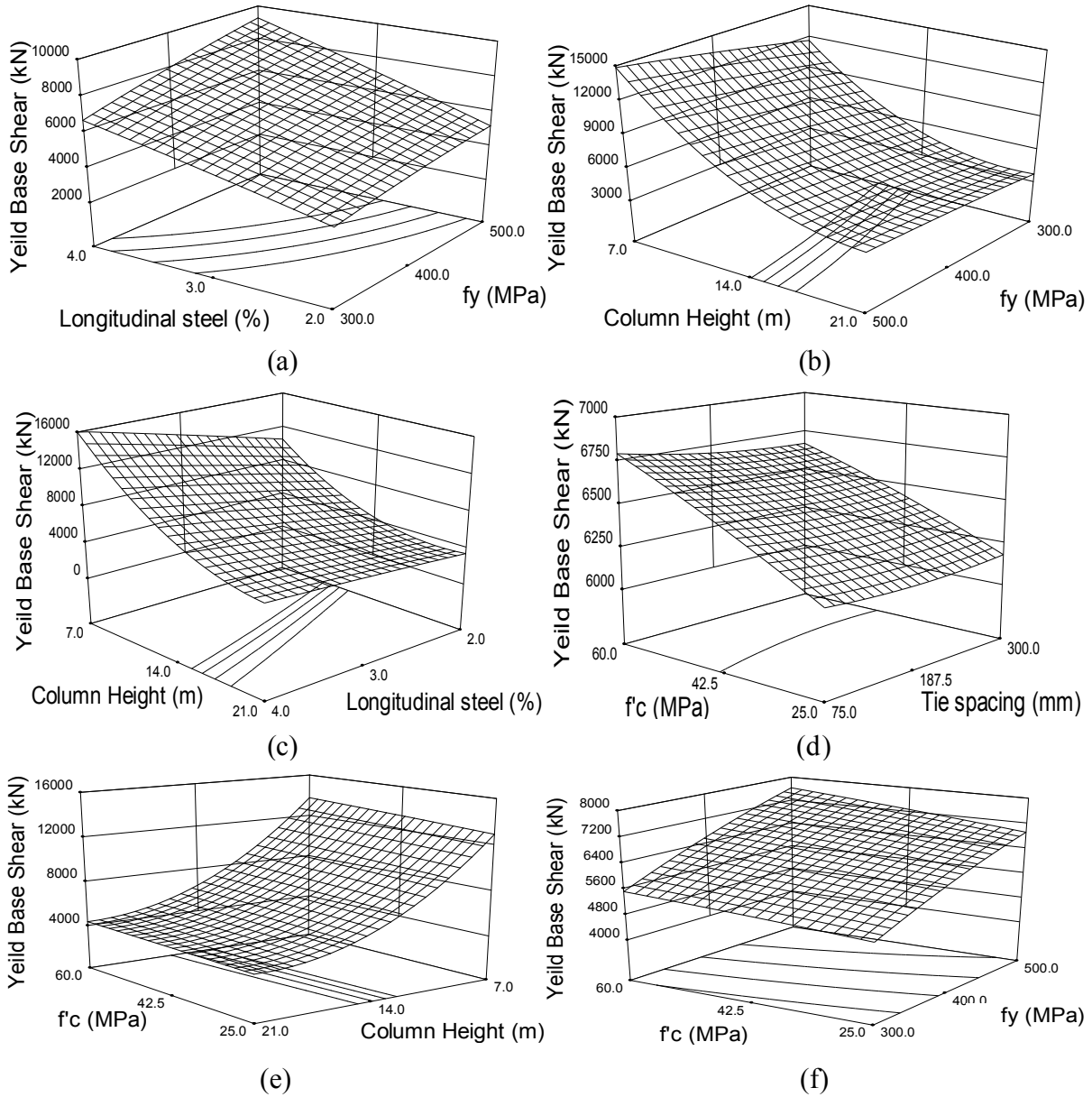
Figure 3-10. Effect of (a) longitudinal steel ratio and f_y of concrete, (b) column height and f_y of concrete, (c) column height and longitudinal steel ratio, (d) tie spacing and f'_c, (e) column height and f'_c, (f) f_y and f'_c on the yield base shear.

As the column height increases, the variation of yield displacement increases over a wider range as depicted in Figure 3-11(a). While determining the percent contribution of different factors on the yield displacement it was observed that f_y has the major contribution on the displacement for first yield as shown in Figure 3-11(b). Compressive strength of concrete and

28

amount of longitudinal reinforcement have also contributions on yield displacement. The effects of interactions among various factors are not significant here. Figure 3-12(c) demonstrates that the tie spacing or confinement of concrete has no effect on the yield displacement. Figures 3-12(a)-3-12(b) show that the yield displacement increases with the increase in f_y; decrease in f'_c; and increase in longitudinal reinforcement ratio. The relationship of these three parameters with yield displacement is linear. f_y, f'_c and longitudinal reinforcement ratio control the section curvature and the yield displacement is obtained by multiplying the square of length with curvature, as shown in Eq. (8). The effects of these factors on yield displacement are more in longer column as shown in Figure 3-12(d). The relationship between yield displacement and column height is almost parabolic ($y = ax^2$).
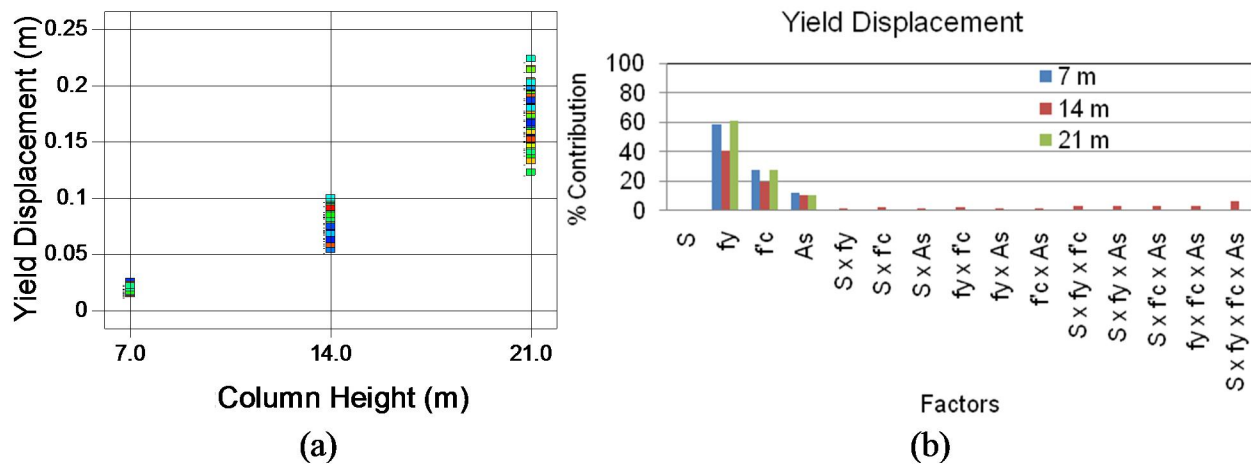
Figure 3-11. (a) Range of yield displacement for different heights of columns, (b) contribution percentage of factors on the change of first yield displacement.

Yield Displacement (m)

0.1
0.09
0.08
0.07
0.06
0.05

60.00 53.00 46.00 39.00 32.00 25.00 300.0 400.0 500.0

f'c (MPa)   fy (MPa)

(a)

Yield Displacement (m)

0.1
0.09
0.08
0.07
0.06
0.05

4.0 3.0 2.0 300.0 400.0 500.0

Longitudinal steel (%)   fy (MPa)

(b)

Yield Displacement (m)

0.1
0.09
0.08
0.07
0.06
0.05

500.0 400.0 300.0 75.0 187.5 300.0

fy (MPa)   Tie spacing (mm)

(c)

Yield Displacement (m)

0.2
0.15
0.1
0.05
0

21.0 14.0 7.0 300.0 400.0 500.0

Column Height (m)   fy (MPa)

(d)
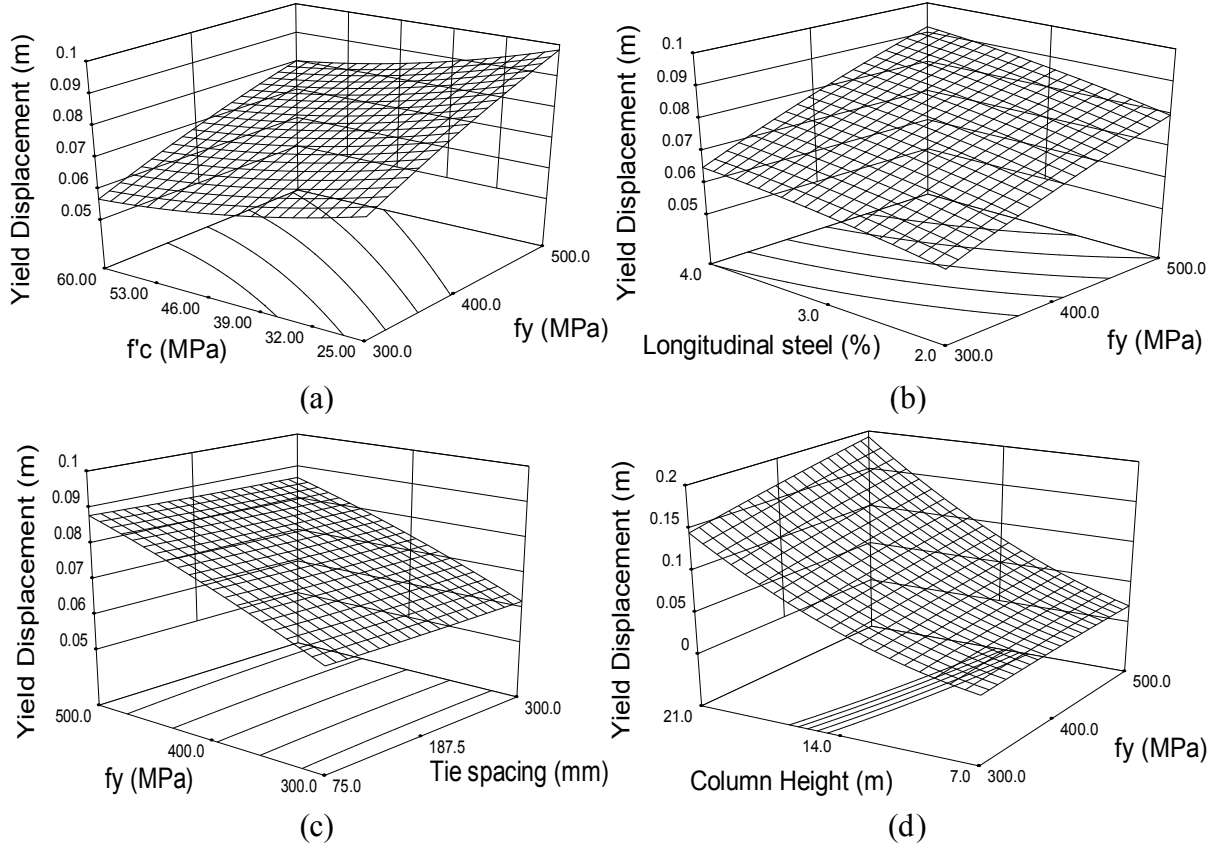
Figure 3-12. Effect of (a) f_y and f'_c, (b) f_y and longitudinal reinforcement ratio, (c) fy and tie spacing, (d) f_y and column on the yield displacement.

3.5.3 First Crushing

3.5.3.1 Analytical effect of factors at first crushing

The curvature ductility for unconfined concrete can be expressed as [Park and Paulay (1975)]

$$\frac{\varphi_u}{\varphi_y} = \frac{\beta_1 E_s \varepsilon_c}{f_y} \frac{1+(\rho+\rho')\,n - \sqrt{\left[(\rho+\rho')^2\,n^2 + 2\left(\rho+\frac{\rho'd'}{d}\right)n\right]}}{\sqrt{\left[\left(\frac{\rho'\varepsilon_c E_s - \rho f_y}{1.7\,f'_c}\right)^2 + \frac{\rho'\varepsilon_c E_s \beta_1 d'}{0.85\,f'_c d}\right]} - \frac{\rho'\varepsilon_c E_s - \rho f_y}{1.7 f'_c}} \tag{3-10}$$

Where, ρ and ρ' are the ratio of longitudinal reinforcement at tension and compression zones respectively; ε_c is the concrete compressive strength at crushing. The unconfined compressive strength in Eq. (3-10) can be replaced by the confined compressive strength. According to Mander et al. (1988b), the confined compressive strength is

$$f'_{cc} = f'_c \left(-1.254 + 2.254 \sqrt{1 + \frac{7.94 f'_l}{f'_{co}}} - 2\frac{f'_l}{f'_{co}} \right) \tag{3-11}$$

Where, f'_c is the unconfined compressive strength of concrete. f'_l is the effective lateral confining stress

$$f'_l = \frac{1}{2} k_e \rho_s f_y \tag{3-12}$$

Where, ρ_s is the volumetric ratio of transverse reinforcement steel to the volume of the core; k_e is the confinement effectiveness coefficient, can be defined as [Mander et al. (1984)]

$$k_e = \left(1 - \Sigma_{i=1}^{n} \frac{(w'_i)^2}{6 b_c d_c} \right) \frac{\left(1 - \frac{s'}{2 b_c} \right)\left(1 - \frac{s'}{2 d_c} \right)}{(1 - \rho_{cc})} \tag{3-13}$$

Where, ρ_{cc} is the ratio of longitudinal reinforcement to area of core section, s' is the clear vertical spacing of the transverse reinforcement; b_c and d_c are the width and depth of the core section and w'_i is the ith clear distance between adjacent longitudinal bars. Total deformation at plastic zone has two parts

$$\Delta_{crush} = \Delta_y + \Delta_p \tag{3-14}$$

Δ_p, the plastic deformation can be derived from equation (3-9) and (3-10), estimating φ_y and φ_u

$$\Delta_p = (\varphi_u - \varphi_y) \, h_p \left(H - \frac{h_p}{2}\right) \tag{3-15}$$

Where, h_p is the plastic hinge length. Therefore, in the plastic deformation zone, all factors have effects on the crushing displacement, and also interactions of different factors are also expected to be prominent. The shear capacity V_{shear} of the section according to Bentz et al. (2006) is presented as

$$V_{shear} = \beta \sqrt{f'_c} b \, d + \frac{A_v f_y d_v \cot\theta}{s} \tag{3-16}$$

Here, b and d are the width and effective depth of the section, s is the center to center distance of transverse reinforcement, A_v is the gross area of the tie bars in a single layer, θ is the angle of shear failure, β is a factor which depends on the average tensile stress in the section.

3.5.3.2 Factorial design at first crushing

The range of base shear at crushing or shear failure is wider than that of yield base shear for each column height (Figure 3-13(a)). Figure 3-13(b) shows that the tie spacing has significant effect on the crushing base shear of 7 m column, however, very little effect on the 14 and 21 m columns. In most of the cases, 7 m columns are shear critical and most of the combinations of 14 and 21 m columns are flexure dominated. Tie spacing, longitudinal steel ratio and f_y play important roles in shear capacity of the column; however, f'_c has little effect on shear capacity, hence, has smaller effect on the base shear at crushing or shear failure of 7 m column. The effect of tie spacing is insignificant on the base shear capacity of flexure dominated column; therefore, it has little effect on the crushing base shear for 14 and 21 m column cases as shown in Figure 3-14(a). Longitudinal steel ratio and f_y are the most effecting parameters in flexure dominated 14 and 21 m height columns. The effect of f_y is more in shorter columns as shown in Figure 3-14(c).

Figure 3-14(d) shows that the crushing base shear increases with the increase of f'_c for 7 m column and decreases with the increase of f'_c. The shear capacity of the column increases with the increase of f'_c [Eq. (16)]. Since, most of the combinations of 7 m column are shear dominated therefore, effect of increase of f'_c on crushing base shear is positive. Due to the P-Δ effect, pushover curve goes downward after reaching the maximum base shear. If the crushing point lies on the downward pushover curve, any increase in crushing displacement will decrease the crushing base shear. The first crushing points of 21 m column combinations lie on the downward pushover curve; i.e. the base shear corresponding to first crushing is less than the maximum base shear capacity due to high slenderness ratio of the 21 m column. Since, the crushing displacement increases with the increase of f'_c, the crushing base shear of the combinations of the 21 m columns decreases with the increase of f'_c and crushing displacement. Figure 3-14(d) shows the decrease in crushing base shear with the increase of f'_c for 21 m column, which is the effect of slenderness; it does not represent the effect of f'_c on the ultimate base shear capacity. Therefore, tie spacing, f'_c and f_y have significant interaction with column height. Moreover, ANOVA analysis suggests that the interaction between tie spacing and longitudinal reinforcement ratio is also significant as shown in Figure 3-14(b). The effect of tie spacing is higher for higher reinforcement ratio.
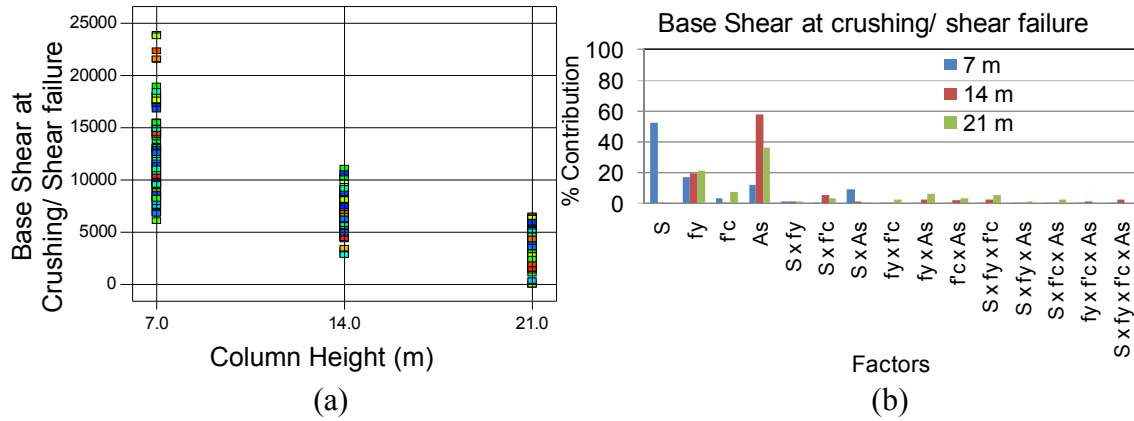
Figure 3-13. (a) Range of base shear for crushing or shear capacity for different heights of columns, (b) contribution percentage of factors on the change of base shear due to first crush or to reach shear capacity.
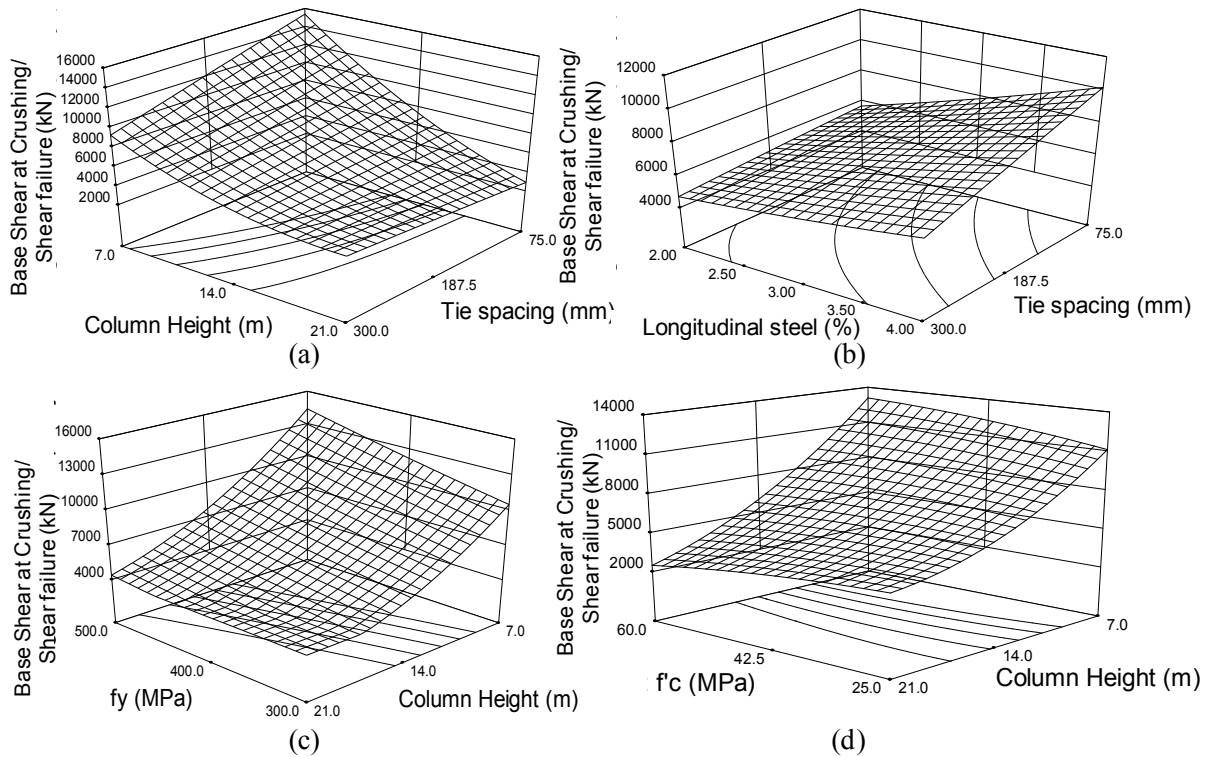
Figure 3-14. Effect of (a) column height and tie spacing, (b) longitudinal reinforcement ratio and tie spacing, (c) column height and f_y, (d) column height and f'_c on the crushing base shear or shear capacity.

Figure 3-15(a) shows that the range of displacement at crushing or shear failure gets wider with the increase of column height. Tie spacing, f'_c and their interaction mostly affects the

crushing displacement for the 7m and 14m height columns. Here, these two factors have significant interaction. The effect of tie spacing decreases with the increase of column height from 7m to 14m and the effect of compressive strength increases. Also, higher order interaction plays some role which is shown in Figure 3-15(b). The effect of confinement is more significant after the first yielding. The 21m column gets unstable before reaching the first crushing for some combinations of the four factors because of the slenderness effect. Figure 3-16 shows the contribution of different factors on the displacement for first crushing or for instability. Figures 3-16(a) and 3-16(c) show that displacement at crushing or shear failure increases with the increase of f'_c, and the effect of f'_c is more for lower tie spacing and longer column height. In the same way, tie spacing has higher effect on the displacement for crushing or shear failure for higher compressive strength of concrete. Although, the percent contribution of tie spacing is higher in shorter column, the difference between highest and lowest displacements is smaller in shorter column (7 m column) than in longer column (14 and 21 m column). Therefore, crushing or shear failure displacement decreases with the increase of tie spacing for 14 and 21 m column, however, the effect of tie spacing is very insignificant in the case of 7 m column as shown in Figure 3-16(d). The displacements at shear failure of most of the combinations of 7 m column are less than the yield displacement. Figure 3-16(b) shows that f_y and longitudinal reinforcement ratio have negligible effect on the displacement at crushing or shear failure. The effects of tie spacing, f'_c, column height, tie spacing-column interaction; f'_c column height interaction and square of f'_c have been found significant on the displacement for crushing or shear failure from ANOVA analysis.
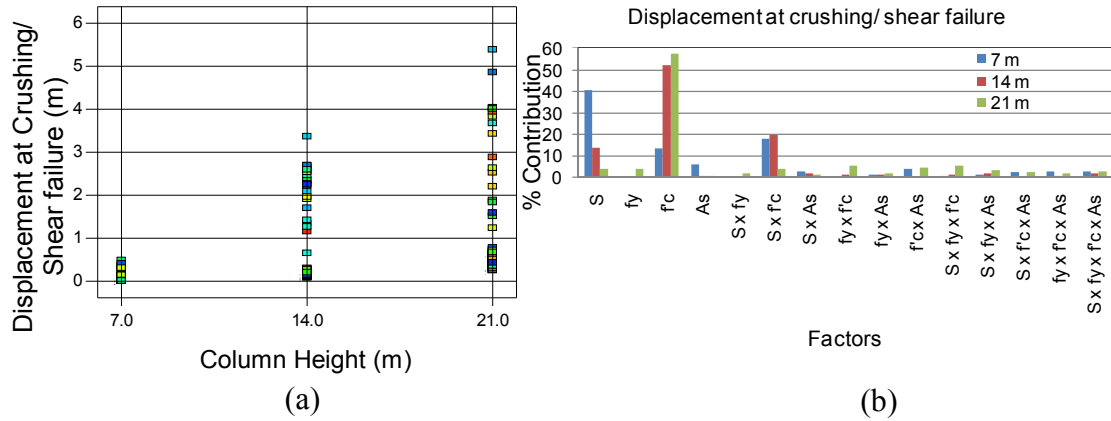
Figure 3-15. (a) Range of displacement for crushing or shear capacity for different heights of columns, (b) contribution percentage of factors on the change of displacement due to first crush or to reach shear capacity.
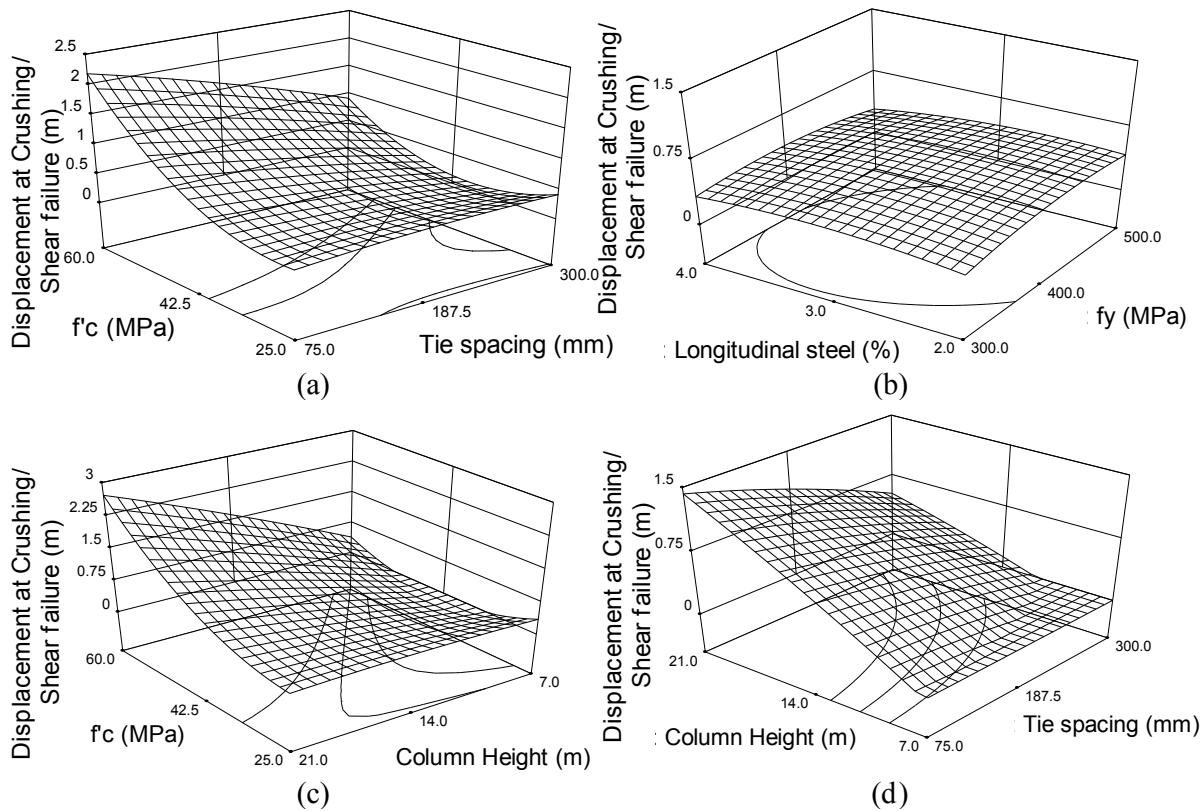
Figure 3-16. Effect of (a) tie spacing and f'_c, (b) f_y and longitudinal reinforcement ratio, (c) column height and f'_c, (d) column height and tie spacing on the displacement at crushing or shear failure.

36

3.5.4 Factorial Design for Displacement Ductility

In this study, ductility is defined as the ratio of displacement at crushing or shear failure to the yield displacement, which is never less than one for flexure dominated column. Among 81 combinations of 7 m column, 45 combinations are shear dominated, and 39 combinations are with virtual ductility, i.e. displacement at shear failure less than the yield displacement, among these shear dominated combinations. On the other hand, only one combination has been found to be shear dominated with ductility of 2.43.

The range of ductility is more for 14 m height column [Figure 3-17(a)]. The effects of tie spacing, f'_c, column height, tie spacing-column interaction; f'_c column height interaction and square of f'_c have been found significant on the ductility as shown in Figure 3-17(b).

(a) (b)
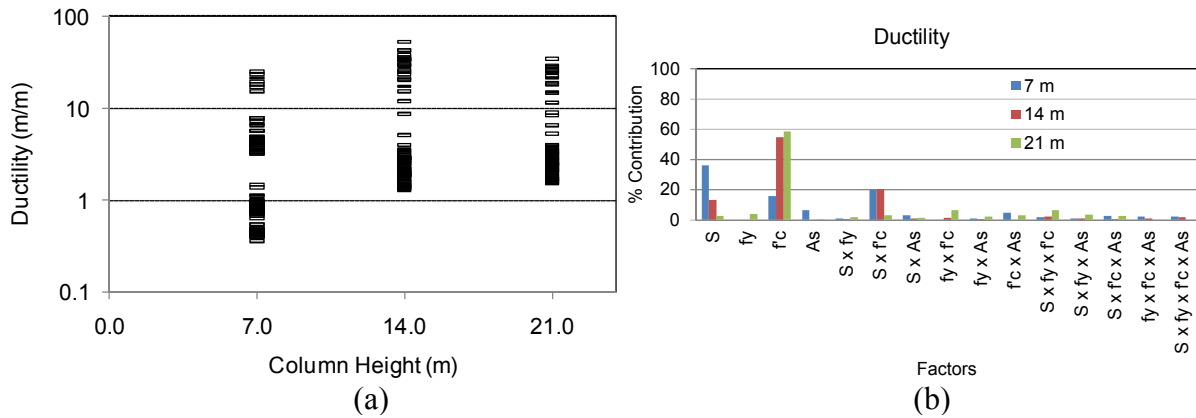
Figure 3-17. Range of ductility for different heights of columns, (b) different factors on ductility (displacement of crushing or shear capacity/yield displacement).

The contributions of factors are almost similar for ductility and displacement at crushing or shear failure. Figure 3-18(a) shows the interaction between tie spacing and f'_c; the effect of f'_c is more for lower tie spacing. Figure 3-18(b) shows that, ductility increases with the increase of column height for 60 MPa concrete, however, ductility increases from 7 m to 14 m column and

decreases from 14 m to 21 m for 25 MPa concrete. Thus, the change in ductility does not follow a common trend with the change in column height and f'_c.
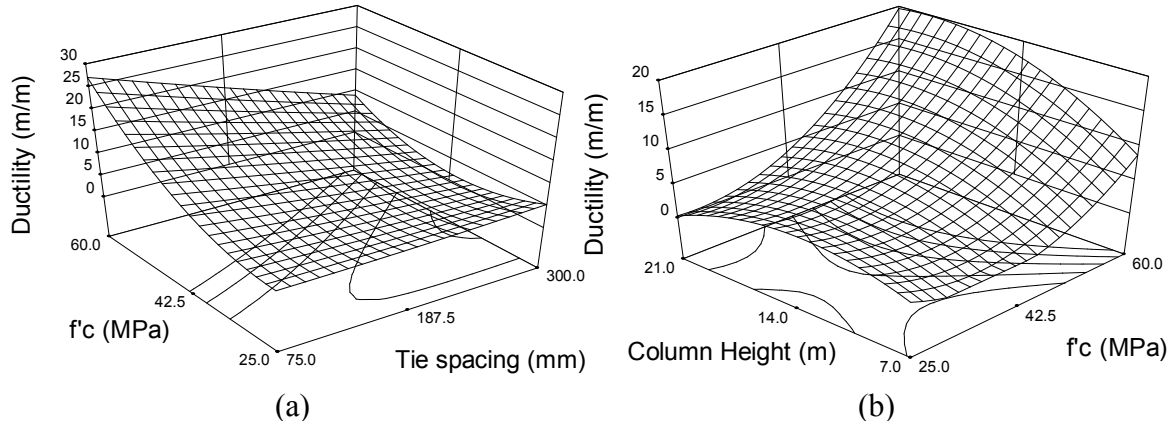
Figure 3-18. Effect of (a) tie spacing and f'_c, (b) f'_c and column height on ductility (displacement of crushing or shear capacity/yield displacement).

3.6 PREDICTED EQUATIONS

Considering the significant factors found from F-test in ANOVA analysis, equations have been developed for cracking base shear, cracking displacement, yield base shear, yield displacement, crushing base shear/shear capacity, displacement at crushing/shear failure and ductility respectively. The general formula is

$$X = \beta + \alpha_1 s + \alpha_2 f_y + \alpha_3 f'_c + \alpha_4 A_s + \alpha_5 H + \alpha_6 s * f_y + \alpha_7 s * f'_c + \alpha_8 s * A_s + \alpha_9 s * H +$$

$$\alpha_{10} f_y * f'_c + \alpha_{11} f_y * A_s + \alpha_{12} f_y * H + \alpha_{13} f'_c * A_s + \alpha_{14} f'_c * H + \alpha_{15} A_s * H + \alpha_{16} s^2 + \alpha_{17}$$

$$f_y^2 + \alpha_{18} f'^2_c + \alpha_{19} A_s^2 + \alpha_{20} H^2 + \alpha_{21} s * f'_c * H + \alpha_{22} s * f'^2_c + \alpha_{23} s * H^2 \qquad + \alpha_{24} f'_c x$$

$$H^2 + \alpha_{25} s * f'c * H^2 \qquad\qquad (3\text{-}17)$$

where, β is constant, α's are the coefficients of the equations, given in Table 3-4. Combined effect of shear and flexure has been taken intentionally in order to check the

formability of the unified equations for crushing/shear failure limit state and ductility. Factors have been used in their actual unit in these equations. s, f'_c, f_y, A_s and H represent the tie spacing in mm, compressive strength of concrete in MPa, yield strength of steel in MPa, longitudinal reinforcement ratio in percentage of concrete gross area and height of column in m, respectively. Figure 3-17 shows the plots of empirical results derived from these equations versus the numerical results derived from finite element analysis.

Four random columns of 7 m, 9 m, 16 m and 21 m heights have been selected in order to validate the equations. Tables 3-5 to 3-7 show that these equations can fairly predict the cracking limit state, yield limit state and crushing base shear or shear capacity. However, generated equations make erroneous prediction on the top displacement at first crushing or shear failure and ductility of the column as shown in Table 3-8. This is due to the presence of high degree of non-linearity in the displacement at post-elastic region or in failure mode of the column. The base shear in the post elastic region, however, is easily predictable, since, the pushover curves flattens after reaching the yield point and there is small difference between the yield and maximum base shear. This study considers three levels for each parameter. Higher level factorial analyses are needed in order to predict the displacement at crushing or shear failure and ductility of a column precisely.
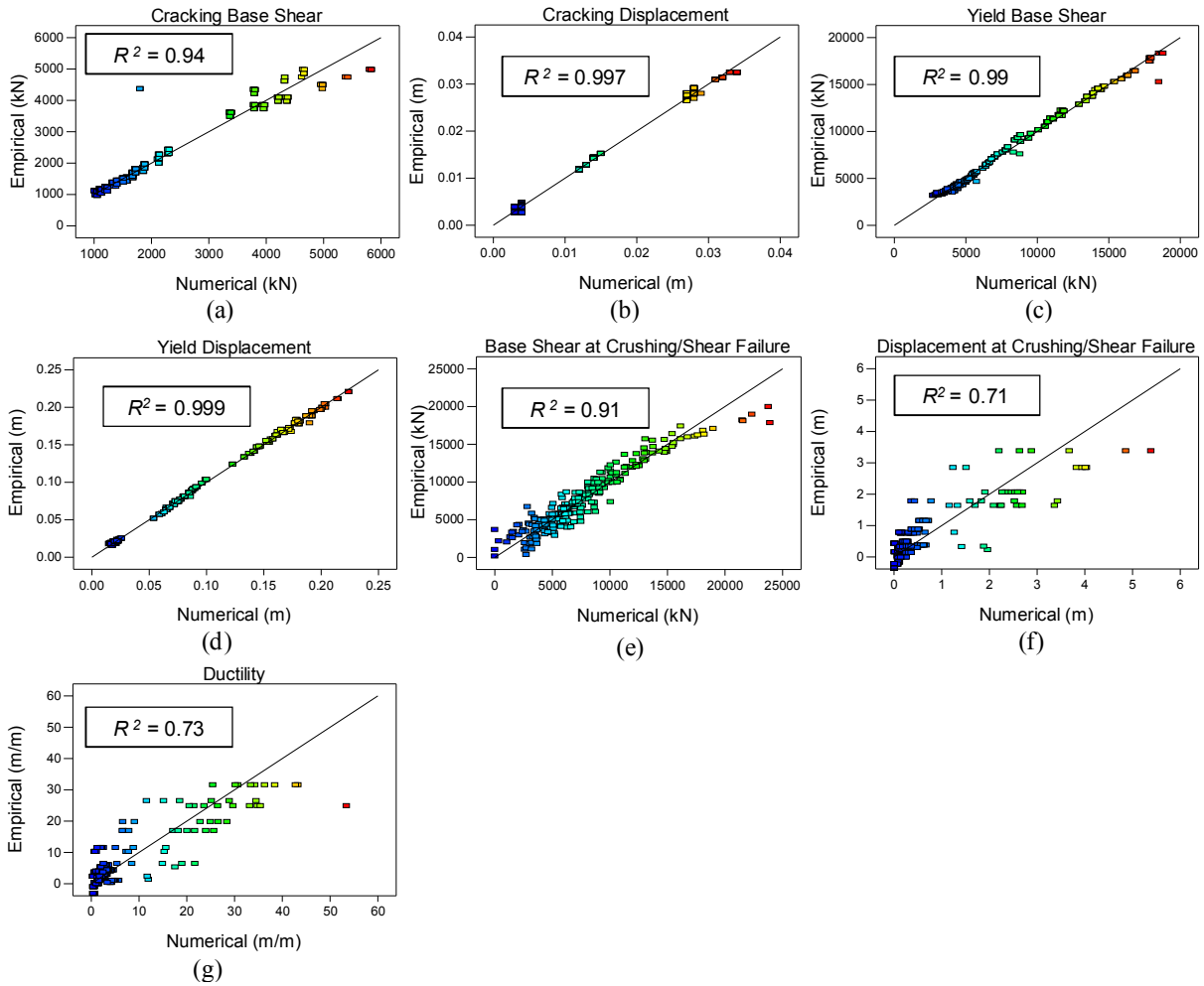
Figure 3-19. Empirical vs. Numerical plots for (a) cracking base shear, (b) cracking displacement, (c) yield base shear, (d) yield displacement, (e) crushing shear/shear capacity, (f) displacement at crushing or shear failure, (g) ductility.

Table 3-4. Coefficient of equations for different limit states of the column.

Factor/ Interaction	Cracking Displacement (m) $R^2 = 0.997$	Cracking Base shear (kN) $R^2 = 0.94$	Yield Displacement (m) $R^2 = 0.999$	Yield Base Shear (kN) $R^2 = 0.99$	Displacement at Crushing/shear failure (m)		Base Shear Crushing/Shear Failure (kN) $R^2 = 0.91$	Ductility (m/m) Cubic $R^2 = 0.73$
					Quadratic $R^2 = 0.71$	Cubic $R^2 = 0.77$		
B	8.92E-03	6748.5	0.022	7746.9	1.824694	1.662474	6232.05	82.288
α_1	0	-4.365	0	0	0.00915	-0.01711	-24.95	-0.120
α_2	0	0	2.17E-06	11.913	0	0.000159	25.622	0
α_3	-3.40E-04	-4.547	-1.36E-04	32.687	-0.1426	-0.07414	102.4239	-3.806
α_4	-1.76E-03	329.43	-8.09E-04	2433.2	0	-0.01857	2679.603	0
α_5	3.45E-04	-588.7	-5.84E-03	-1204.5	-0.04553	0.151059	-1174.49	-6.318
α_6	0	0	0	0	0	0	0	0
α_7	0	0	0	0	-0.00017	0.000871	0	0.0073
α_8	0	0	0	0	0	0.0000	-6.090	0
α_9	0	0	0	0	-0.0002	0.000458	2.322	0
α_{10}	0	0	-4.24E-07	0	0	0	0	0
α_{11}	0	0	9.26E-06	3.177	0	0	0	0
α_{12}	0	0	1.55E-05	-0.834	0	0	-0.878	0
α_{13}	0	0	0.00E+00	0	0	0	0	0
α_{14}	-8.48E-06	-1.258	-5.87E-05	-1.19	0.004652	-0.0106	-7.157	0.2109
α_{15}	3.84E-05	-12.486	6.23E-04	-141.306	0	0	0	0
α_{16}	0	0.012	0.00E+00	0	-4.3E-06	0	0	0
α_{17}	0	0	-1.28E-07	0	0	0	0	0
α_{18}	4.59E-06	0.454	7.78E-06	0	0.00169	0.000426	0	0.0375
α_{19}	2.96E-04	0	-1.07E-03	0	0	0	0	0
α_{20}	+ 6.87E -5	16.675	3.94E-04	48.478	-0.00111	0	27.46	0.2020
α_{21}	-	-	-	-	-	-	-	-
α_{22}	-	-	-	-	-	-9.6E-06	-	-0.0001
α_{23}	-	-	-	-	-	-	-	-
α_{24}	-	-	-	-	-	0.00021	-	-0.0067
α_{25}	-	-	-	-	-	-	-	-

Table 3-5. Validation of generated equations for cracking limit state.

H (m)	A_s (%)	f'_c (Mpa)	f_y (Mpa)	s (mm)	Cracking displacement (m)			Cracking base shear (kN)		
					Equation	Original	Error (%)	equation	original	Error (%)
7	2.4	56	310	275	0.003572	0.004	10.71	4408	5110	13.72
9	2.8	42	390	250	0.004637	0.006	22.717	3201	3147	1.739
16	3.2	35	420	130	0.016462	0.017	3.165	1340	1569	14.597
18	3.6	29	460	100	0.02201	0.023	4.306	1207	1432	15.69

Table 3-6. Validation of generated equations for first yield limit state.

H (m)	A_s (%)	f'_c (MPa)	f_y (MPa)	s (mm)	Yeilding displacement (m)			Yeilding base shear (kN)		
					Equation	Original	Error (%)	Equation	Original	Error (%)
7	2.4	56	310	275	0.018019	0.016	12.62	10768	10399	3.54
9	2.8	42	390	250	0.031075	0.031	0.24	10196	9362	8.92
16	3.2	35	420	130	0.108223	0.101	7.15	5583	5497	1.57
18	3.6	29	460	100	0.151834	0.142	6.93	5538	5398	2.59

Table 3-7. Validation of generated equation for base shear at first crushing.

H (m)	A_s (%)	f'_c (Mpa)	f_y (Mpa)	s (mm)	Crushing base shear (kN)		
					Equation	Original	Error (%)
7	2.4	56	310	275	7811	7101	9.997
9	2.8	42	390	250	8243	8321	0.939
16	3.2	35	420	130	6528	6395	2.091
18	3.6	29	460	100	6807	6562	3.73

Table 3-8. Validation of generated equations for displacement at crushing/shear failure and ductility.

H (m)	A_s (%)	f'_c (Mpa)	f_y (Mpa)	s (mm)	Displacement at crushing/shear failure (m)		Ductility (m/m)
					Quadratic	Cubic	Cubic
					Error (%)	Error (%)	Error (%)
7	2.4	56	310	275	8826	97077	32
9	2.8	42	390	250	1783	11303	1132
16	3.2	35	420	130	134	451	33
18	3.6	29	460	100	21	98	109

3.7 SUMMARY

In this study, variations in three limit states: cracking, yielding of longitudinal bar and first crushing of concrete, with the change of four parameters (s, f'_c, f_y and A_s) have been investigated using design of experiments. Pushover analyses have been performed with 81 numerical models for each three different column heights in order to measure those limit states in terms of base shear and displacement. The effects of the four factors on the limit states have been determined with those 81 combinations by 3^4 factorial analyses. In order to take the effect of height into the Design of Experiment, the analyses were turned into 3^5 factorial analyses. The results demonstrated that three level factorial analyses are adequate to predict the limit states except the inelastic displacement and ductility of the bridge piers.

CHAPTER 4: SEISMIC PERFORMANCE EVALUATION OF A MULTI-SPAN RC BRIDGE WITH IRREGULAR COLUMN HEIGHTS OF VARYING DUCTILITY LEVELS

4.1 GENERAL

Bridges are essential elements in a modern transportation network and play significant roles in a country's economy. However, it has always been a major challenge to keep bridges safe and serviceable. Due to river geometry and topological profile, different irregularities are introduced in bridges. The most common form of irregularities in bridges is non-uniform height of columns over a basin. This causes earlier failure of shorter columns due to large deformation demand. The objective of this study is to assess the seismic performance a four equal span RC box-girder bridge monolithically connected to columns of irregular heights. Here, different column height configurations and four ductility levels have been considered where their performance has been assessed through static pushover analyses, incremental dynamic analyses (IDA) and fragility analyses. Static pushover (SPO) analysis gives static pushover curves identifying different limit states and ductility capacity. Dynamic pushover curves have been generated from IDA results and compared with the SPO curves. IDA results have also been utilized in order to develop fragility curves for two regular and two irregular column height combinations of bridges with two different tie spacing. Thus, the effects of column height irregularities and different levels of ductility on the vulnerability of the bridge in longitudinal direction have been examined.

4.2 BRIDGES WITH DIFFERENT DUCTILITY LEVELS AND NON-UNIFORM COLUMN HEIGHTS

Vulnerability of bridges increases with the presence irregularity (Akbari 2010). Displacement ductility demand for short columns in bridges with irregular column heights increases significantly during an earthquake. This study will demonstrate the effect of irregularity in column heights on the performance of bridges using pushover analysis. Here, column of heights 7 m, 14 m and 21 m have been considered to make eight cases with different combinations of column height. Table 4-1 shows the combinations of column height variations for 7 m, 14 m and 21 m columns, which corresponds to short (S), medium (M) and long (L), respectively. Figure 4-1 shows one combination case SML case, which can be interpreted as column heights of 7 m, 14 m and 21 m, respectively.
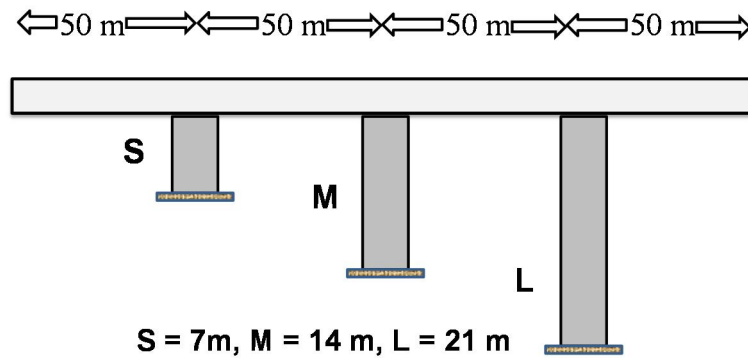
Figure 4-1. Bridges with irregular column height combination.

Table 4-1. Different column height combinations.

Case	C1	C2	C3
SSS	7 m	7 m	7 m
MMM	14 m	14 m	14 m
LLL	21 m	21 m	21 m
MLL	14 m	21 m	21 m
SLL	7 m	21 m	21 m
SML	7 m	14 m	21 m
MSL	14 m	7 m	21 m
SLM	7 m	21 m	14 m

Current seismic design codes/standards emphasize on providing adequate lateral reinforcement in bridge columns to achieve sufficient ductility during earthquakes. Previously tie spacing of 300 mm was very common in bridge columns designed before 1970 (Ruth and Zhang 1999). However, in CHBDC 2010 (CSA-S6-06), the recommended tie spacing is six times the longitudinal bar diameter where tie should cover every alternate longitudinal bar. This study will assess the seismic performance of four-span bridges with four ductility levels by considering the tie spacings of 75 mm, 100 mm, 150 mm and 200 mm. Tie spacing is allowed up to 150 mm for compression member in modern code. Confinement factor has been determined according to Park et. al. (1982).

4.3 MODELING OF THE BRIDGE

A box girder bridge with four equal spans of length 50 m each has been modeled with SeismoStruct (2010). The description of this software is presented in Chapter 3. Table 4-2 shows the property of the bridge superstructure. 1500 mm x 3000 mm columns with 2% longitudinal

bars have been considered at all pier locations irrespective of the height of columns. 16 mm tie bar is used at every alternate longitudinal bar (Figure 4-2). Supports at each abutment are considered fixed in transverse and vertical directions, however, longitudinal direction is considered free. Fixed supports are considered at the base of each column. Column-deck connections are considered fixed. Deck and column have been modeled as inelastic displacement-based elements. 11.1 tonne/m and 20.2 tonne/m uniformly distributed mass have been assigned to the column and deck, respectively.

Table 4-2. Sectional properties of bridge deck.

EA (kN)	EI (kN-m2)	EI (kN-m2)	GJ (kN-m2)
2.0187×10^8	1.4926×10^8	2.3198×10^9	1.9747×10^8
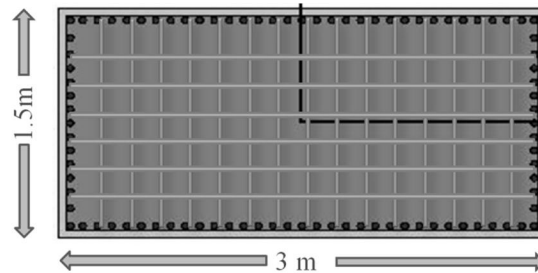
Figure 4-2. Column cross section.

The compressive strength of concrete and yield strength of steel are used as 35 MPa and 500 MPa, respectively. Cracking strain of concrete and yield strain of steel in tension are assumed to be 0.000133 and 0.025, respectively. Crushing strain of unconfined concrete varies from 0.0025 to 0.006 (MacGregor and Wight 2005). According to Paulay and Priestley (1992), crushing strain for confined concrete is much higher and it varies from 0.015 to 0.05. In the present study, crushing strain of confined concrete is considered to be 0.015. Static non-linear

pushover analyses have been conducted with SeismoStruct (2010) using the concrete and steel models described in Chapter 3.

4.4 STATIC PUSHOVER ANALYSIS

The performance of a bridge can be defined by limit states, related to strain limits. First cracking, first yielding and first crushing have been considered as the limit states of the bridges in this study. Static pushover (SPO) analyses have been conducted in the longitudinal direction in order to identify the limit states for all column combinations (Table 4-1). Base shears and lateral displacements of the bridges for the each of the limit states have been determined from the pushover curves. The effect of irregularity due to column height will be observed by comparing the performance of bridges with different column height combinations.

4.4.1 Effect of Tie Spacing on Bridge Performance

Figures 4-3 to 4-5 show the bridge responses with regular column heights of 7 m, 14 m and 21 m, respectively, for different tie spacings of 75 mm, 100 mm, 150 mm and 200 mm obtained from pushover analyses. Effect of confinement has been found significant after the first yielding. The bridge with smaller tie spacing has higher total base shear capacity and can undergo larger deformation before concrete crushing. However, tie spacing does not have significant effect on the yield strength and strain. In the case of SSS, pushover curve remains flat after reaching the first crushing for 75 mm tie spacing whereas it undergoes a sharp fall for larger spacings of tie. The behaviour is the same in the cases of MMM and LLL. The columns of regular bridge did not show uniform pushover curves due to the initial deformation of deck under dead load. In the case of rigid deck, the behaviour of all three columns would be the same.
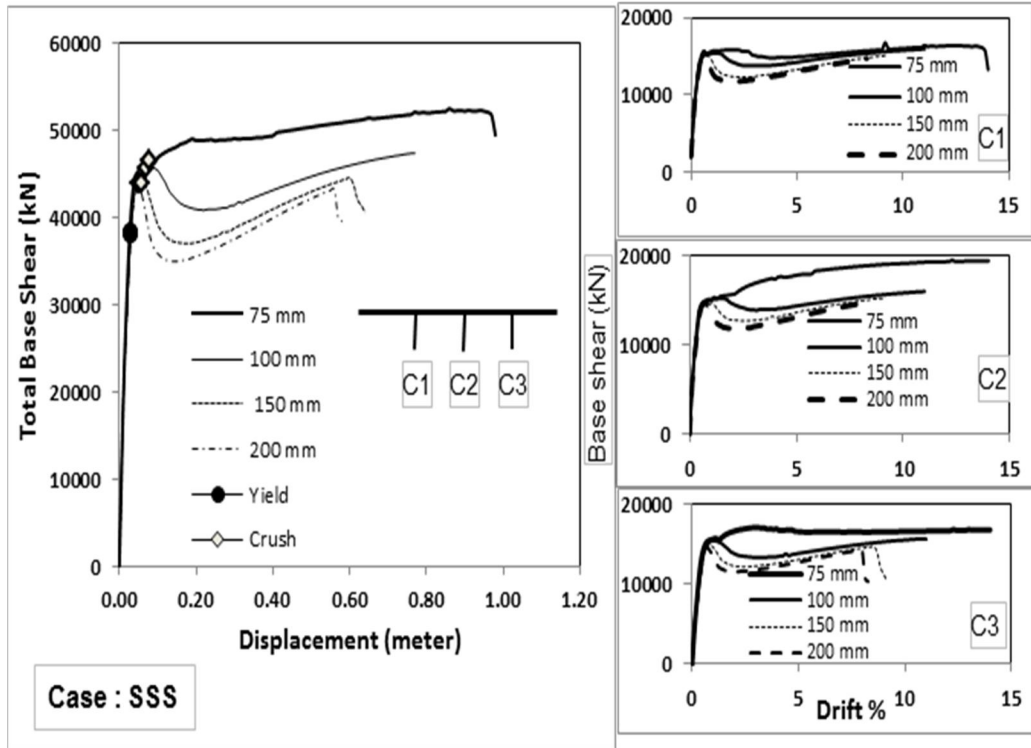
Figure 4-3. Results of pushover analysis in longitudinal direction for Case: SSS.
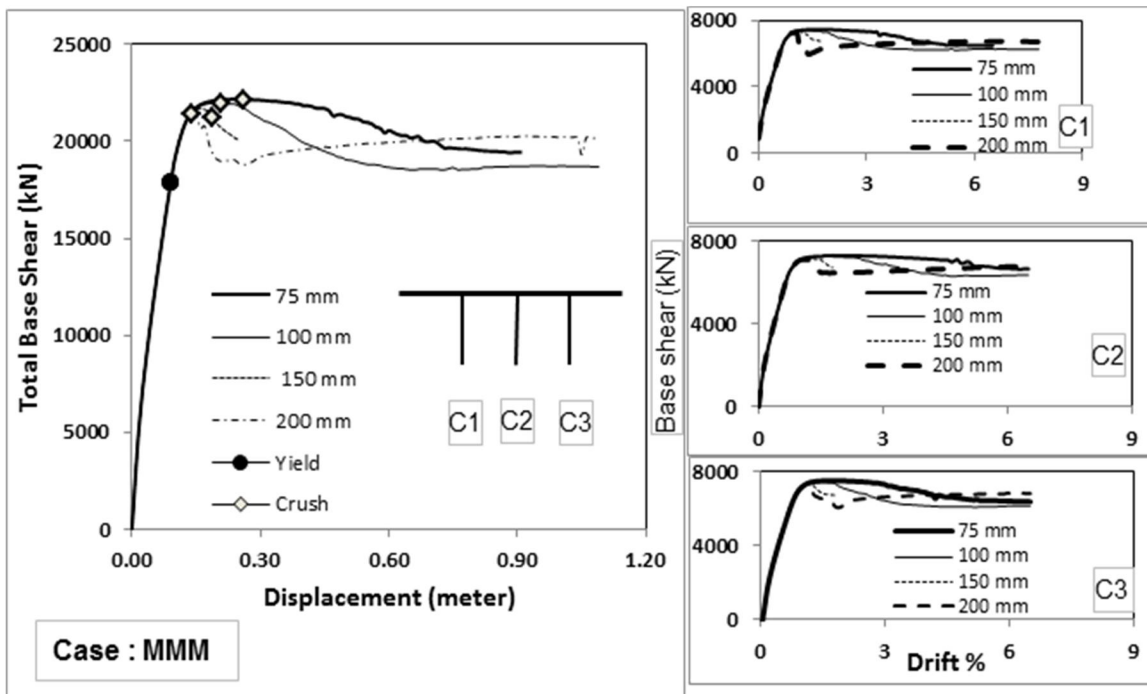
Figure 4-4. Results of pushover analysis in longitudinal direction for Case: MMM.
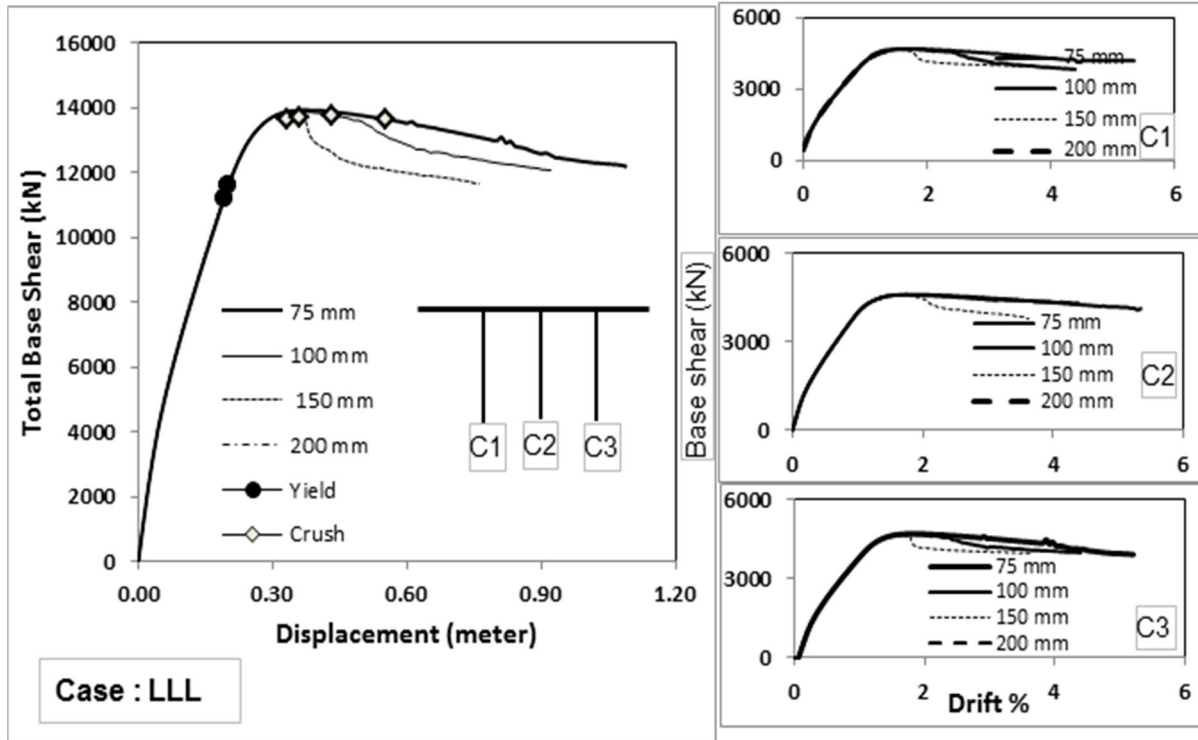
Figure 4-5. Results of pushover analysis in longitudinal direction for Case: LLL.

While considering irregular column height combinations, SLL and MLL are the irregular forms of the case LLL. Here, the stiffness of the column increases with the reduction of length and, thus, the shorter column attracts more load than the other two columns, which are shown in Figures 4-6 and 4-7. Pushover curves show more ductile behaviour for smaller tie spacing. The pushover curves for tie spacing of 200 mm falls just after it reaches the crushing load, which indicates its brittle behaviour. The ties start comes into action after the start of the concrete crush, therefore, pushover curves falls down and goes up due to strain hardening of tie bars.

4.4.2 Effect of Irregularity on Bridge Performance

Pushover analyses are conducted considering irregularities in column height for five different combinations of column heights. The pushover curves of irregular bridges are given in Figures 4-6 to 4-8. In the cases of MLL and SLL, they have higher total base shear capacity than

that of case LLL, however those reaches to the yield and crush limit in lower strain. For the same deck displacement in longitudinal direction, the shorter column is subjected to more drift and since, it has more stiffness, it attracts more base-shear than the longer columns.
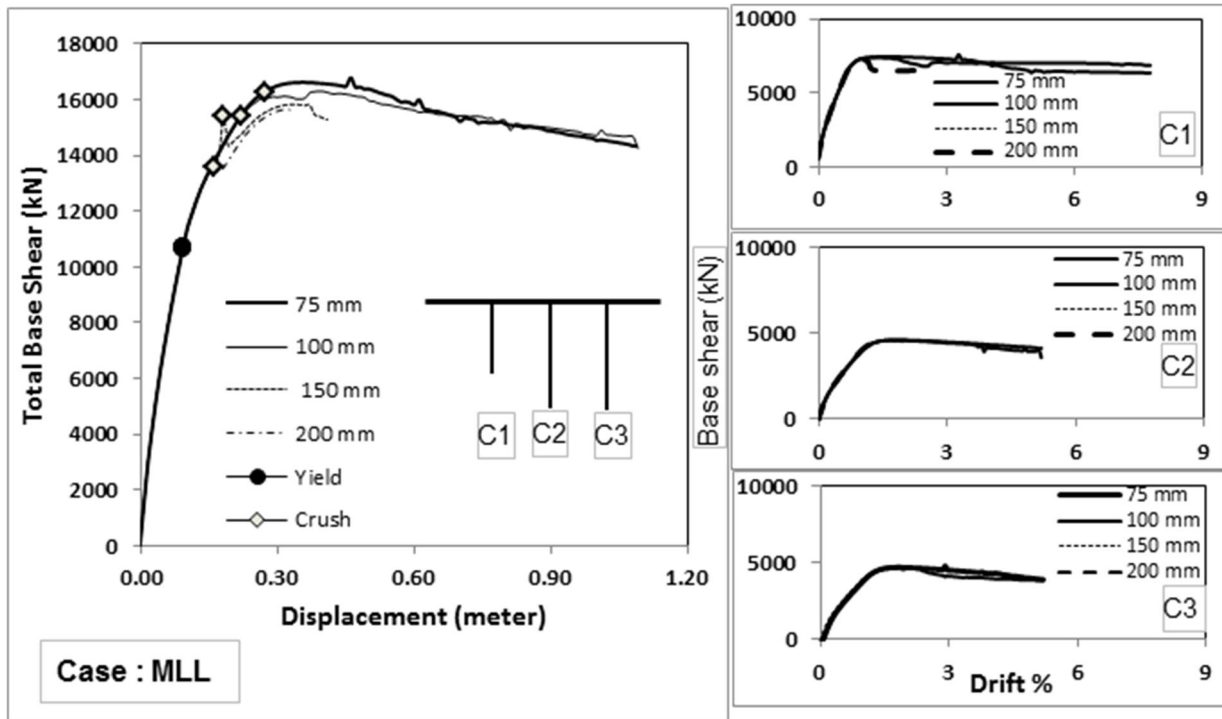
Figure 4-6. Results of pushover analysis in longitudinal direction for Case: MLL.

Tables 4-3 and 4-4 show the strengths and displacements of bridges with different column height combinations corresponding to yielding and crushing, respectively. For all cases, it is observed that tie spacing has little effect on the first cracking and first yielding limit states, however, it has significant effect on the first crushing limit state. The displacements needed for crushing and yielding of the cases MLL match with that of the cases MMM. The similar results were observed for SLL, SML, SLM and MSL and SSS cases. Therefore, the shortest column of the bridge determines the displacements corresponding to the first yielding and crushing. The

shortest column has the highest stiffness in the lateral direction; therefore, it controls the seismic behaviour and capacity of the bridge. The shortest column height in the cases of SML, MSL, SLM is 7m, however, the arrangements of different height of columns are different in these cases and hence the similar performance in terms of first yielding and crushing displacements are observed. The patterns of pushover curves for these three cases are also similar. Therefore, bridges, with of the same column height configuration with different orders, behaves the same in longitudinal direction.
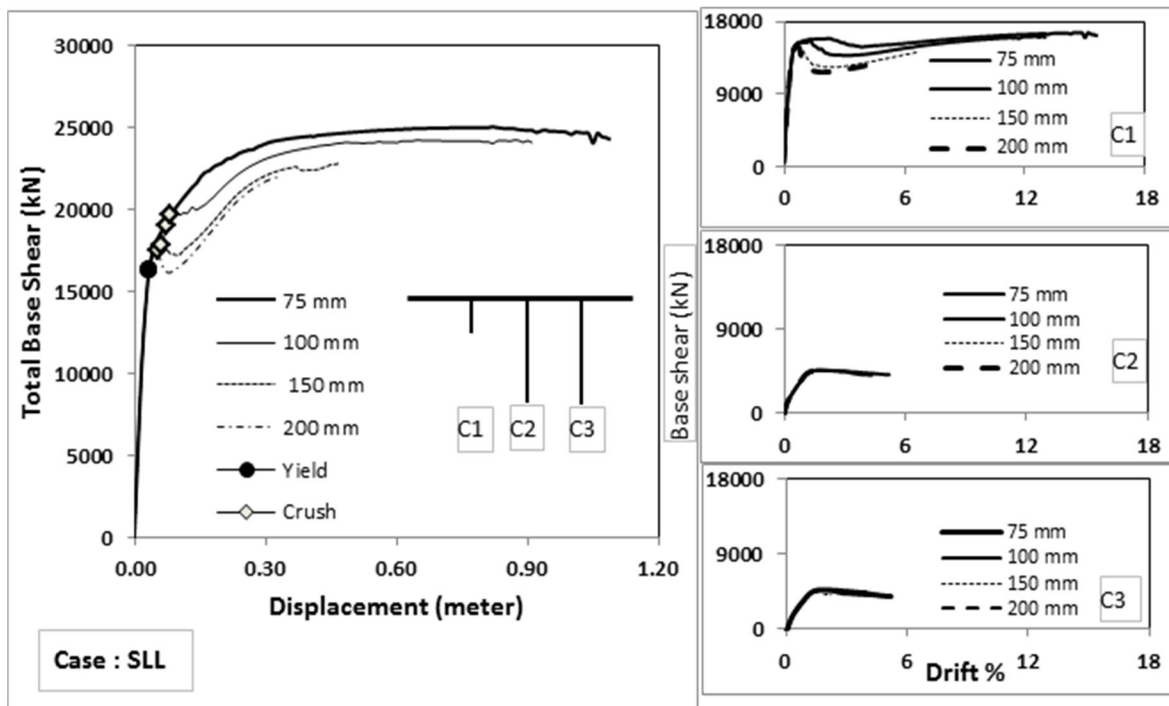
Figure 4-7. Results of pushover analysis in longitudinal direction for Case: SLL.
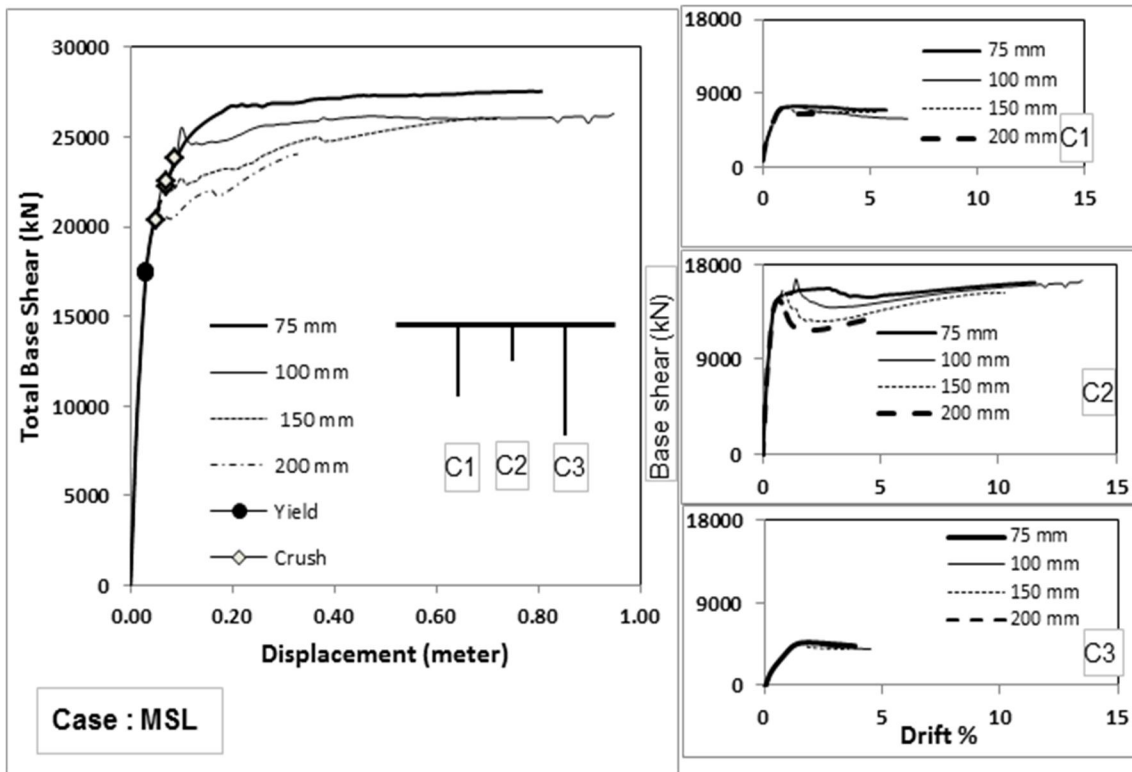
Figure 4-8. Results of pushover analysis in longitudinal direction for Case: MSL.

Figure 4-9 shows the pushover curves for the cases LLL, SSS, SML and SLL for tie spacing of 75 mm. Although, all cases with a 7m column have almost the same yielding and crushing displacement; SSS possesses base shear capacity almost twice of the capacity of SLL and almost three times the capacity of SML. Since, the main portion of the bridge total mass is lumped in the deck, all four cases in Figure 4-9 show similar seismic force due to a particular earthquake event. Two cases with regular column height configurations: SSS, with high base shear capacity, and LLL, with high displacement tolerance, are expected to behave better in earthquake excitation. SLL and MLL are of irregular column heights. Among these, SLL is the most irregular, since the stiffness of the side column drastically increases and hence, the worst performance resulted. SML performs better than the Case SLL, because it has the irregularity in lower level with higher displacement tolerance.

Table 4-3. Yield strength and displacement for different column height combinations.

	Yielding							
	75 mm spacing		100 mm spacing		150 mm spacing		200 mm spacing	
Case	Displacement (m)	Total base shear (kN)	Displacement (m)	Total base shear (kN)	Displacement (m)	Total base shear (kN)	Displacement (m)	Total base shear (kN)
SSS	0.02	38185	0.02	38190	0.02	38225	0.02	38265
MMM	0.09	17823	0.09	17800	0.09	17855	0.09	17880
LLL	0.2	11594	0.2	11598	0.2	11218	0.2	1SML6
MLL	0.09	10673	0.09	10678	0.09	10695	0.09	10710
SLL	0.03	16302	0.03	16300	0.03	16307	0.03	16280
SML	0.03	18021	0.03	18018	0.03	18030	0.03	18043
MSL	0.03	17422	0.03	17425	0.03	17444	0.03	17461
SLM	0.03	17851	0.03	17877.55	0.03	17891	0.03	17900
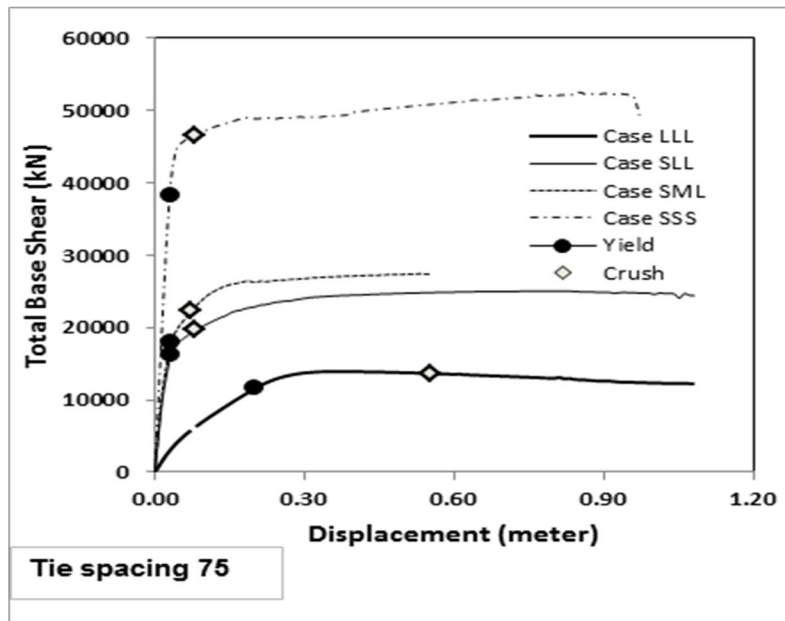
Figure 4-9. Results of pushover analysis in longitudinal direction for Cases: LLL, SLL, SML and SSS considering 75 mm tie spacing.

Table 4-4. Crushing strength and displacement for different column height combinations.

| Case | Crushing | | | | | | | |
| | 75 mm spacing | | 100 mm spacing | | 150 mm spacing | | 200 mm spacing | |
	Displacement (m)	Total base shear (kN)	Displacement (m)	Total base shear (kN)	Displacement (m)	Total base shear (kN)	Displacement (m)	Total base shear (kN)
SSS	0.07	46643	0.06	45704	0.05	44066	0.04	43996
MMM	0.26	22174	0.21	21982	0.19	21229	0.14	21445
LLL	0.55	13657	0.43	13784	0.36	13710	0.33	13662
MLL	0.27	16277	0.22	15395	0.18	15395	0.16	13595
SLL	0.08	19661	0.07	19002	0.06	17839	0.05	17542
SML	0.08	22231	0.08	21998	0.06	20806	0.05	18504
MSL	0.09	23792	0.07	MMM3	0.07	22492	0.05	20320
SLM	0.08	22810	0.07	21845	0.06	20639	0.05	19780

4.4.3 Ductility

Figure 4-10 shows the ductility ratio at first crushing (CALTRANS, 2004) in the case of SLL for different tie spacings. It is well know that increase in tie spacing causes a decrease in confinement. Consequently, ductility decreases with the increase of tie spacing.
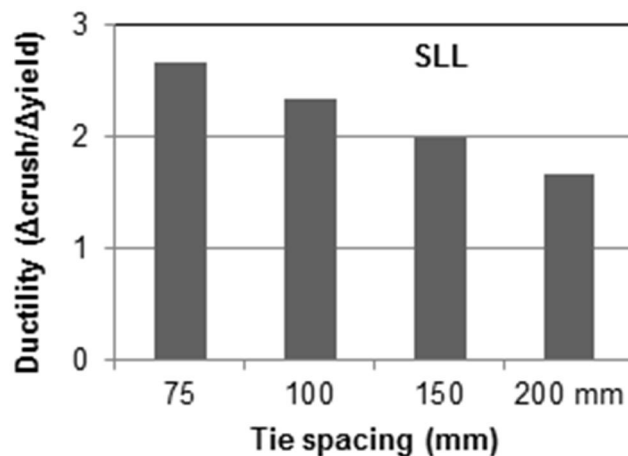
Figure 4-10. Ductility of the bridge with column height configuration SLL for different tie spacing.

4.5 INCREMENTAL DYNAMIC ANALYSIS

SPO analysis gives the structural response under increasing static lateral load. However, lateral load due to earthquakes are truly dynamic in nature and structural response to the earthquake loads cannot be accurately predicted by SPO analysis. In order to overcome the drawbacks of SPO curves, Luco and Cornell (1998) introduced a technique, which performs a series of nonlinear dynamic analyses of the FE model of the structure for an ensemble of ground motions of increasing intensity resulting a set of dynamic response data corresponding to the lateral load with respect to the increment of ground motion intensity. This technique, called the incremental dynamic analysis (IDA), ensures the response of the structure under lateral load which is dynamic in nature (Vamvatsikos and Cornell 2001). Since, IDA generates a set of structural response data for increasing intensity level of ground motions, a dynamic pushover (DPO) curve can be generated by plotting the maximum displacements and corresponding base shear of the structure. Due to high computational cost of IDA, bridges with four column height combinations of LLL, SSS, SLM and SLL for two tie spacings of 75 mm and 200 mm tie spacing have been selected for IDA in this study. The SPO curves have been compared with DPO curves and to conduct fragility curve results have been generated from IDA results in order to observe the effect of bridge irregularity due to varying column heights and tie spacing of the columns.

4.5.1 Description of Ground Motion Properties

The properties of earthquake ground motions vary in terms of predominant period, duration and peak ground acceleration (PGA). Therefore, time history analysis of a structure for a single ground motion may not represent the worst case scenario. Time history analyses with an ensemble of ground motions of varying characteristics gives a fair prediction of structural

56

response under an earthquake. Considering the variation in properties in terms of PGA to PGV ratio 10 earthquake ground motions have been selected for IDA. The magnitudes and epicentral distances of these ground motions are presented in Table 4-5. The acceleration response spectra (5% damped) for the selected ground motion sets are shown in Figure 4-11.
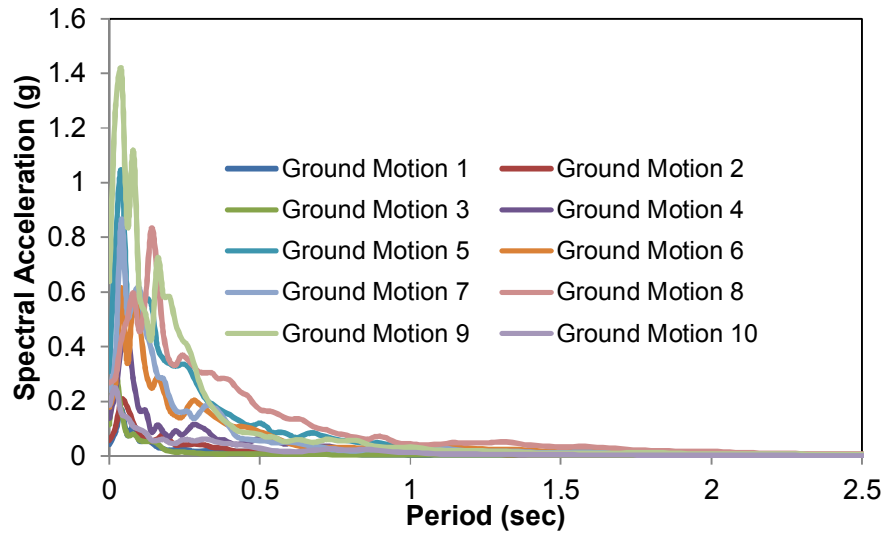
Figure 4-11. Spectral acceleration for the chosen earthquake ground motions.

Table 4-5. Selected earthquake ground motion records.

No	Event	Year	Record Station	M[1]	R[2] (km)	PGA (g)	PGA/PGV
1	Imperial Valley	1979	Plaster City	6.5	31.7	0.042	1.3
2	Imperial Valley	1979	Plaster City	6.5	31.7	0.057	1.05
3	Imperial Valley	1979	Westmoreland Fire Sta.	6.5	15.1	0.11	0.8
4	Imperial Valley	1979	El Centro Array#13	6.5	21.9	0.139	1.06
5	Loma Prieta	1989	Coyote Lake Dam	6.5	22.3	0.179	0.93
6	Loma Prieta	1989	Anderson Dam	6.9	21.4	0.244	1.2
7	Loma Prieta	1989	Hollister Diff. Array	6.9	25.8	0.279	0.79
8	Imperial Valley	1979	Cucapah	6.9	23.6	0.309	0.85
9	Loma Prieta	1989	16 LGPC	6.9	16.9	0.605	1.19
10	Superstation Hill	1987	Wildlife liquefaction array	6.7	24.4	0.132	1.03

[1] Moment Magnitudes [2] Closest Distances to Fault Rupture
PEER Strong Motion Database, http://peer.berkeley.edu/svbin

4.5.2 Dynamic Pushover Curves

Figures 4-12 to 4-19 show the total base shear versus lateral displacement plots for bridges with columns height combinations of LLL, SSS, SLM and SLL and of two different tie spacing of 75 mm and 200 mm based on the results of IDA. Shapes of the IDA curves are also included. DPO points closely coincide with the SPO curves before the first yield of the longitudinal bars. IDA show higher base shear capacity compared to that of SPO between the first yield and first crushing of the concrete, however, the variation of DPO and SPO is within 10% for the cases of SSS, SLM and SLL and is about 30% for the cases of LLL. Therefore, the ductility calculated based on the first yield of rebar and crushing of the concrete is acceptable. The DPO base shear capacity is lower than that of SPO beyond crushing point.
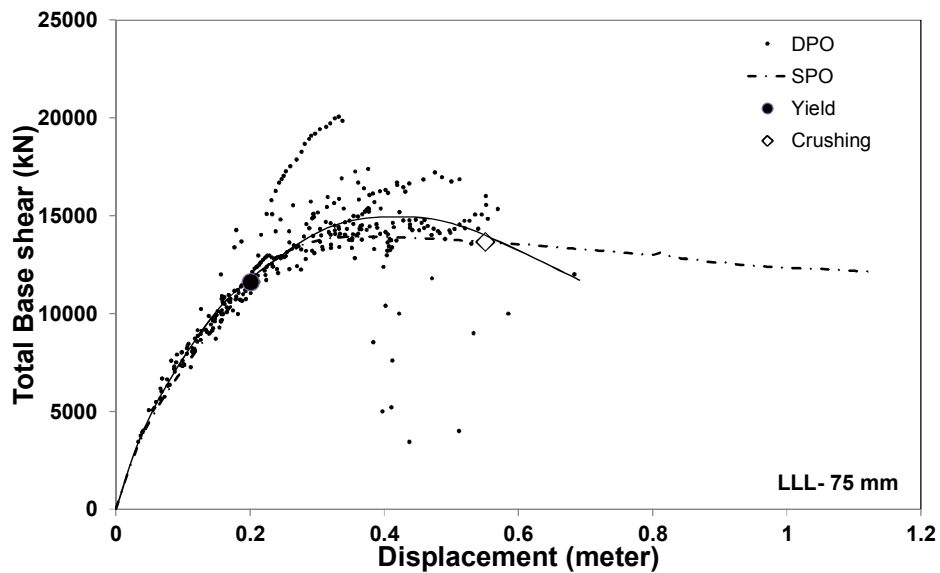
Figure 4-12. Dynamic and static pushover curve for LLL with columns of 75 mm tie spacing.
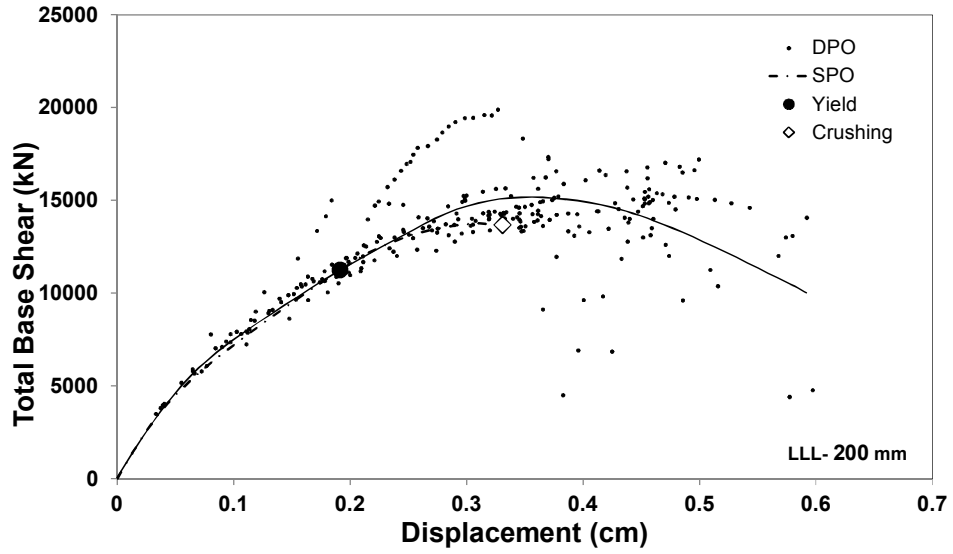
Figure 4-13. Dynamic and static pushover curve for LLL with columns of 200 mm tie spacing.
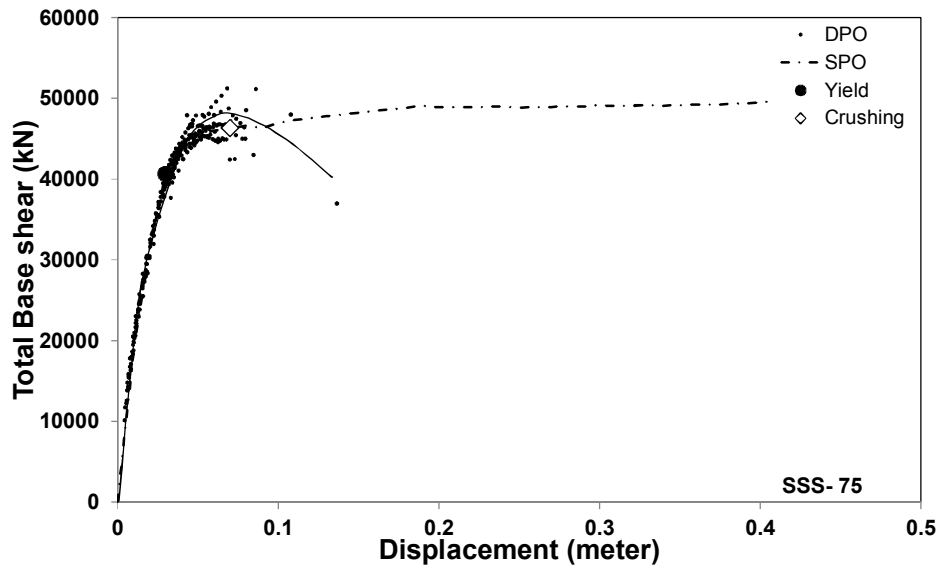
Figure 4-14. Dynamic and static pushover curve for SSS with columns of 75 mm tie spacing.
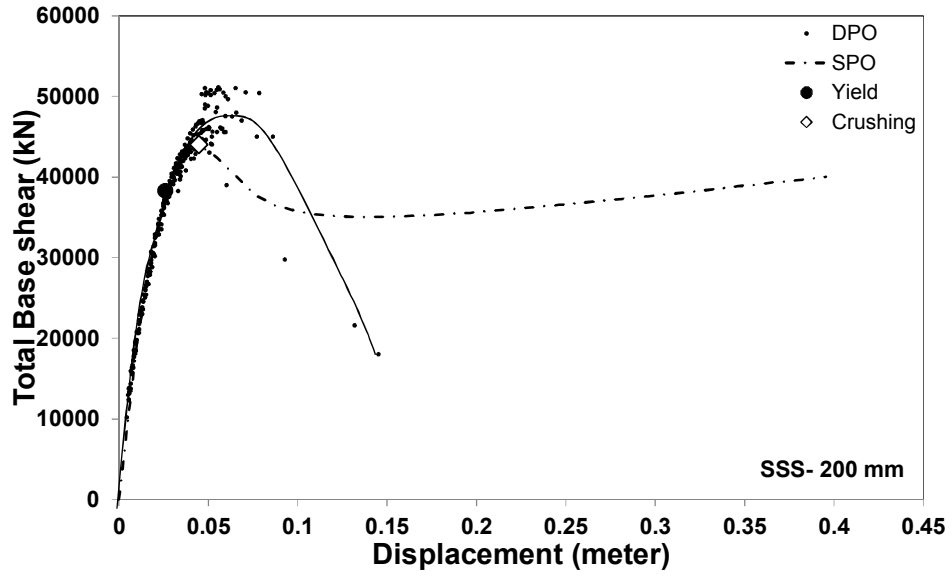
Figure 4-15. Dynamic and static pushover curve for SSS with columns of 200 mm tie spacing.
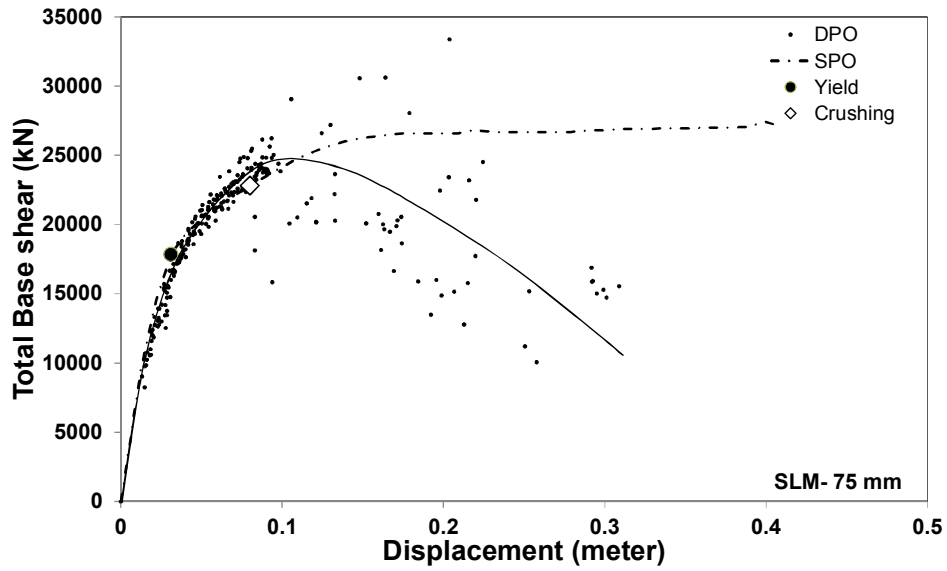
Figure 4-16. Dynamic and static pushover curve for SLM with columns of 75 mm tie spacing.
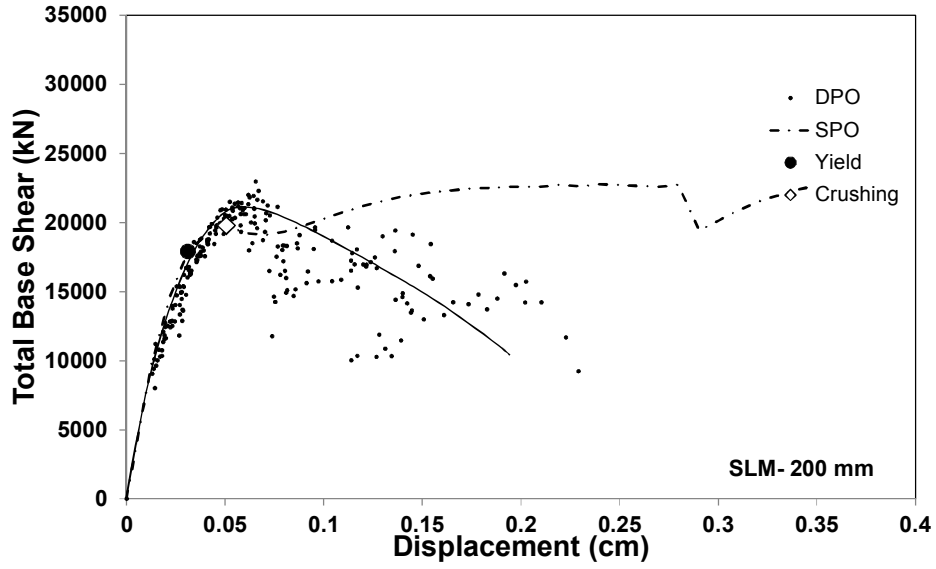
Figure 4-17. Dynamic and static pushover curve for SLM with columns of 200 mm tie spacing.
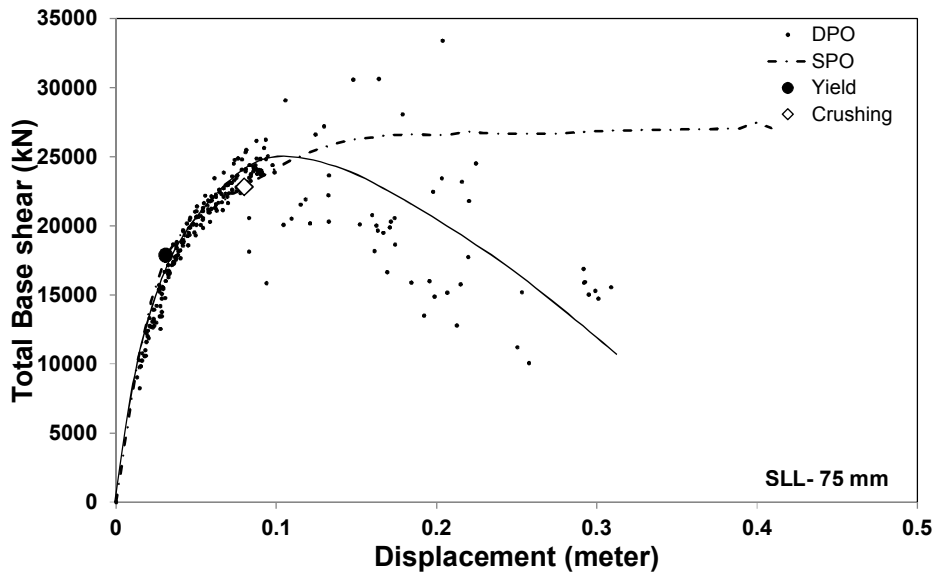
Figure 4-18. Dynamic and static pushover curve for SLL with columns of 75 mm tie spacing.
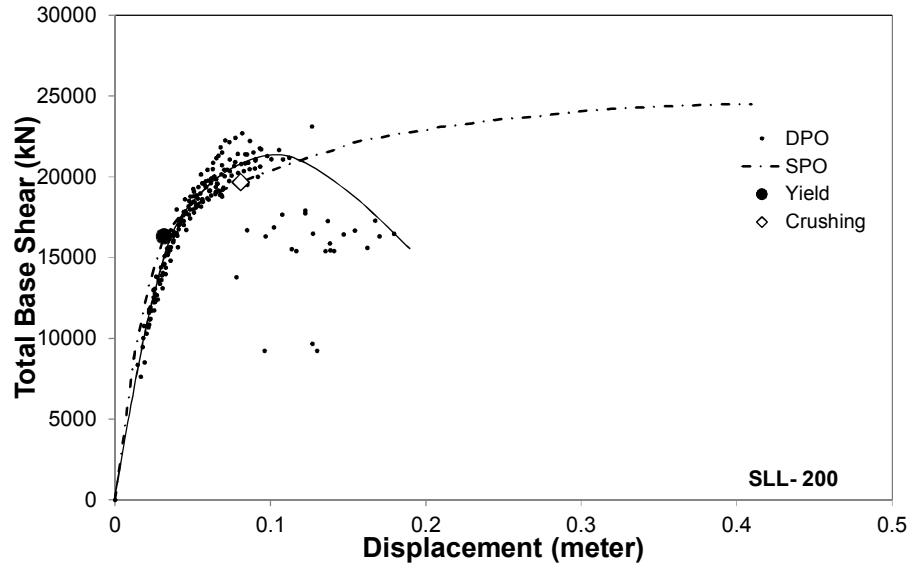
Figure 4-19. Dynamic and static pushover curve for SLL with columns of 200 mm tie spacing.

4.6 FRAGILITY ANALYSIS

Fragility curves represent the probability of reaching or exceeding a certain damage level of a structure under the earthquake ground motion excitation. Fragility curves can be generated empirically or analytically. The empirical fragility curves are generated by surveying bridge conditions after earthquakes, which is often impractical due to the lack of damage data (Padget and DesRoches 2008). In the analytical method of fragility analysis, linear/nonlinear time-history analyses can be utilized (Hwang et al. 2001, Choi et al. 2004, Mackie and Stojadinovic, 2004). In this study, the effect of irregularity in column heights and effect of tie spacing have been observed by deriving the analytical fragility curves by probabilistic seismic demand model (PSDM) with IDA results for bridges with two regular and two irregular column height combinations with two different tie spacing of 75 mm and 200 mm.

4.6.1 Characterization of Damage States

In order to develop the fragility curves, the damage states need to be established. Different damage criteria have been established in order to assess the bridge condition, for example, column drift ratio (Dutta and Mander 1999), energy dissipation capacity and ductility demand (Park and Ang 1985, Caltrans 2004) etc. In this study, four damage states have been taken: slight damage, moderate damage, extensive damage and collapse. Ductility has been taken as the engineering demand parameter (EDP) for each damage state as specified in Hwang et al. 2001 for RC bridge column.

4.6.2 Fragility Function Methodology

The probabilistic seismic demand model (*PSDM*) can be obtained by the scaling approach (Zhang and Huo 2009) or by the cloud approach (Choi et al. 2004; Nielson and Desroches 2007). In this study, the cloud method has been used in order to evaluate the seismic fragility functions of the four span bridges with different column height combinations and various tie spacing.

Ductility and PGA have been considered as the engineering demand parameters (*EDP*) and the ground intensity measures (*IM*), respectively. A correlation between *EDP* and *IM* is to be established in the *PSDM*. Cornell et al. (2002) gives a logarithmic correlation between median *EDP* and selected *IM*:

$$EDP = a\ (IM)^b\ \ or,\ \ ln\ (EDP) = ln\ (a) + b\ ln\ (IM) \tag{4-1}$$

where, *a* and *b* are regression coefficients as shown in Figure 4-20. Table 4-6 shows the values of *a* and *b* for bridges with column height combinations of LLL, SSS, SLM and SLL with 75 mm and 200 mm tie spacing.

IDA gives the response of the structure for low to high ground motion intensities. It is necessary to obtain intermediate responses in the cloud approach. The dispersion of the demand, $\beta_{EDP|IM}$, conditioned upon the *IM* can be derived as (Baker and Cornell, 2006):

$$\beta_{EDP|IM} = \sqrt{\frac{\sum_{i=1}^{N}(ln(EDP)-ln(aIM^b))^2}{N-2}} \qquad (4\text{-}2)$$

where, N is the number of data points. $\beta_{EDP|IM}$ for different combinations of bridges are shown in Table 4-6. $\beta_{EDP|IM}$ decreases with the increase of the tie spacing.

Table 4-6. PSDMs for bridges with four different column height combinations with two tie spacings.

Column combination	*ln (a)*	*b*	$\beta_{EDP|IM}$
LLL- 75	0.655	0.538	0.300
LLL- 200	0.688	0.583	0.226
SSS- 75	1.182	1.111	0.612
SSS- 200	1.180	1.140	0.513
SLM- 75	2.454	1.074	1.113
SLM- 200	2.511	1.102	1.021
SLL- 75	2.454	0.905	1.113
SLL- 200	2.478	0.936	0.943
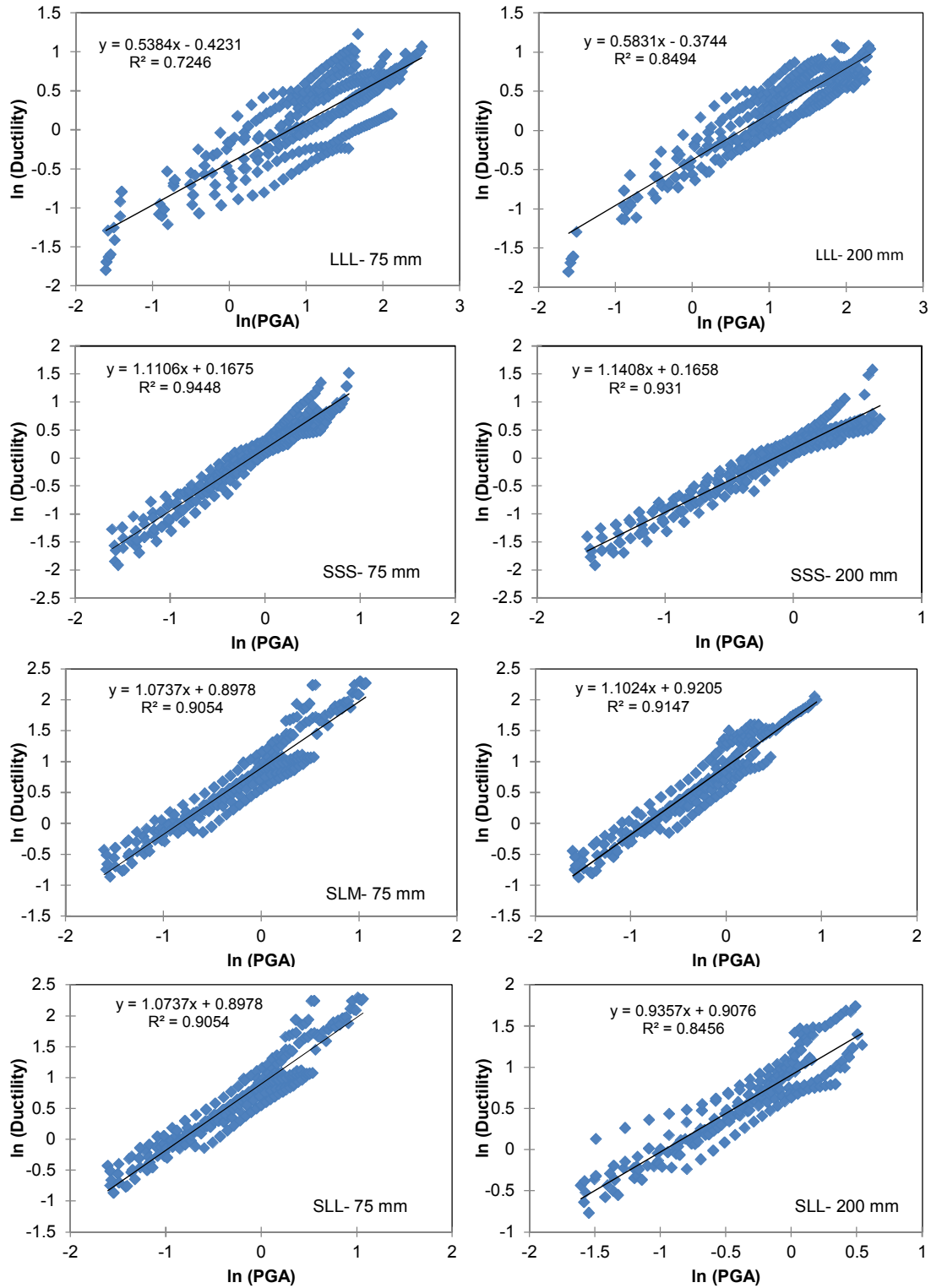
Figure 4-20. Comparison of the PSDMs for LLL, SSS, SLM and SLL for 75 mm and 200 mm tie spacing.

Now, the *PSDM* can be expressed as (Nielson, 2005):

$$P[LS|IM] = \varphi\left[\frac{ln(IM)-ln(IM_n)}{\beta_{comp}}\right]$$
(4-3)

Where, $ln(IM_n)$ is the median value of the intensity measure for the chosen damage state (slight, moderate, extensive, collapse). $ln(IM_n)$ can be derived as

$$ln(IM_n) = \frac{ln(S_c)-ln(a)}{b}$$
(4-4)

and β_{comp}, is the dispersion component, can be determined as

$$\beta_{comp} = \frac{\sqrt{\beta_{EDP|IM}+\beta_c^2}}{b}$$
(4-5)

where, S_c is the median value and β_c is the dispersion of the capacity of the structure. S_c and β_c are the lognormal parameters for damage states. Fragility curves are generated by describing the structural capacity and seismic demand to a lognormal distribution, which represent the probability of reaching or exceeding a specific damage state. S_c and β_c values are given in Table 4-7 for the specified damage state of RC bridges (Hwang et al. 2001).

Table 4-7. Limit states for RC bridge.

Damage state	S_c	β_c
slight	1	0.59
moderate	1.2	0.51
extensive	176	0.64
collapse	4.76	0.65

4.6.3 Fragility Curves Results

The results of the PSDM for bridges with column height combinations of LLL, SSS, SLM and SLL and of two different tie spacing of 75 mm and 200 mm are presented in Figures 4-21 to 4-24 for reaching or exceeding slight, moderate, extensive and collapse damage states. In the case of LLL, the bridge has the lowest probability of damage among all combinations. It can be observed from the fragility curves that the bridges with regular column height combination (SSS, LLL) needs higher intensity of ground motion excitation than the bridges with irregular column heights (SLM, SLL) for reaching the same damage level. Bridges with smaller tie spacing are less vulnerable for all column height combinations, however, the effect of irregularity in column height has been found to have more effect than that of variation in tie spacing from 75mm to 200mm.
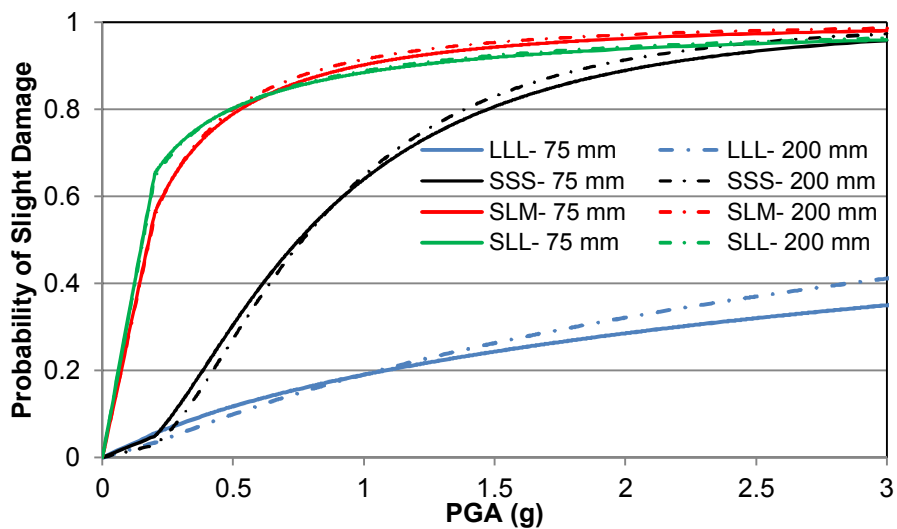
Figure 4-21. Comparison of fragility curves for bridges with different column height combinations for 75 mm and 200 mm tie spacing for slight damage.
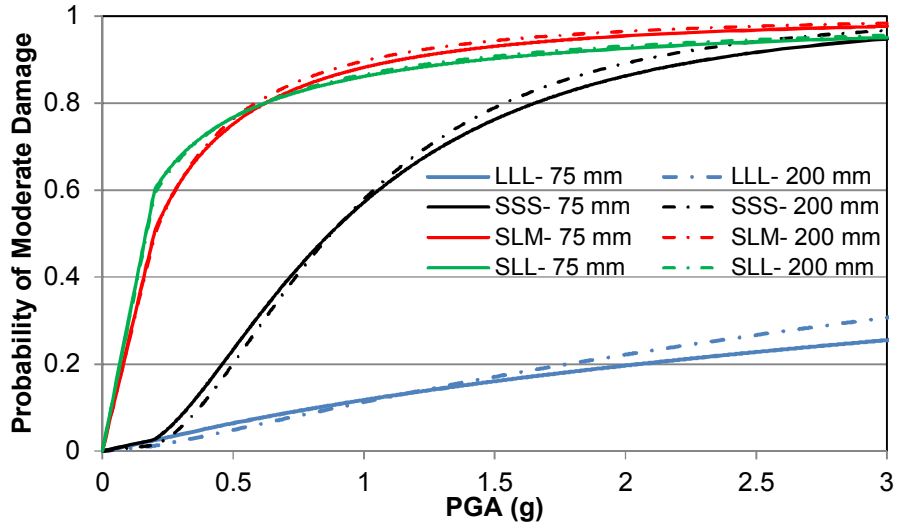
Figure 4-22. Comparison of fragility curves for bridges with different column height combinations for 75 mm and 200 mm tie spacing for moderate damage.
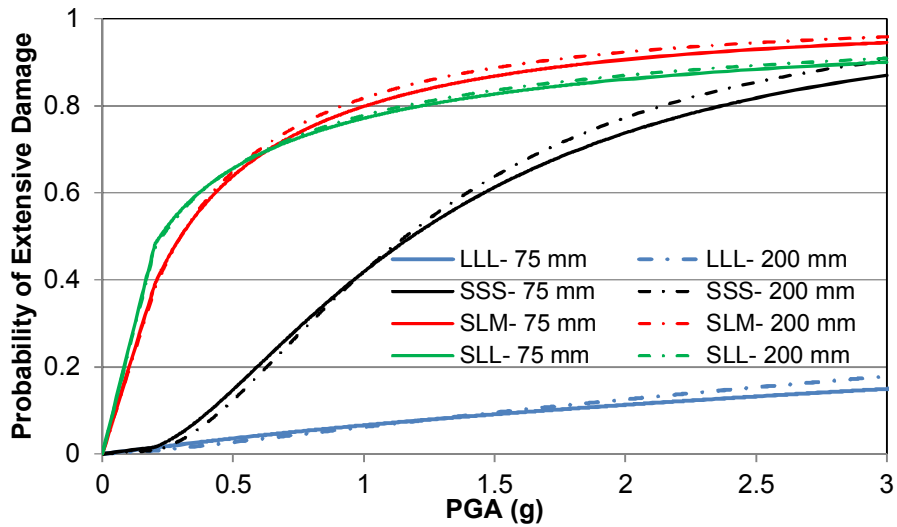
Figure 4-23. Comparison of fragility curves for bridges with different column height combinations for 75 mm and 200 mm tie spacing for extensive damage.
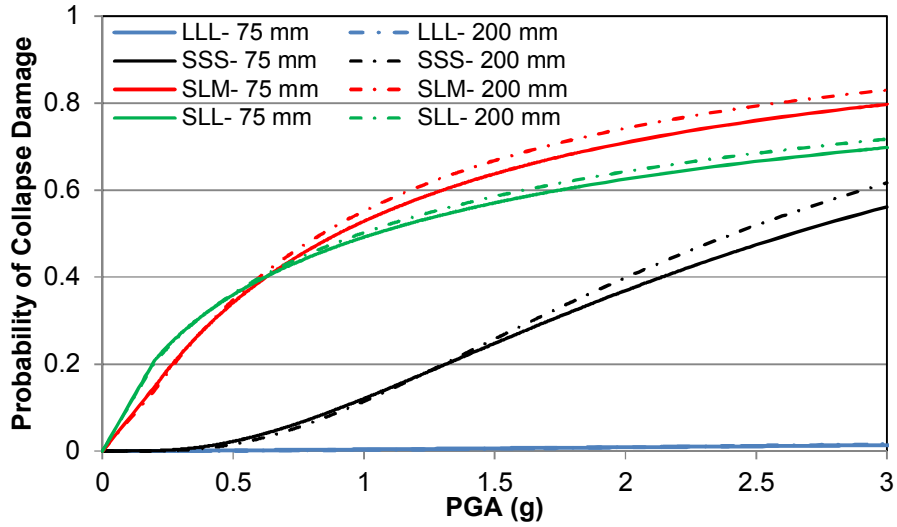
Figure 4-24. Comparison of fragility curves for bridges with different column height combinations for 75 mm and 200 mm tie spacing for collapse damage.

4.7 SUMMARY

In this study, static pushover analyses and incremental dynamic analyses have been conducted for bridges in longitudinal direction considering irregularity in column height with varying tie spacing in bridge column. This study included the comparison of SPO and DPO, and the development of fragility curves show the effect of irregularity in column heights and tie spacing on the seismic performance of bridges.

CHAPTER 5: COMPARISON OF DIRECT DISPLACEMENT-BASED DESIGN AND FORCE-BASED DESIGN IN CANADIAN CONTEXTS

5.1 GENERAL

Economic bridge design is a great challenge, especially in an earthquake prone zone while ensuring safety. Canadian Highway Bridge Design Code (CHBDC 2010) and AASHTO 2007, like other traditional design codes follow force-based design (FBD) method, which is focused at the target force resistance capacity of the structure. On the other hand, displacement-based design approach aims to ensure a target maximum displacement of the bridge during the earthquake in a specific zone. In this study, the columns of a bridge with irregular column heights have been designed according to direct displacement-based design (DDBD) method and FBD as per Canadian standards and AASHTO 2007 considering seismic loading. Seismic performances of the bridge designed in two different methods have been compared by non-linear dynamic analyses in the longitudinal direction in terms of maximum and residual displacements and energy dissipation capacity. This study outlines the necessity of possible modification in the current Canadian seismic design standards as well as displacement-based design for bridges with irregular column heights.

5.2 SAMPLE BRIDGE

A box girder highway bridge having four equal spans of 50 m with varying column heights has been considered in this study. The bridge is assumed to be located in Vancouver, BC, Canada. Figure 5-1 shows the column height irregularity considered in this study. The height of the middle column is 21 m and the heights of the side columns are 7 m and 14 m, respectively as

shown in Figure 5-1. The columns have been designed for the seismic loading in the longitudinal direction. Table 5-1 shows the property of the bridge superstructure. Supports at the abutments are considered to be fixed in the transverse and vertical directions; however, the longitudinal direction is considered as free. The support at the base as well as column-deck connection of each column is considered as fixed. Uniformly distributed mass of 11.1 tonne/m and 20.2 tonne/m have been assigned to the column and deck, respectively. Compressive strength of concrete and yield strength of steel used in this study are 35 MPa and 400 MPa, respectively.
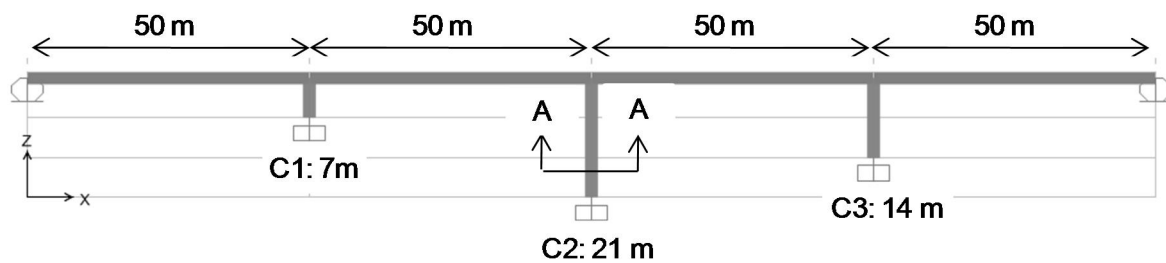
Figure 5-1. Elevation of the bridge with irregular column heights.

Table 5-1. Sectional properties of bridge deck.

EA (kN)	EI2 (kN-m^2)	EI3 (kN-m^2)	GJ (kN-m^2)
2.0187 x 10^8	1.4926 x 10^8	2.3198 x 10^9	1.9748 x 10^8

5.3 BRIDGE COLUMN DESIGN

Design moment and shear of the columns of the sample bridge have been determined according to DDBD and FBD. The design procedures of these two methods are shown in Figure 5-2. The longitudinal reinforcement has been designed from the bending moment demand. Shear resistance of the column section has been checked using Modified Compression Field Theory

(Vecchio and Collins 1986), which predicts the experimentally determined shear failure within 1% error (Bentz et al. 2006).
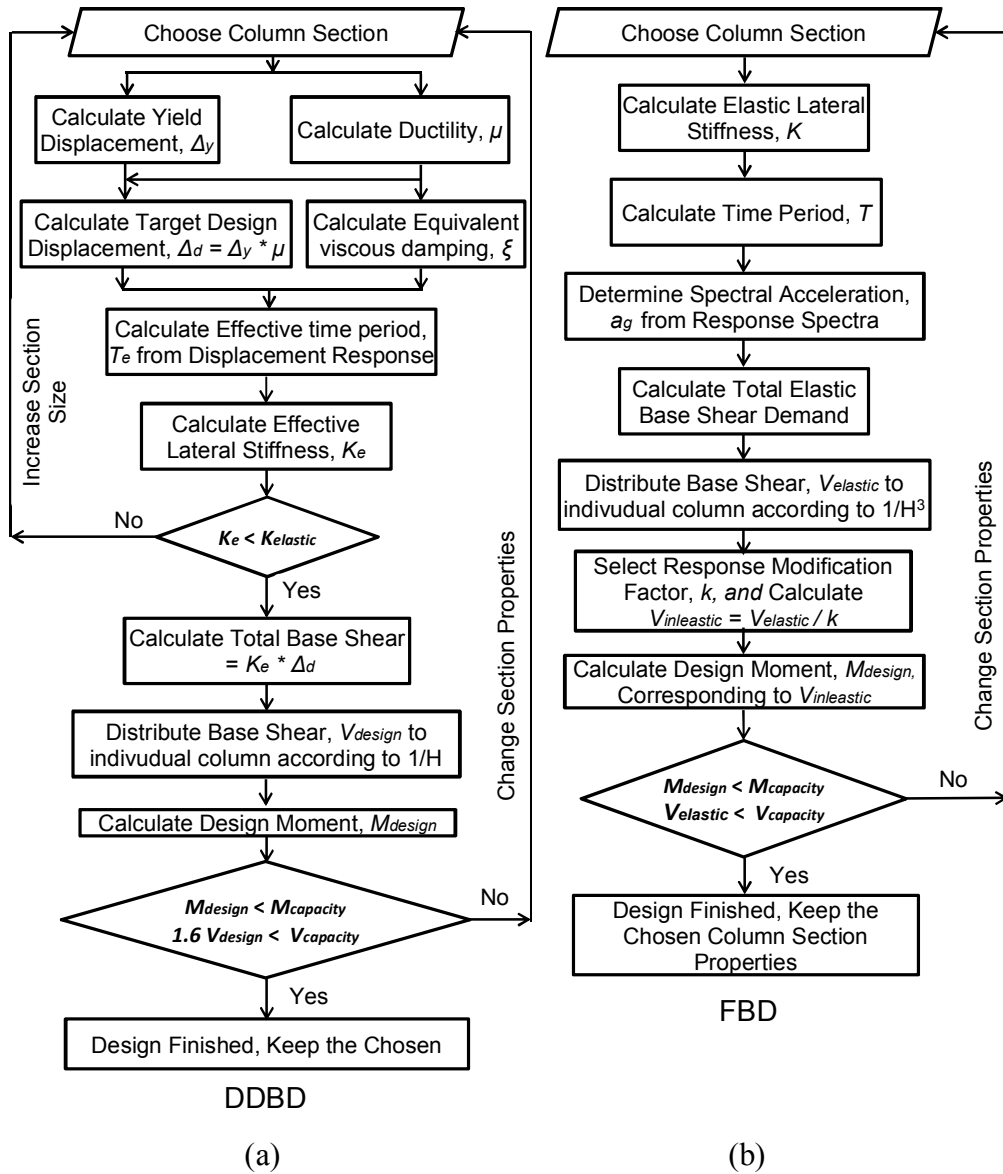
Figure 5-2. Flowcharts showing step by step procedures: (a) displacement-based and (b) force-based design.

5.3.1 Direct Displacement-Based Design (DDBD)

In displacement-based approach, a target displacement and effective stiffness of the bridge have to be determined in order to calculate the base shear demand. The procedure described in Priestley et al. (2007) has been adopted in this study. In DDBD a number of design solutions are possible by choosing column section size and level of ductility. Therefore, the designer has options in choosing column size and tie spacing. In this study 3m x 1.5m section is chosen. Since column C1 is the shortest column, the yield displacement and target displacement of the bridge are governed by the column, C1. From section size, the yield displacement has been found to be 22.9 mm. Confinement reinforcement in C1 is provided as 12mm tie @ 135 mm c/c, the target displacement for damage control limit state is found to be 111.8 mm. Therefore, the corresponding ductility for C1, C2 and C3 are 4.89, 0.54 and 1.22, respectively. Hence, the equivalent viscous damping ratio of an individual column has been derived as per equation 5-1 (Priestley et al., 2007).

$$\xi_{eq} = 0.05 + 0.444 \left(\frac{\mu - 1}{\pi \, \mu} \right) \qquad\qquad (5\text{-}1)$$

Here, the first part of the equation is for 5% material damping of concrete and the second part is for hysteresis damping, calculated from ductility (μ). The equivalent viscous damping ratios for C1, C2 and C3 have been found to be 0.162, 0.05 and 0.076 respectively. The equivalent viscous damping ratio for the whole system is derived according to equation 5-2.

$$\xi_{sys} = \frac{\sum_m V_i \xi_i}{\sum_m V_i} \qquad\qquad (5\text{-}2)$$

Where, V_i is the distributed base shear in each column. Base shear distribution in the column is proportional to the inverse of the column height in DDBD. The equivalent viscous

damping of the bridge has been found to be 11.83%. The displacement spectra for Vancouver at 11.83% damping has been derived by applying the spectral reduction factor (equation 3) to the 5% damped displacement spectrum, as show in Figure 5-3.

$$R_\xi = \left(\frac{0.07}{0.02+\xi_{sys}} \right)^{0.5} \tag{5-3}$$

The effective time period (T_e) of the system for the target displacement of 111.83 mm is 1.747 sec, which is determined from the displacement response spectrum of Vancouver. The effective weight (W_e) of the bridge is 101,043 kN. The effective stiffness of the structure has been determined according to equation 5-4.

$$K_e = \frac{4\pi^2 W_e}{gT_e^2} = 133,363 \text{ kN/m} \tag{5-4}$$

Displacement Response Spectra
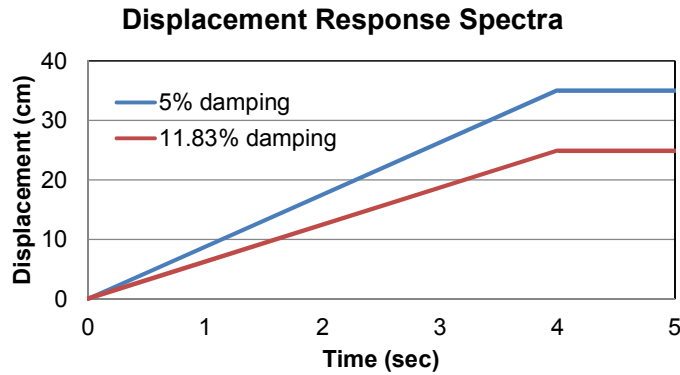
Figure 5-3. Design displacement spectra for Vancouver.

Total base shear demand has been calculated as 14,912 kN by multiplying the effective stiffness and the target displacement. This base shear is distributed to each column in inverse proportion to the height of the column. Therefore, columns will be subjected to equal bending moments, which leads to equal design longitudinal reinforcement. The design base shear and bending moment in each column is given in Table 5-2. The design reinforcement is provided in

Table 5-3. Design longitudinal reinforcement for each column is 92-35 mm bar. The shear capacity of the column should be greater than 1.6 times the base shear corresponding to the design moment (Wang et al. 2008). Tie bar for C1 is 12mm-135 mm c/c as mentioned previously. The required lateral reinforcement in C2 and C3 are 12 mm at 600 mm and 400 mm, respectively. Due to lower ductility demand and lower base shear demand, the required lateral reinforcements in C2 and C3 are low. However, tie spacing more than 300 mm is not very common. The maximum tie spacing allowed in CHBDC 2010 is 150 mm whereas there is no strict guideline for DDBD. Therefore, the comparison between DDBD and FDB are as following:

i)   Bridge designed as per DDBD where longitudinal and lateral reinforcements are governed by flexure and shear demand

ii)   Bridge designed as per DDBD for longitudinal rebar; however, with limited tie spacing as specified in CHBDC (2010)

iii) Bridge designed as per DDBD for longitudinal rebar; however, an intermediate tie spacing of 144 mm has been selected between 135 mm and 150 mm.

5.3.2 Force Based Design (FBD)

The base shear demand has been computed through elastic response spectrum analysis, which has been conducted considering the acceleration response spectrum of Vancouver (NBCC 2010). Elastic response spectrum analysis is performed by calculating the elastic base shear demand for the natural period of the bridge. The response spectrum for Vancouver is shown in Figure 5-4. The initial stiffness and natural period of the bridge in longitudinal direction have been determined as 576,276 kN/m and 0.84 sec, respectively. The elastic base shear demand has

been calculated as 30,102 kN by multiplying the mass of the bridge with the spectral acceleration corresponding to the natural period of the structure. According to CHBDC 2010, the response modification factor (R) is 3. Therefore, the inelastic base shear demand is one third of the elastic base shear demand. Inelastic base shear demand is 10,034 kN. The total base shear has been distributed to each of the three columns according to their initial stiffness, which is given in Table 5-2. The design reinforcement for the columns is given in Table 5-3. The shear capacity of the column should be greater than the elastic shear load (CHBDC 2010). The longitudinal reinforcement in column C1 is 92-35 mm bars with 12 mm tie bar at 55 mm c/c. Minimum 1% reinforcement governs in columns C2 and C3 for design of longitudinal reinforcement. Maximum 150 mm spacing has been provided for 10 mm tie bar, used for the longitudinal bars of 25 mm, at each alternate longitudinal bar. According to CHBDC 2010 the maximum tie spacing is the smallest of six times the longitudinal bar diameter or 0.25 times the minimum component dimension or 150 mm and tie should cover every longitudinal bar.
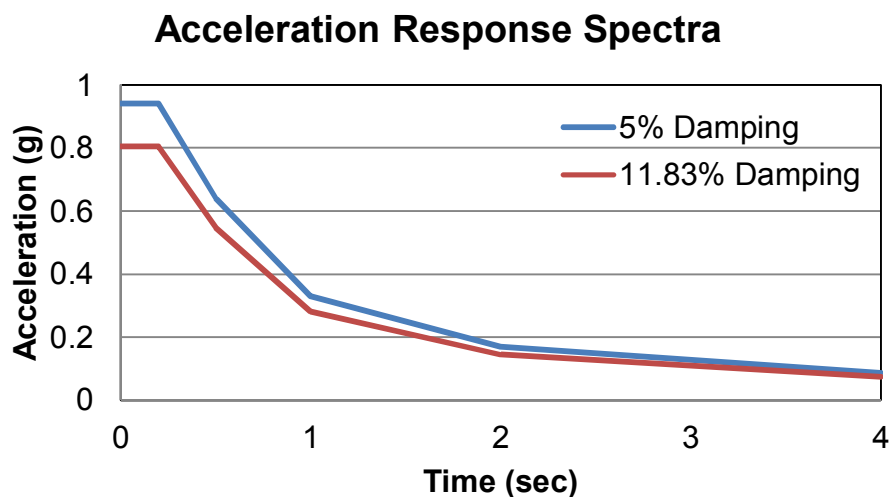
Figure 5-4. Design acceleration spectra for Vancouver.

Table 5-2. Design shear and moment in columns.

Design Method	C1		C2		C3	
	V (kN)	M (kN-m)	V (kN)	M (kN-m)	V (kN)	M (kN-m)
DDBD	8606	30122	2869	30122	4303	30122
FBD	25905	30223	960	3358	3237	7556

Table 5-3. Design reinforcement in columns.

		DDBD (Direct Displacement-Based Design)	DDBD (Tie Spacing Limited by CHBDC)	DDBD (Equal Tie Spacing in Columns)	FBD (Force-Based Design)
	C1	92-35 mm Tie bar 12mm-135 mm c/c	92-35 mm Tie bar 12mm-135 mm c/c	92-35 mm Tie bar 12mm-144 mm c/c	92-35 mm Tie bar 12mm-55mm c/c
	C2	92-35 mm Tie bar 12mm-400 mm c/c	92-35 mm Tie bar 12mm-150 mm c/c	92-35 mm Tie bar 12mm-144 mm c/c	92-25 mm Tie bar 10 mm-150mm c/c
	C3	92-35 mm Tie bar 12mm-600 mm c/c	92-35 mm Tie bar 12mm-150 mm c/c	92-35 mm Tie bar 12mm-144 mm c/c	92-25 mm Tie bar 10 mm-150mm c/c

3.0 m

1.5 m

A-A
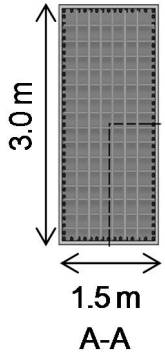
5.3.3 Comparison between DDBD and FBD

For bridges with irregular column heights, the distribution of total base shear demands for flexure and shear design of columns are different in DDBD and FBD. In DDBD the total base shear in an individual column is inversely proportional to the column height, resulting equal bending moment demand in each column, which can be expressed as

$$V_i = \frac{1/H_i}{1/H_1 + \cdots + 1/H_n} V \qquad (5\text{-}5)$$

Where, V_i is the base shear of an individual column and V is the total base shear and H_i is the height of the column. Therefore, the longitudinal reinforcement for each column is the same.

77

However, in FBD, the base shear distribution is inversely proportional to the cube of the column heights (equation 5-6), resulting design moments in the columns are inversely proportional to the square of the column heights

$$V_i = \frac{1/H_i{}^3}{1/H_1{}^3 + \cdots + 1/H_n{}^3} \, V \qquad (5\text{-}6)$$

As per FBD, the required amount of longitudinal reinforcement is significantly less in longer column than shorter columns compared to that of DDBD. In case of this bridge, the amount of longitudinal reinforcement in the longer columns is governed by the minimum steel-concrete ratio of 1%. Therefore, longitudinal reinforcement in the longer columns is higher than required. The main differences in the two design methods include:

a) DDBD considers 1.6 times the base shear corresponding to the design moments and FBD takes the elastic base shear demand according to Canadian Code, which ensures a conservative design for shear resistance;

b) In the case of shear design, base shear in the 7 m column has been 88% more for FBD than that of DDBD design, which causes 59% smaller tie spacing in FBD than the DDBD. However, in cases of 14 m and 21 m columns base shears in FBD are 52% and 79% lower, respectively than those in DDBD. The tie spacing in longer columns has been limited by the Canadian code. Since, DDBD does not have any upper limit for tie spacing; the required tie spacing in longer columns have been found even more than 300 mm.

5.4 NON-LINEAR DYNAMIC ANALYSIS

Non-linear dynamic time history analysis (NTHA) involves with higher computational cost than the other methods of structural performance evaluation, for example capacity spectrum

method (ATC 40). However, this method gives an accurate response of a structure subjected to a particular ground motion. In order to evaluate the dynamic performances of the three DDBD and one FBD bridges finite element models have been generated in SeismoStruct (2010), which is based on the fiber modeling approach. NTHA has been used for the simulation of bridge response to the selected earthquake ground motions.

5.4.1 Selection and Scaling of Ground Motions

The structural response depends on the ground motion properties of the earthquake, which can vary in a wide range in terms of predominant period, peak ground acceleration (PGA), peak ground velocity (PGV) and duration. Since, the upcoming earthquake characteristics in any area is truly unpredictable, a set of earthquake ground motions is generally selected containing a different ground motion characteristics in order to predict the worst structural response through NTHA. In this study, an ensemble of seventeen ground motion records has been selected. The properties of these ground motions are provided in Table 5-4. The predominant period of the structure is varied from 0.09 to 4.55 sec, whereas, the PGA varies from 0.22 to 0.73 g. The acceleration spectra of the ground motions are shown in Figure 5-5. Since, the bridges have been designed for Vancouver region involving firm soil with 10% probability of exceedance in fifty years, the original earthquake ground motions need to be scaled to fit the design spectra of Vancouver for 5% damping, which is shown in Figure 5-3. In this study, the earthquake ground motions have been scaled using the method proposed by Shome et al. (1998). In this method, scaling factor for each ground motion is determined so that the spectral acceleration of that ground motion matches to the design spectral acceleration at the first-mode period of the structure. The first modal periods for the bridges designed in DDBD and FBD are 0.692 and 0.696 sec respectively, which are very close. The scale factors have been determined at the

spectral period of 0.69 s. Figures 5-5 and 5-6 show the acceleration spectra for original and scaled ground motions, respectively. The spectral acceleration of scaled ground motions merge at the period of 0.69 sec.
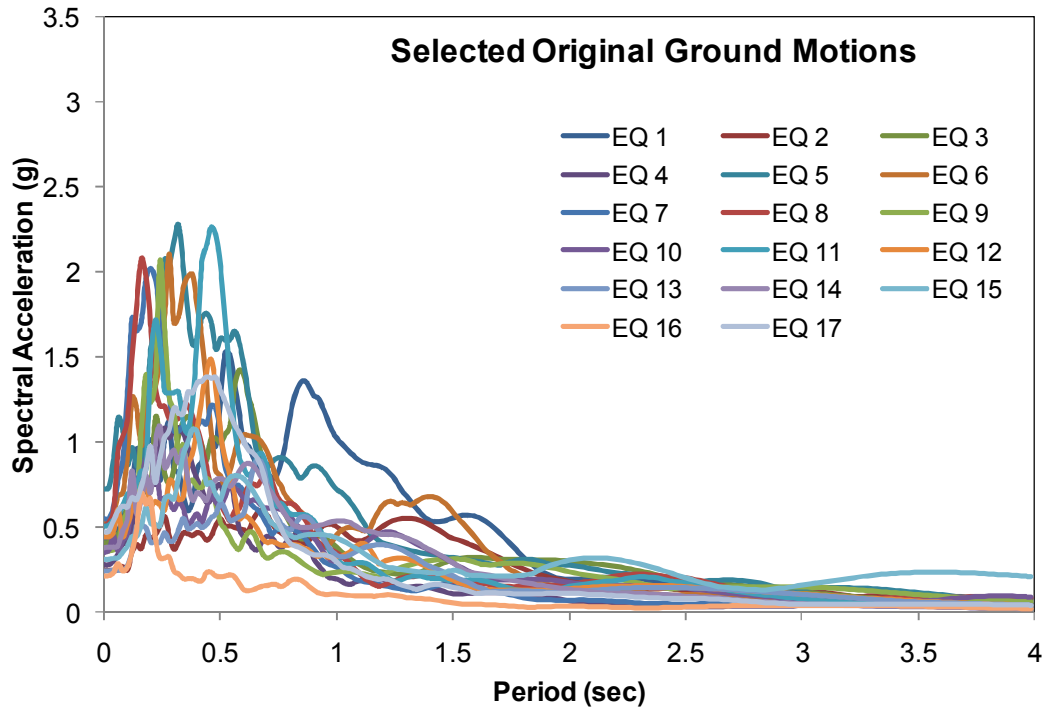
Figure 5-5. Spectral acceleration for original earthquake ground motions.
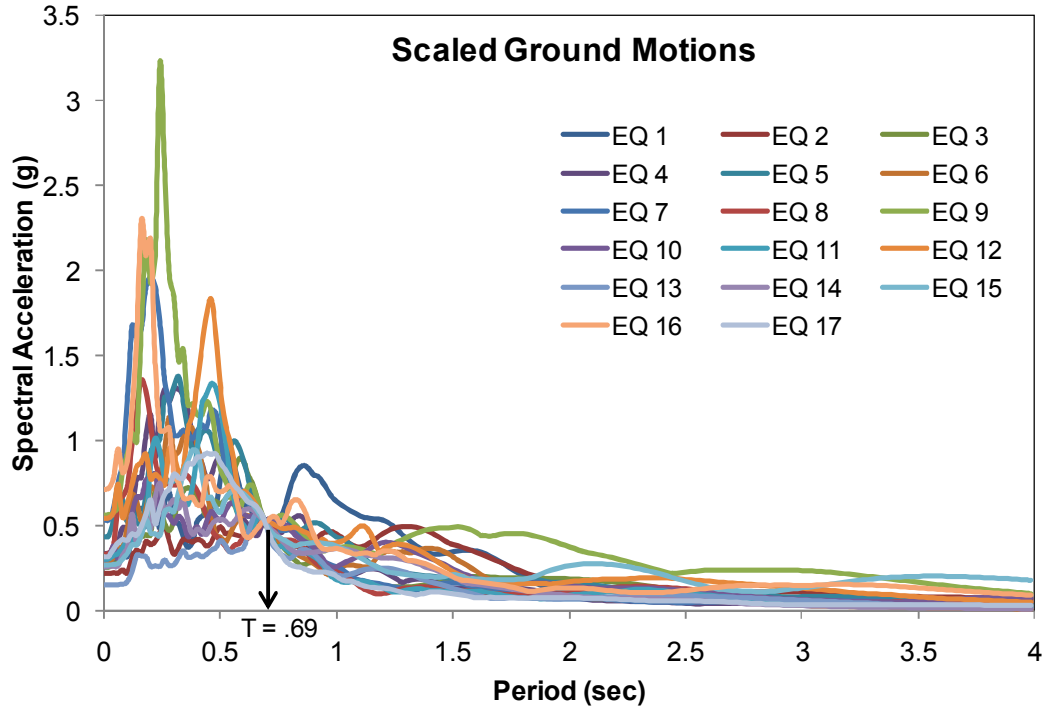
Figure 5-6. Spectral acceleration for scaled earthquake ground motions.

5.4.2 Time History Analysis Results

Longitudinal responses of the bridge have been simulated by NTHA using SeismoStruct (2010) for 17 scaled ground motions. Collapse of bridge in time history analysis is defined for instability or exceeding the 5% drift (Dutta and Mander 1998) of the column. The FBD bridge collapsed for the scaled ground motion of EQ 2. The DDBD bridge collapsed in EQ 2 and 9. The DDBD bridge with limited tie spacing and equal tie spacing of 144 mm survived all 17 earthquakes. Maximum displacement demand, residual displacement and energy dissipation have been set as the parameters in order to compare the seismic performance of the bridges designed in two methods. In order to compare between the four cases; mean (μ) and standard deviation (σ) have been determined for these parameters excluding EQs 2 and 9, since collapse occurred in some of these cases in these two earthquake ground motions. Mean plus standard deviation and mean plus twice standard deviation represents 68% and 95% data are within the limit.

Table 5-4. Earthquake ground motion properties.

No	Earthquake			Recording Station	Epicentral Distance (km)	PGA (g)	PGV (cm/s.)	Predominant Period (s)
	M	Year	Name	Name				
EQ1	6.7	1994	Northridge	Beverly Hills - Mulhol	13.3	0.42	58.95	0.759
EQ2	7.3	1992	Landers	Yermo Fire Station	86	0.24	52	4.551
EQ3	6.7	1994	Northridge	Canyon Country-WLC	26.5	0.41	42.97	0.63
EQ4	7.3	1992	Landers	Coolwater	82.1	0.28	26	0.64
EQ5	7.1	1999	Duzce, Turkey	Bolu	41.3	0.73	56.44	1.078
EQ6	6.9	1989	Loma Prieta	Capitola	9.8	0.53	35	0.683
EQ7	6.9	1989	Loma Prieta	Gilroy Array #3	31.4	0.56	36	0.745
EQ8	7.4	1990	Manjil, Iran	Abbar	40.4	0.51	43	1.781
EQ9	6.5	1979	Imperial Valley	El Centro Array #11	29.4	0.36	34.44	4.096
EQ10	6.5	1987	Superstition Hills	El Centro Imp. Co.	35.8	0.36	46	0.09
EQ11	6.9	1995	Kobe, Japan	Nishi-Akashi	8.7	0.51	37.28	1.28
EQ12	6.7	1994	Nothridge	Rinaldi	7.5	0.38	59.7	0.301
EQ13	6.7	1994	Nothridge	Olive View	6.4	0.72	120	2.341
EQ14	7.0	1992	Cape Mendocino	Rio Dell Overpass	22.7	0.39	44	0.509
EQ15	7.5	1999	Kocaeli, Turkey	Duzce	98.2	0.31	59	0.836
EQ16	7.5	1999	Kocaeli, Turkey	Arcelik	53.7	0.22	17.69	1.205
EQ17	7.6	1999	Chi-Chi, Taiwan	TCU045	77.5	0.47	37	1.205

5.5 PERFORMANCE COMPARISON DDBD AND FBD BRIDGE

The data of maximum and residual displacements and dissipated energy by the bridges have been extracted from the simulated responses to the ground motions, which have been scaled to match the response spectrum of Vancouver. Maximum displacement is the primary indicator of the structural response to an earthquake. Probability of inelastic deformation and damage of the structure increases with the increase of maximum displacement demand. Therefore, the structure with lower maximum displacement is expected to perform better than the structure with higher displacement demand during an earthquake. The residual displacement indicates the level

of damage and reusability of the structure after an earthquake. The higher residual displacement is also involved with higher repair and rehabilitation cost. Energy dissipation capacity of the structure is also an important parameter for seismic performance of the structure. Higher energy dissipation capacity indicates the better ductile behaviour of the structure under dynamic loading. The comparison of the bridges based on these performance criteria are as following.

5.5.1 Maximum Displacement

Figure 5-7 shows the displacement demand comparison between the four cases and the maximum, μ, $\mu + \sigma$ and $\mu + 2\sigma$ values for the ground motion excitations, which did not cause any collapse of the bridges, are given in Table 5-5. Among the three DDBD bridges, the bridge with limited tie spacing has the lowest displacement demand in terms of μ, $\mu + \sigma$ and $\mu + 2\sigma$. The displacement demand of FBD bridge is lower than that of the DDBD bridges, although, it is very close to the original DDBD bridge and DDBD bridge with limited tie spacing. The DDBD bridge with equal tie spacing is the worst among the four bridges.

Table 5-5. Displacement demand of DDBD and FBD bridges from NTHA.

Maximum Displacement (mm)	DDBD	DDBD (Limited tie spacing)	DDBD (Equal Tie spacing of 144 mm)	FBD
Max	151	152	192	143
μ	77	75	80	76
$\mu + \sigma$	103	101	115	101
$\mu + 2\sigma$	128	126	150	125
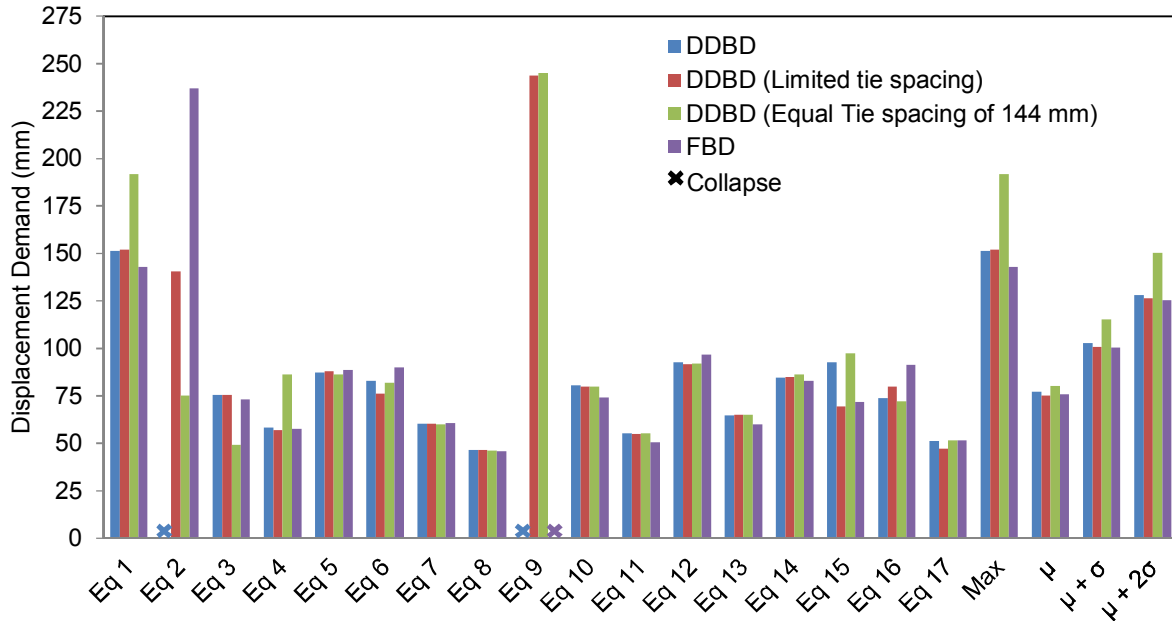
Figure 5-7. Maximum displacement demand of bridges designed in displacement-based and force-based approach.

5.5.2 Residual Displacement

Figure 5-8 shows the residual displacement of bridges under ground motion excitations and the maximum, μ, $\mu + \sigma$ and $\mu + 2\sigma$ values for the ground motion excitations, which did not cause any collapse of the bridges, are given in Table 5-5. The DDBD bridge with limited tie spacing performs the best with respect to residual displacement among the DDBD bridges in terms of μ, $\mu + \sigma$ and $\mu + 2\sigma$. The residual displacement of DDBD bridge with limited tie spacing is less than half of that of the original DDBD bridge, which indicates that, the performance of DDBD bridge can be significantly improved by imposing the maximum allowable tie spacing rule as per Canadian code. Residual displacement is the lowest in the case of FBD bridge, which implies the better capability of FBD bridge to restore its original position.
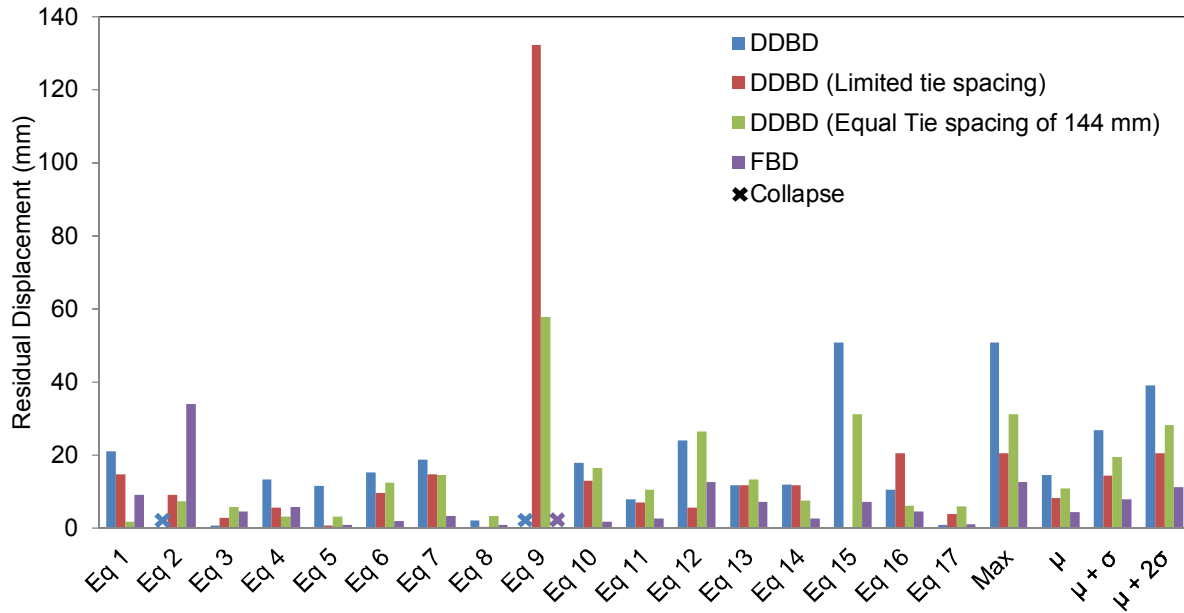
Figure 5-8. Residual displacement of bridges designed in displacement-based and force-based approach.

Table 5-6. Residual displacement of DDBD and FBD bridges from NTHA.

Residual Displacement (mm)	DDBD	DDBD (Limited tie spacing)	DDBD (Equal Tie spacing of 144 mm)	FBD
Max	51	21	31	13
μ	15	8	11	4
$\mu + \sigma$	27	14	19	8
$\mu + 2\sigma$	39	21	28	11

5.5.3 Energy Dissipation

The energy dissipation under seismic loading is maximum in the case of FBD bridge and and the maximum, μ, $\mu + \sigma$ and $\mu + 2\sigma$ values for the ground motion excitations, which did not cause any collapse of the bridges, are given in Table 5-5. The minimum energy dissipation in the case of DDBD bridge with limited tie spacing in terms of μ, $\mu + \sigma$ and $\mu + 2\sigma$, which is shown in Figure 5-9. The FBD bridge shows the highest energy dissipation capacity. However, variation in energy dissipation among the four cases is very low and is less than 6% for μ, $\mu + \sigma$ and $\mu + 2\sigma$.

Table 5-7. Energy dissipation of DDBD and FBD bridges from NTHA.

Energy Dissipation (kN-m)	DDBD	DDBD (Limited tie spacing)	DDBD (Equal Tie spacing of 144 mm)	FBD
Max	5430	5363	4978	5782
μ	2978	2945	2996	3031
$\mu + \sigma$	4200	4081	4121	4257
$\mu + 2\sigma$	5421	5217	5245	5483
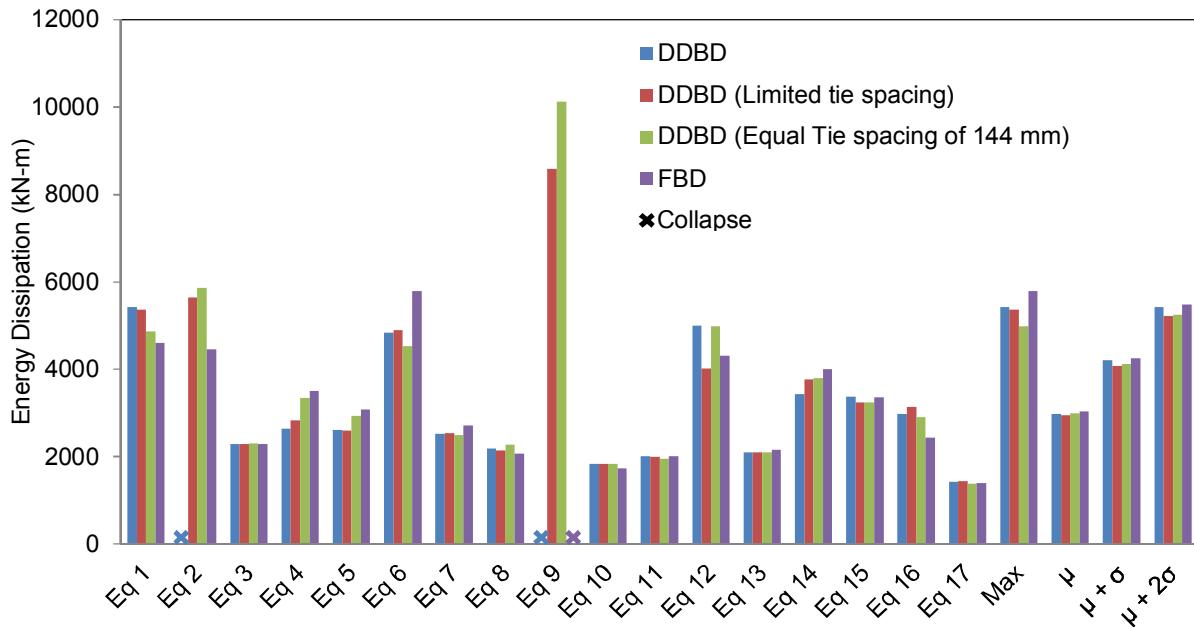
Figure 5-9. Dissipated energy of bridges designed in displacement-based and force-based approach in time history analyses.

5.5.4 Base Shear Demand

Figures 5-10 to 5-12 show the base shear demand in columns C1, C2 and C3, respectively for the ground motion excitations. Base shear demands in each column have been found lower than the shear capacity, therefore, no shear failure has been observed. Since FBD takes the elastic base shear for shear design, the shear capacity of 7 m column in the FBD bridge is more than twice that of the base shear demand; however, the design moment is 23% lower than the

demand. Both of the design base share for shear design and base share corresponding to design moment for 14 m and 21 m column are lower than those of the base shear demands from time history analyses. Since the provided longitudinal and transverse reinforcement in 14 m and 21 m columns are governed by the code specified minimum amount, the actual capacity of these columns are higher than the demand. Therefore, these columns did not fail in the time history analyses. FBD is not accurate in determining the design load in shorter and longer columns. It was observed that the shear capacity of 7 m column in DDBD bridge is 21% higher than the base shear demand. The design moment of 7m column in DDBD is almost equal to that of FBD; however, FBD experienced higher demand by 20% compared to that of DDBD. In longer column, unlike FBD, the design moment as per DDBD is equal to that of shorter column, whereas it is smaller by 24% and 19% in the case of 14 m and 21 m FBD columns compared to that of 7m FBD columns, respectively. The shear capacities of 14 m and 21 m columns in DDBD bridges are 21% and 29% higher than those of the demand base shear, respectively. Hence, the shear capacity for all short and long columns in DDBD is fairly well above the demand, and its moment capacity is slightly lower than the demand, however, this method ensures an even distribution of base shear to the columns of different heights.
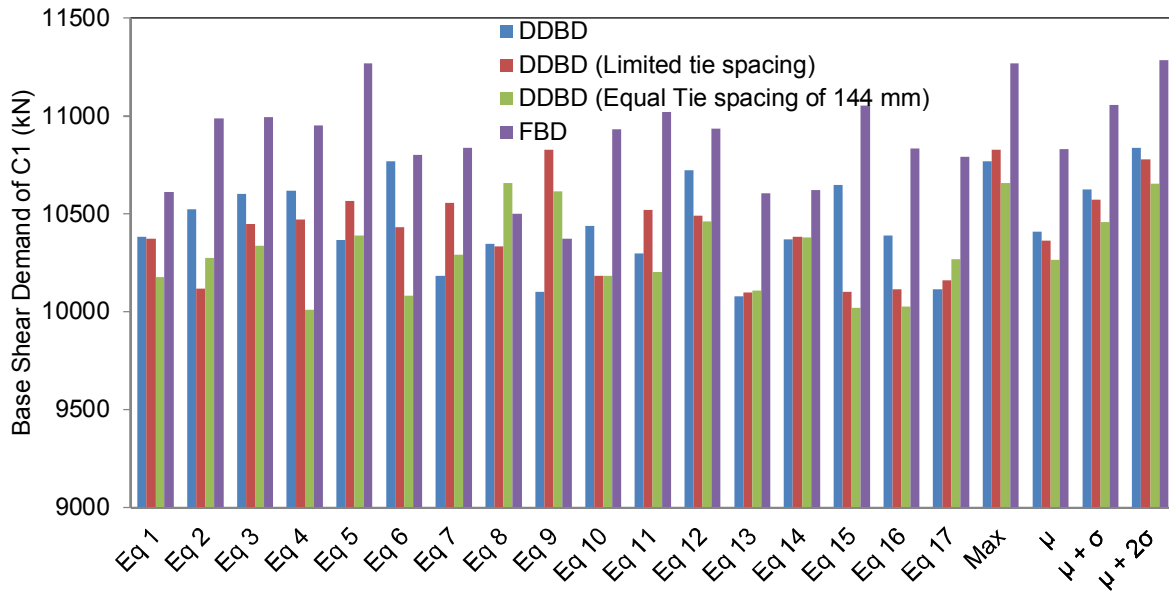
Figure 5-10. Comparison of base shear demand of C1 of bridges designed in displacement-based and force-based approaches through time history analyses.
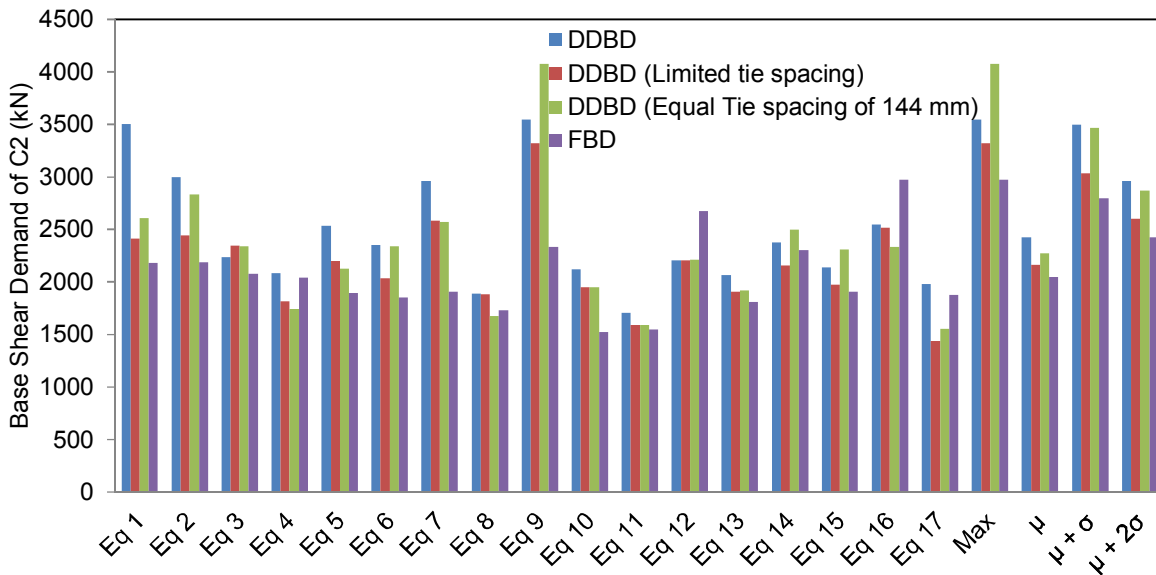
Figure 5-11. Comparison of base shear demand of C2 of bridges designed in displacement-based and force-based approaches through time history analyses.
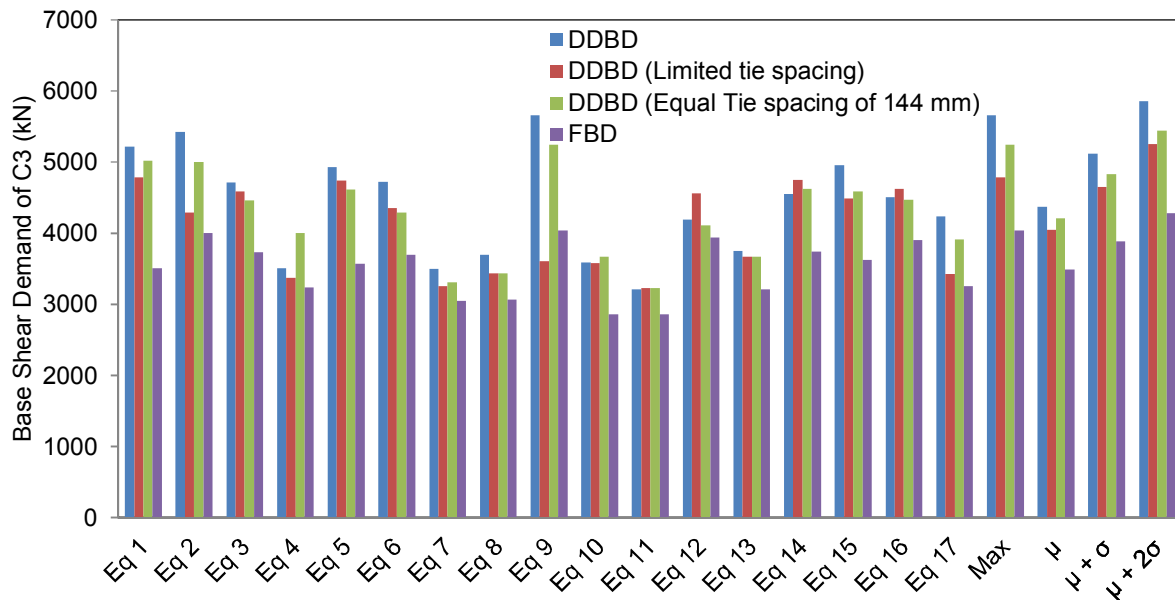
Figure 5-12. Comparison of base shear demand of C3 of bridges designed in displacement-based and force-based approaches through time history analyses.

5.6 DISCUSSION

Results obtained from dynamic time history analysis indicate that the FBD bridge performs better than the DDBD bridges in terms of displacement demand, residual displacement and energy dissipation capacity considering μ, $\mu + \sigma$ and $\mu + 2\sigma$. However, the original DDBD bridge and the FBD bridge experienced collapse under two and one ground motion excitations respectively among the 17 earthquake records. On the other hand, the DDBD bridges with limited tie spacing and equal tie spacing did not fail in any of the earthquake time history analyses. Therefore, the DDBD with limited tie spacing suggested by CHBDC 2010 has been found to be more balanced compared to the other three design methods. It is also observed that the FBD method highly overestimates the base shear for the shortest column in shear design, however, predicts design moment lower than the demand by the same amount of DDBD case.

However, the prediction of base shear for shear design and design moment for the design of longer columns are significantly lower than the demand in the case of FBD method.

5.7 SUMMARY

In this study, an irregular bridge with varying column heights has been designed in conventional force-based approach and displacement-based approach. The limitations of the two methods have been identified by the seismic performance evaluation of the bridges.

CHAPTER 6: CONCLUSIONS

6.1 SUMMARY

This thesis explores the effects of concrete and steel properties, amount of longitudinal reinforcement and confinement on the limit states of single RC bridge piers, which helps understanding the performance of old and modern bridge pier during earthquake events. The combined effect of piers of different heights has been investigated by analyzing the seismic performance of irregular bridges with varying column heights. The effect of tie spacing has been compared with the effect of column height irregularity, which is the most common form of irregularity in bridges considering seismic performance.

This study includes the design of a RC bridge with irregular column height configuration in conventional force-based approach and displacement-based approach. The dynamic performances of these bridges have been assessed in order to identify the limitations of both approaches while designing the bridges with irregular column height combinations.

6.2 LIMITATIONS OF THE STUDY

The main limitations of the current study are

- Only one column cross-section with fixed column ends has been taken for factorial analysis.

- This study only considered continuous bridges with fixed column-deck connection.

- A particular deck property has been taken for bridges.

- Irregular bridge with only one combination of varying column heights has been considered for comparisons between displacement-based and force-based design methods.

6.3 CONCLUSIONS

Based on the results obtained from the factorial analysis, the following conclusions are drawn:

- Columns of 7 m height considered in this study are mostly shear dominated.

- Crushing displacement of flexure dominated column is always greater than its yield displacement resulting ductility greater than one.

- The ductility of a shear dominated column will be greater than one if the displacement due to shear failure is more than the yield displacement. Otherwise, the displacement at shear failure is less than the yield displacement, yield point cannot be reached and the virtual ductility can be calculated with respect to virtual yield displacement, which is less than one.

- The tendency of shifting to flexure dominance from shear dominance increases with the increase of the length of the column.

- Effect of confinement does not have significant effect on the column performance before yielding in flexure dominated cases. However, it has significant effect in plastic zone on crushing displacement and ductility of the column especially for shorter column.

- The effect of tie spacing or confinement is more in high strength concrete.

- The amount of longitudinal reinforcement has significant effect on yield and crushing base shear, but, it has little effect on the yield and crushing displacement for flexure dominated columns.

- Compressive strength of concrete mainly controls the cracking base shear.

- Cracking displacement is not affected by the four factors.

- Three level factorial analyses have been found adequate in order to develop generalized formula to predict cracking limit state, yield limit state and base shear at first crushing or shear capacity, however, have been found inadequate to develop formula in order to predict displacement at first crushing or shear failure and ductility. Higher level factorial analysis is needed to predict the post elastic displacement of the column.

Based on the results obtained from seismic performance evaluation of irregular bridges with varying column heights, the following conclusions can be drawn:

- Effect of confinement has little effect on the first cracking and first yielding limit states.

- Since, the smaller tie spacing increases the effect of confinement; it provides higher base shear capacity for first crushing and increases the ductility of the bridge.

- The bridge with a moderate change in column height performs better than the bridge, which has rapid change in column height.

- Smaller tie spacing helps both regular and irregular bridges to perform better.

- The effect of the order of columns in the bridge with irregular column heights has been found insignificant along longitudinal direction.

- Static pushover curve closely matches with the dynamic pushover curve until the concrete reaches the first crushing strain. Therefore, cracking, yielding and crushing limit states found from static pushover curves are reliable.

- Fragility curve results indicate that the presence of irregularity in column heights and larger tie spacing in columns makes bridges more vulnerable to earthquakes.

Based on the results obtained from DDBD and FBD design of bridges with irregular column heights and different confinements, the following conclusions can be drawn:

- The distribution of base shear to columns of different heights is different in DDBD that results in equal design moments in columns of different heights leading to equal longitudinal reinforcement.

- The distribution of base shear to columns of different heights is different in FBD that predicts higher design base shear in the shortest column, and lower design base shear in longer columns compared to the base shear demands found from non-linear time history analyses. However, the provided longitudinal reinforcements in longer columns are higher than the design moments, since, minimum 1% reinforcement governed.

- FBD takes elastic base shear for shear design, which leads to a large base shear demand and high lateral reinforcement ratio in the shortest column. However, base shear in longer column is small and code specified maximum tie spacing is governed in the longer columns.

- The required tie spacing in 14 m and 21 m columns in DDBD have been found to be 400 mm and 600 mm, respectively. DDBD bridge with tie spacing of longer columns limited by the maximum allowed tie spacing in CSA Standard S6-06 (CSA 2010) has performed better than the original DDBD bridge.

6.4 RECOMMENDATIONS FOR FUTURE RESEARCH

Since the present study considers columns with the same cross-section and end condition in the factorial analysis of limit states, further research is necessary considering columns of different dimensions and fixity conditions in order to normalize the column dimensions and fixity condition in the formula for computation of the limit states.

Further research is required to observe the effect on the unequal span bridges with and without column-deck isolation devices.

Further research is necessary to optimize the base shear distribution to shorter and longer column in FBD and to optimize the maximum allowed tie spacing in longer columns in DDBD considering irregular bridges with various column height combinations.

REFERENCES

Akbari, R. 2010. Cyclic response of Rc continuous span bridges with irregular configuration in longitudinal direction. *Structure and Infrastructure Engineering*, DOI: 10.1080/15732479.2010.510528 1-11.

Alam, M. S., Nehdi, M., and Youssef, M., A. 2009. Seismic performance of concrete frame structures reinforced with superelastic shape memory alloys. *Smart Structures and Systems*, 5(5): 565-585.

Alam, M.S., Youssef, M.A., and Nehdi, M. 2008. Analytical prediction of the seismic behaviour of superelastic shape memory alloy reinforced concrete elements. *Eng. Structures*, 30(12): 3399-3411.

ATC-49, 2003. Recommended LFRD guidelines for the seismic design of highway bridges. MCEER/ATC-49, Applied Technology Council and Multidisciplinary Center for Earthquake Engineering Research, Redwood City, Calif.

Baker J.W. and Cornell, C.A. 2006. Vector-valued ground motion intensity measures for probabilistic seismic demand analysis. PEER report 2006/08. Berkeley: Pacific Earthquake Engineering Research Center, University of California Berkeley.

Bardakis, V. G. and Fardis, M. N. 2010. A displacement-based seismic design procedure for concrete bridges having deck integral with the piers. *Bull Earthquake Eng.*, DOI 10.1007/s10518-010-9215-5.

Bentz, E. C., Vecchio, F. J., and Collins, M. P. 2006. Simplified modified compression field theory for calculating shear strength of reinforced concrete elements. *ACI Structural Journal*, American Concrete Institute, 103(4): 614-624.

Box, G. E. P., Hunter, W. G. and Hunter, J. S. 1978. Statistics for Experimenters. *Wiley and Sons Inc.*, New York.

Boys, A., Bull, D., Pampanin, S. 2008. Seismic performance assessment of inadequately detailed reinforced concrete columns. *New Zealand Society of Earthquake Engineering (NZSEE) Conference*, Wairakei, New Zealand.

Canadian Standards Association (CSA). 1974. Canadian Highway Bridge Design Code. *CSA Standard S6-074*. Canadian Standards Association, Rexdale, Ontario.

CALTRANS, 2004. California Department of Transportation, Seismic Design Criteria, Sacramento, CA.

Calderone, A.J., Lehman, D.E., and Moehle, J.P. 2000. Behavior of reinforced concrete bridge columns having varying aspect ratios and varying lengths of confinement. *Pacific Earthquake Engineering Research Center Report 2000/08*.

California Department of Transportation. 1999. Seismic Design Criteria Version 1.1. *Engineering Service Center, Earthquake Engineering Branch*, Sacramento, CA, July 1999.

Calvi G.M. and Kingsley G.R. 1995. Displacement based seismic design of multi-degree-of-freedom bridge structures. *Earthquake Engineering and Structural Dynamics*, 24(9): 1247-1266.

Canadian Standards Association (CSA). 1978. Canadian highway bridge design code. *CAN3- S6-M78*. Canadian Standards Association, Rexdale, Ontario.

Canadian Standard Association CSA. 2004. Design of concrete structures. *CSA No. A23.3-04*, Mississauga, Canada.

Canadian Standards Association (CSA). 2010. Canadian highway bridge design code. *CAN/CSA S6-06*. Canadian Standards Association, Rexdale, Ontario.

Chen, W., and Duan, L. 2000. Bridge engineering handbook, *CRC Press*.

Choi, E., DesRoches, R. and Nielson, B.G. 2004. Seismic fragility of typical bridges in moderate seismic zones, *Engineering Structures,* 26(2): 187-199.

Cornell A.C., Jalayer, F., and Hamburger, R.O. 2002. Probabilistic basis for 2000 SAC federal emergency management agency steel moment frame guidelines. *Journal of Structural Engineering*; 128:526–532.

Dutta, A. and Mander, J.B. 1999. Seismic fragility analysis of highway bridges, *Proceedings of the Center-to-Center Project Workshop on Earthquake Engineering in Transportation Systems*, Tokyo, Japan.

Fragiadakis, M., and Papadrakakis, M. 2008. Modeling, analysis and reliability of seismically excited structures: computational issues, *International Journal of Computational Methods*, 5(4): 483-511.

Hassoun, M. N. 1998. Structural Concrete: Theory & Design. *Addison-Wesley Publishing Company, Inc.*, 3rd edition.

Hwang, H., Liu, J. B., and Chiu, Y. H. 2001. Seismic fragility analysis of highway bridges. Technical Report, *MAEC RR-4 Project*, Mid-America Earthquake Center.

Kappos, A. and Konstantinidis D. 1999. Statistical analysis of confined high strength concrete. *Materials and Structures*, 32(10): 734-748.

Kappos, A. J., Manolis, G. D. and Moschonas, I. F. 2002. Seismic assessment and design of R/C bridges with irregular configuration, including SSI effects. *Engineering Structures,* 24(10): 1337-1348.

Kowalsky, M. J. 2000. Deformation limit states for circular reinforced concrete bridge columns. *Journal of Structural Engineering*, New York, N.Y., 126(8): 869-878.

Kowalsky M.J., 2002. A Displacement-based approach for the seismic design of continuous concrete bridges, *Earthquake Engineering and Structural Dynamics*, 31(3): 719-747.

Kowalsky M.J., Priestley M.J.N. and MacRae G.A. 1995. Displacement-based design of RC bridge columns in seismic regions, *Earthquake Engineering and Structural Dynamics*, 24(12): 1623-1643.

Luco, N. and Cornell, C. A. 1998. Effects of random connection fractures on the demands and reliability for a three-story pre-Northridge (SMRP) structure, Proc. of the sixth *U.S. National Conf. on Earthquake Eng.*, Earthquake Engineering Research Institute, Oakland, California.

MacGregor, J.G. and Wight, J.K. 2005. Reinforced concrete mechanics and design. *Prentice Hall*, Fourth Edition.

Mackie, K. R, Stojadinovi¢, B. 2004. Fragility curves for reinforced concrete highway overpass bridges, *Proc. of 13th World Conference on Earthquake Engineering*. paper no. 1553.

McDaniel, C. 1997. Scale effects on the shear strength of circular reinforced concrete columns. thesis, presented to University of California, San Diego, in partial fulfillment of the requirements for the degree of Doctor of Philosophy.

Madas, P. 1993. Advanced modelling of composite frames subjected to earthquake loading. thesis, presented to Imperial College, University of London, London, UK, in partial fulfillment of the requirements for the degree of Doctor of Philosophy.

Mander J.B., Priestley, M.J.N., and Park, R. 1988a. Observed stress-strain behavior for confined concrete. *Journal of Structural Engineering*, ASCE, 114(8), 1827-1849.

Mander,J. B., Priestley, M. J. N., and Park, R. 1988b. Theoretical stress-strain model for confined concrete. *Journal of Structural Engineering*, 114(8): 1804-1826, DOI 10.1061/(ASCE)0733-9445(1988)114:8(1804).

Martinez-Rueda, J.E. and Elnashai, A.S. 1997. Confined concrete model under cyclic load. *Materials and Structures*, 30(197): 139-147.

Mitchell, D., Paultre, P., Tinawi, R., Saatcioglu, M., Tremblay, R., Elwood, K.J., Adams, J., DeVall, R. 2010. Evolution of seismic design provisions in the national building code of Canada, *Canadian Journal of Civil Engineering*, 37(9): 1157-1170.

Mitchell, D., Sexsmith, R.G. and Tinawi, T. 1994. Seismic retrofit techniques for bridges- A state of the art report, *Canadian Journal of Civil Engineering* 21(5): 823-835.

Mo, Y. L., and Nien, I. C. 2002. Seismic performance of hollow high-strength concrete bridge columns, *Journal of Bridge Engineering*, ASCE, ISSN 1084-0702/2002/6-338–349, 7(6): 338-349.

Montgomery, D.C. 2001. Design and analysis of experiments. 5th edition, *Wylie and Sons Inc.*, New York.

Monti, G., and Nuti, C. 1992. Nonlinear cyclic behaviour of reinforcing bars including buckling. *Journal of Structural Engineering*, 118(12): 3268-3284.

Moustafa, K. F., Sanders, D., M. Saiidi, M. S., and Saad El-Azazy, S. 2011. Seismic Performance of Reinforced Concrete Bridge Bents. *ACI Structural Journal*, 108(1): 23-33.

Nagashima, T., Sugano, S., Kimura, H., and Ichikawa, A. 1992. Monotonic axial compression tests on ultra high strength concrete tied columns. *Proceedings of the Tenth World Conference on Earthquake Engineering*, Madrid, Spain, 2983-2988.

Nielson, B.G. and DesRoches, R. 2007b. Seismic fragility methodology for highway bridges using a component level approach. *Earthquake Engineering and Structural Dynamics,* 36: 823–839.

NRCC. 1941. National Building Code of Canada, Associate Committee on the National Building Code, *National Research Council of Canada,* Ottawa, ON.

NRCC. 1953. National Building Code of Canada, Associate Committee on the National Building Code, *National Research Council of Canada,* Ottawa, ON.

NRCC. 1960. National Building Code of Canada, Associate Committee on the National Building Code, *National Research Council of Canada,* Ottawa, ON.

NRCC. 1965. National Building Code of Canada, Associate Committee on the National Building Code, *National Research Council of Canada,* Ottawa, ON.

NRCC. 1970. National Building Code of Canada, Associate Committee on the National Building Code, *National Research Council of Canada,* Ottawa, ON.

NRCC. 1975. National Building Code of Canada, Associate Committee on the National Building Code, *National Research Council of Canada,* Ottawa, ON.

NRCC. 1977. National Building Code of Canada, Associate Committee on the National Building Code, *National Research Council of Canada,* Ottawa, ON.

NRCC. 1980. National Building Code of Canada, Associate Committee on the National Building Code, *National Research Council of Canada,* Ottawa, ON.

NRCC. 1985. National Building Code of Canada, Associate Committee on the National Building Code, *National Research Council of Canada,* Ottawa, ON.

NRCC. 1990. National Building Code of Canada, Associate Committee on the National Building Code, *National Research Council of Canada,* Ottawa, ON.

NRCC. 1995. National Building Code of Canada, Associate Committee on the National Building Code, *National Research Council of Canada,* Ottawa, ON.

NRCC. 2005. National Building Code of Canada, Associate Committee on the National Building Code, *National Research Council of Canada,* Ottawa, ON.

NRCC. 2010. National Building Code of Canada, Associate Committee on the National Building Code, *National Research Council of Canada,* Ottawa, ON.

Padgett, J. E. and DesRoches, R. 2006. Comparative study of the seismic performance of retrofitted multi-span steel bridges. *7th International Conference on Short and Medium Span Bridges*, Montreal, Canada.

Ortiz, J. 2006. Displacement-based design of continuous concrete bridges under transverse seismic excitation. European School for Advanced Studies in Reduction of Seismic Risk (ROSE School).

Padgett, J.E., and DesRoches, R. 2008. Methodology for the development of analytical fragility curves for retrofitted bridges. *Earthquake Engineering and Structural Dynamics*, 37: 1157-74.

Papanikolaou, V. K. and Kappos, A. J. 2009. Numerical study of confinement effectiveness in solid and hollow reinforced concrete bridge piers: Methodology. *Computers and Structures,* 87: 1427–1439.

Park, Y.J. and Ang, A.H.S. 1985. Mechanistic seismic damage model for reinforced concrete. *ASCE Journal of Structural Engineering*, 111(4):722–39.

Park, R. and Paulay, T. 1975. Reinforced Concrete Structures. *JhonWiley & Sons Inc*.

Park R, Priestley MJN, Gill, W.D. 1982. Ductility of square confined concrete columns. *J Struct Div*, ASCE; 108(4): 929–90.

Paulay, T. and Priestley, M.J.N. 1992. Seismic design of reinforced concrete and masonry buildings. *J. Wiley*, New York.

Paultre, P., and Légeron, F. 2008. Confinement reinforcement design for reinforced concrete columns. *Journal of Structural Engineering*, ASCE, 134(5), 738–749.

Priestley, M.J.N., Calvi, G. M., and Kowalsky, M. J. 2007. Displacement-based seismic design of structures. *IUSS Press*, Pavia, Italy.

Priestley, M. J. N., Seible, F., and Calvi, G. M. Seismic Design and Retrofit of Bridges. *John Wiley & Sons, Inc.,* New York, 1996.

Ranf, R. T., Nelson, J. M., Price, Z., Eberhard, O. M., and Stanton, J., F. 2006. Damage Accumulation in Lightly Confined Reinforced Concrete Bridge Columns. *Pacific Earthquake Engineering Research Center,* PEER Report 2005/08.

Razvi, S.R., and Saatcioglu, M. 1994. Strength and deformability of confined high-strength concrete columns. *ACI, Struct. J.*, 91(6): 678-687.

Ruth, C., and Zhang, H. 1999. Personal correspondence. *Washington State Department of Transportation (WSDOT)*, Olympia, Washington.

Saatcioglu, M. and Razvi, S. R. 2002. Displacement Based Design of Reinforced Concrete Columns for Confinement. *ACI Structural Journal,* American Concrete Institute, 99(1): 3-11.

Sebai, D. E. 2009. Comparisons of International Seismic Code Provisions for Bridges. thesis, Department of Civil Engineering and Applied Mechanics, McGill University, Montreal, Quebec, Canada.

SeismoStruct. 2010. version 5.0.5, *www.seismosoft.com*.

Senthilvasan, J., Thambiratnam, D. P., and Brameld, G. H. 2002. Dynamic Response of a Curved Bridge Under Moving Truck Load. *Engineering Structures,* 24(10): 1283–1293.

Sevgili, G. and Caner, A. 2009. Improved seismic response of multi-span skewed bridges retrofitted with link slabs. *Journal of Bridge Engineering*, 14(6): 452-459.

Sheikh, S.A., and Uzumeri, S.M. 1982. Analytical model for concrete confined in tied columns. *Journal of the Structural Division*, ASCE, 108(12): 2703-2722.

Shibata, A. and Sozen, M. A. 1976. Substitute structure method for seismic design in R/C. *Journal of the Structural Division*, ASCE, 102(1): 1-18.

Shome, N., Cornell, C. A., Bazzurro, P., and Carballo, J. E. 1998. Earthquakes, records, and nonlinear responses. *Earthquake Spectra*, 14(3), 469 – 500.

State-of-the-Art Report on High-Strength Concrete. 1997. ACI Committee 363.

Stone, W.C. and Cheok, G.S. 1989. Inelastic behavior of full scale bridge columns subjected to cyclic loading. *NIST Building Science Report No. 166*, U.S Department of Commerce, National Institute of Standards and Technology, Gaithersburg, MD, 252.

Suarez, V. and Kowalsky, M. 2006. Implementation of displacement based design for highway bridges. Fifth National Seismic Conference on Bridges & Highways, San Francisco, Canada.

Takemura, H. and Kawashima, K. X. 1997. Effect of loading hysteresis on ductility capacity of reinforced concrete bridge piers. *Journal of Structural Engineering*, Japan, 43A: 849-858.

Vamvatsikos, D. and Cornell, C. A. 2002. Incremental dynamic analysis, *Earthquake Engineering & Structural Dynamics,* 31(3): 491–514.

Vecchio, F., J., and Collins, M. P. 1986. The modified compression-filed theory for reinforced concrete elements subjected to shear. *American Concrete Institute*, 83(2): 219-231.

Veletsos, A, Newmark, N. M., 1960. Effect of inelastic behavior on the response of simple systems to earthquake motions. *Proceedings of 2nd World Conference on Earthquake Engineering*, 2: 895–912.

Wang, D. S., Ai, Q. H., Li, H. N., Si, B. J., and Sun, Z. G. 2008. Displacement Based Seismic Design of Rc Bridge Piers: Method and Experimental Evaluation. *The 14th World Conference on Earthquake Engineering*, Beijing, China, 2008.

Zanetell, D. 2010. The Colorado River Bridge at Hoover Dam - overview. *HPC Bridge Views*, the Federal Highway Administration and the National Concrete Bridge Council, Issue 63.

Zhang, J. and Huo, Y. 2009. Evaluating effectiveness and optimum design of isolation devices for highway bridges using the fragility function method, *Engineering Structures,* 31(8): 1648-1660.

Zhu, L., Elwood, K. J. and Haukaas, T. 2007. Classification and seismic safety evaluation of existing reinforced concrete columns, *Journal of Structural Engineering*, ASCE, 133(9): 1316-1330.

APPENDIX

Table A-1. Limit states of columns for factorial analyses.

Column HeightH (m)	Longitudinal reinforcement A_s (%)	Compressive Strenght, f'_c (MPa)	Yield strenght, f_y (MPa)	Tie spacing, s (mm)	Cracking base shear (kN)	Cracking displacement (m)	Yield base shear (kN)	Yield displacement (m)	Crushing base shear (kN)	Shear Capacity (kN)	Displacement at crushing or shear failure (m)	DUCTILITY (m/m)
7	2	25	300	75	3366	0.004	8832	0.018	9683	21599	0.084	4.67
7	2	25	300	150	3381	0.004	8832	0.018	9067	12023	0.058	3.22
7	2	25	300	300	3402	0.004	8851	0.018	7909	7235	0.012	0.68
7	2	25	400	75	3364	0.004	10085	0.021	11449	26932	0.092	4.38
7	2	25	400	150	3373	0.004	10065	0.021	10913	14400	0.070	3.33
7	2	25	400	300	3393	0.004	10081	0.021	10062	8134	0.015	0.70
7	2	25	500	75	3366	0.004	10944	0.023	13181	33198	0.098	4.26
7	2	25	500	150	3368	0.004	10892	0.023	12538	17533	0.074	3.22
7	2	25	500	300	3386	0.004	10903	0.023	11795	9701	0.019	0.83
7	2	40	300	75	3951	0.004	9369	0.017	10158	20611	0.097	5.71
7	2	40	300	150	3968	0.004	9394	0.017	9529	11877	0.067	3.94
7	2	40	300	300	3980	0.004	9416	0.017	8720	7510	0.011	0.64
7	2	40	400	75	3944	0.004	10507	0.019	11980	26433	0.110	5.79
7	2	40	400	150	3961	0.004	10538	0.019	11335	14788	0.081	4.26
7	2	40	400	300	3976	0.004	10572	0.019	10466	8966	0.014	0.75
7	2	40	500	75	3939	0.004	11478	0.021	13752	32601	0.120	5.71
7	2	40	500	150	3956	0.004	11514	0.021	13117	17778	0.087	4.14
7	2	40	500	300	3972	0.004	11563	0.021	11984	10366	0.018	0.85
7	2	60	300	75	4967	0.004	9541	0.015	11947	20260	0.360	24.00
7	2	60	300	150	1807	0.004	9551	0.015	10921	12417	0.110	7.33
7	2	60	300	300	4987	0.004	9562	0.015	9803	8495	0.011	0.74
7	2	60	400	75	4952	0.004	10674	0.017	13011	26602	0.341	20.06

7	2	60	400	150	4982	0.004	10754	0.017	12537	15371	0.133	7.82
7	2	60	400	300	4987	0.004	10760	0.017	11583	9755	0.014	0.82
7	2	60	500	75	4985	0.004	11618	0.019	13073	32218	0.488	25.68
7	2	60	500	150	1802	0.004	11766	0.019	14944	17513	0.291	15.32
7	2	60	500	300	4987	0.004	11800	0.019	13451	10493	0.016	0.83
7	3	25	300	75	3787	0.004	11130	0.019	12281	19667	0.079	4.16
7	3	25	300	150	3802	0.004	11128	0.019	11681	10609	0.017	0.88
7	3	25	300	300	3821	0.004	11143	0.019	10432	6080	0.075	3.95
7	3	25	400	75	3785	0.004	12937	0.022	14850	21781	0.085	3.86
7	3	25	400	150	3794	0.004	12913	0.022	14193	11862	0.019	0.87
7	3	25	400	300	3813	0.004	12930	0.022	12983	6903	0.009	0.41
7	3	25	500	75	3786	0.004	14493	0.025	17387	26740	0.092	3.68
7	3	25	500	150	3789	0.004	14428	0.025	16666	14342	0.025	0.99
7	3	25	500	300	3807	0.004	14042	0.024	15546	8142	0.011	0.48
7	3	40	300	75	4358	0.004	11716	0.018	12878	19902	0.091	5.06
7	3	40	300	150	4374	0.004	11745	0.018	12057	11168	0.016	0.88
7	3	40	300	300	4385	0.004	11546	0.017	10856	6801	0.008	0.44
7	3	40	400	75	4351	0.004	13338	0.020	15523	25724	0.101	5.05
7	3	40	400	150	4368	0.004	13375	0.020	14731	14079	0.023	1.15
7	3	40	400	300	4381	0.004	13413	0.020	13417	8257	0.010	0.50
7	3	40	500	75	4346	0.004	14603	0.022	18100	32156	0.108	4.91
7	3	40	500	150	4362	0.004	14648	0.022	17765	17059	0.033	1.48
7	3	40	500	300	4378	0.004	14712	0.022	15976	9510	0.012	0.55
7	3	60	300	75	5407	0.004	11840	0.016	14289	19728	0.274	17.13
7	3	60	300	150	4327	0.003	11872	0.016	13633	11601	0.015	0.94
7	3	60	300	300	4327	0.003	11874	0.016	12126	7537	0.007	0.45
7	3	60	400	75	5385	0.004	13770	0.019	16748	25705	0.412	21.68
7	3	60	400	150	4324	0.003	13862	0.019	19038	14474	0.022	1.14

7	3	60	400	300	4327	0.003	13870	0.019	14660	8858	0.009	0.49
7	3	60	500	75	4622	0.003	18501	0.022	23913	32093	0.148	6.73
7	3	60	500	150	4321	0.003	15358	0.021	19952	17281	0.029	1.39
7	3	60	500	300	5426	0.004	15413	0.021	17457	10262	0.012	0.56
7	4	25	300	75	4207	0.004	13491	0.020	14836	20620	0.075	3.75
7	4	25	300	150	4221	0.004	13482	0.020	14133	11394	0.015	0.74
7	4	25	300	300	4240	0.004	13489	0.020	12645	6781	0.007	0.37
7	4	25	400	75	4205	0.004	15910	0.023	18194	26771	0.082	3.57
7	4	25	400	150	4214	0.004	15881	0.023	17433	14469	0.020	0.87
7	4	25	400	300	4232	0.004	15897	0.023	15924	8318	0.010	0.42
7	4	25	500	75	4206	0.004	17912	0.026	21504	32922	0.087	3.35
7	4	25	500	150	4209	0.004	17836	0.026	20670	17545	0.025	0.98
7	4	25	500	300	4226	0.004	17840	0.026	19243	9856	0.012	0.47
7	4	40	300	75	3791	0.003	13877	0.018	15528	22247	0.085	4.72
7	4	40	300	150	3803	0.003	13910	0.018	14525	12672	0.015	0.83
7	4	40	300	300	3812	0.003	13940	0.018	13244	7884	0.008	0.44
7	4	40	400	75	3786	0.003	16265	0.021	18971	27427	0.093	4.43
7	4	40	400	150	3799	0.003	16306	0.021	17980	14895	0.015	0.73
7	4	40	400	300	3809	0.003	16352	0.021	16302	8629	0.009	0.42
7	4	40	500	75	3782	0.003	17855	0.023	22341	33693	0.099	4.30
7	4	40	500	150	3794	0.003	17904	0.023	21387	18028	0.023	1.01
7	4	40	500	300	3806	0.003	17977	0.023	19571	9447	0.010	0.44
7	4	60	300	75	5818	0.004	14229	0.017	17629	21966	0.310	18.24
7	4	60	300	150	4666	0.003	14266	0.017	16956	12583	0.013	0.77
7	4	60	300	300	5836	0.004	14268	0.017	14592	8217	0.007	0.41
7	4	60	400	75	4639	0.003	16733	0.020	21573	27139	0.158	7.90
7	4	60	400	150	4664	0.003	16839	0.020	19739	15477	0.017	0.86
7	4	60	400	300	4667	0.003	16860	0.020	18829	9548	0.009	0.44

7	4	60	500	75	5803	0.004	18501	0.022	23774	33265	0.144	6.55
7	4	60	500	150	4661	0.003	18731	0.022	23112	18442	0.022	0.98
7	4	60	500	300	5836	0.004	18797	0.022	21534	11030	0.011	0.50
14	2	25	300	75	1572	0.015	4157	0.065	4456	23510	0.084	1.29
14	2	25	300	150	1580	0.015	4211	0.067	4333	13288	0.125	1.87
14	2	25	300	300	1590	0.015	4223	0.067	5194	8410	0.098	1.46
14	2	25	400	75	1572	0.015	4787	0.080	5322	27406	0.230	2.88
14	2	25	400	150	1576	0.015	4778	0.080	5230	15329	0.158	1.98
14	2	25	400	300	1586	0.015	4788	0.080	4466	9290	0.118	1.48
14	2	25	500	75	1572	0.015	5177	0.089	6119	30751	0.261	2.93
14	2	25	500	150	1574	0.015	5190	0.090	5911	16711	0.181	2.01
14	2	25	500	300	1582	0.015	5160	0.089	5547	9692	0.142	1.60
14	2	40	300	75	1673	0.013	4420	0.061	4794	22489	0.183	3.00
14	2	40	300	150	1681	0.013	4435	0.061	4585	13430	0.129	2.11
14	2	40	300	300	1687	0.013	4447	0.061	4772	8901	0.134	2.20
14	2	40	400	75	1670	0.013	4979	0.072	5575	28386	0.251	3.49
14	2	40	400	150	1678	0.013	4996	0.072	5404	15812	0.162	2.25
14	2	40	400	300	1685	0.013	5014	0.072	5721	9773	0.248	3.44
14	2	40	500	75	1668	0.013	5403	0.081	6362	29879	0.299	3.69
14	2	40	500	150	1676	0.013	5378	0.080	6204	16807	0.187	2.34
14	2	40	500	300	1683	0.013	5402	0.080	6069	10270	0.144	1.80
14	2	60	300	75	2127	0.013	4569	0.054	2943	23471	2.339	43.31
14	2	60	300	150	2135	0.013	4585	0.054	4430	14413	1.162	21.52
14	2	60	300	300	2135	0.013	4586	0.054	5026	9884	0.104	1.93
14	2	60	400	75	2118	0.013	5107	0.065	3213	24879	2.361	36.32
14	2	60	400	150	2134	0.013	5023	0.065	5061	16767	1.336	20.55
14	2	60	400	300	2135	0.013	5136	0.065	5748	9737	0.168	2.58
14	2	60	500	75	2107	0.013	5553	0.075	5071	29927	1.911	25.48

14	2	60	500	150	2131	0.013	5568	0.074	2829	17308	2.576	34.81
14	2	60	500	300	2135	0.013	5584	0.074	6278	10999	0.654	8.84
14	3	25	300	75	1672	0.014	5320	0.071	5774	18497	0.195	2.75
14	3	25	300	150	1679	0.014	5322	0.071	5563	10369	0.134	1.89
14	3	25	300	300	1688	0.014	5333	0.071	4875	6306	0.097	1.37
14	3	25	400	75	1671	0.014	6185	0.085	6977	24556	0.230	2.71
14	3	25	400	150	1676	0.014	6175	0.085	6755	13324	0.161	1.89
14	3	25	400	300	1685	0.014	6185	0.085	6172	7708	0.120	1.41
14	3	25	500	75	1672	0.014	6831	0.096	8171	30172	0.261	2.72
14	3	25	500	150	1673	0.014	6802	0.096	7921	16132	0.188	1.96
14	3	25	500	300	1682	0.014	6807	0.096	7498	9112	0.144	1.50
14	3	40	300	75	1724	0.012	5561	0.066	6083	17857	0.197	2.98
14	3	40	300	150	1731	0.012	5542	0.065	5745	10548	0.129	1.98
14	3	40	300	300	1714	0.012	5556	0.065	6300	6893	0.262	4.03
14	3	40	400	75	1721	0.012	6400	0.078	7293	22730	0.247	3.17
14	3	40	400	150	1728	0.012	6374	0.077	7041	12984	0.159	2.06
14	3	40	400	300	1717	0.012	6394	0.077	3444	8111	0.125	1.62
14	3	40	500	75	1719	0.012	7048	0.088	8497	29927	0.284	3.23
14	3	40	500	150	1726	0.012	7012	0.087	8229	16382	0.191	2.20
14	3	40	500	300	1733	0.012	7041	0.087	6446	9609	0.145	1.67
14	3	60	300	75	2134	0.012	5653	0.059	4960	18255	2.269	38.46
14	3	60	300	150	2141	0.012	5673	0.059	6092	11197	2.091	35.44
14	3	60	300	300	2141	0.012	5671	0.059	6622	7668	0.301	5.10
14	3	60	400	75	2126	0.012	6570	0.072	5874	22961	2.468	34.28
14	3	60	400	150	2140	0.012	6576	0.072	7189	13550	1.703	23.65
14	3	60	400	300	2141	0.012	6585	0.072	7465	8845	0.163	2.26
14	3	60	500	75	2288	0.012	8784	0.086	9088	28331	2.642	30.72
14	3	60	500	150	2138	0.012	7203	0.081	5805	16148	2.690	33.21

14	3	60	500	300	2141	0.012	7225	0.081	8652	10057	1.268	15.65
14	4	25	300	75	1860	0.014	6414	0.073	7015	22634	0.199	2.73
14	4	25	300	150	1867	0.014	6416	0.073	6775	12877	0.134	1.84
14	4	25	300	300	1876	0.014	6428	0.073	6155	7649	0.097	1.33
14	4	25	400	75	1859	0.014	7585	0.088	8614	27145	0.227	2.58
14	4	25	400	150	1863	0.014	8334	0.164	8696	14194	1.965	11.98
14	4	25	400	300	1872	0.014	7584	0.088	7721	9028	0.121	1.38
14	4	25	500	75	1860	0.014	8411	0.099	10197	33198	0.249	2.52
14	4	25	500	150	1861	0.014	8442	0.100	9874	17533	0.174	1.74
14	4	25	500	300	1869	0.014	8446	0.100	9368	9701	0.145	1.45
14	4	40	300	75	1881	0.012	6651	0.068	7365	22347	0.198	2.91
14	4	40	300	150	1887	0.012	6668	0.068	7020	13289	0.130	1.91
14	4	40	300	300	1892	0.012	6684	0.068	7791	8760	0.193	2.84
14	4	40	400	75	1878	0.012	7775	0.081	8983	28268	0.238	2.94
14	4	40	400	150	1885	0.012	7798	0.081	9140	16190	1.422	17.56
14	4	40	400	300	1890	0.012	7823	0.081	8536	10151	0.123	1.52
14	4	40	500	75	1876	0.012	8663	0.092	10587	31459	0.269	2.92
14	4	40	500	150	1883	0.012	8615	0.091	10234	17419	0.188	2.07
14	4	40	500	300	1889	0.012	8648	0.091	8427	10399	0.145	1.59
14	4	60	300	75	2304	0.012	6795	0.063	6235	23298	2.696	42.79
14	4	60	300	150	2311	0.012	6816	0.063	7339	14239	3.368	53.46
14	4	60	300	300	2311	0.012	6811	0.063	7485	9710	0.139	2.21
14	4	60	400	75	2297	0.012	7947	0.076	8097	28729	2.539	33.41
14	4	60	400	150	2310	0.012	7943	0.075	8668	16651	2.229	29.72
14	4	60	400	300	2311	0.012	7951	0.075	8760	10612	0.154	2.05
14	4	60	500	75	2288	0.012	8784	0.086	9170	30718	2.597	30.20
14	4	60	500	150	2308	0.012	8813	0.085	10634	17646	2.252	26.49
14	4	60	500	300	2311	0.012	8842	0.085	11260	11110	0.207	2.44

21	2	25	300	75	1025	0.034	2725	0.155	2610	23948	0.500	3.23
21	2	25	300	150	1030	0.034	2721	0.154	2608	13815	0.349	2.27
21	2	25	300	300	1011	0.033	2723	0.153	2500	8748	0.259	1.69
21	2	25	400	75	1024	0.034	3074	0.181	3063	27500	0.603	3.33
21	2	25	400	150	1027	0.034	3068	0.181	3080	15422	0.442	2.44
21	2	25	400	300	1008	0.033	3067	0.180	3018	9383	0.312	1.73
21	2	25	500	75	1025	0.034	3355	0.204	3541	33538	0.675	3.31
21	2	25	500	150	1025	0.034	3307	0.201	3553	18441	0.488	2.43
21	2	25	500	300	1006	0.033	3311	0.201	3505	10893	0.367	1.83
21	2	40	300	75	1054	0.028	2884	0.139	2733	24923	0.557	4.01
21	2	40	300	150	1059	0.028	2887	0.138	2748	14790	0.380	2.75
21	2	40	300	300	1063	0.028	2889	0.137	2082	9723	0.276	2.01
21	2	40	400	75	1052	0.028	3229	0.161	3207	28527	0.638	3.96
21	2	40	400	150	1057	0.028	3232	0.160	3221	16450	0.454	2.84
21	2	40	400	300	1061	0.028	3246	0.160	1	10411	1.884	11.78
21	2	40	500	75	1050	0.028	3487	0.179	3669	34023	0.727	4.06
21	2	40	500	150	1055	0.028	3501	0.179	3699	16447	0.536	2.99
21	2	40	500	300	1060	0.028	3507	0.178	3840	10138	0.364	2.04
21	2	60	300	75	1331	0.028	2985	0.123		23471		
21	2	60	300	150	1336	0.003	2990	0.123		14413		
21	2	60	300	300	1336	0.028	2990	0.123	1056	9884	1.837	14.93
21	2	60	400	75	1325	0.028	3335	0.146	1	29510	3.675	25.17
21	2	60	400	150	1335	0.028	4064	0.144		14784	3.829	26.59
21	2	60	400	300	1336	0.028	3341	0.144	3305	11394	0.780	5.42
21	2	60	500	75	1318	0.028	3617	0.166		29927		
21	2	60	500	150	1381	0.029	3767	0.174		17308		
21	2	60	500	300	1336	0.028	3625	0.162		10999		
21	3	25	300	75	1102	0.032	3453	0.162	3444	17179	0.509	3.14

21	3	25	300	150	1107	0.032	3454	0.162	3438	9869	0.355	2.19
21	3	25	300	300	1113	0.032	3455	0.161	3278	6215	0.257	1.60
21	3	25	400	75	1101	0.032	4003	0.192	4203	22052	0.575	2.99
21	3	25	400	150	1104	0.032	3995	0.192	4167	12306	0.431	2.24
21	3	25	400	300	1110	0.032	4003	0.192	4030	7433	0.311	1.62
21	3	25	500	75	1102	0.032	4400	0.215	4955	29333	0.638	2.97
21	3	25	500	150	1103	0.032	4378	0.215	4895	15788	0.497	2.31
21	3	25	500	300	1108	0.032	4368	0.214	4761	9015	0.365	1.71
21	3	40	300	75	1128	0.027	3615	0.147	3630	17496	0.529	3.60
21	3	40	300	150	1132	0.027	3627	0.147	3572	10438	0.371	2.52
21	3	40	300	300	1135	0.027	3628	0.146	3657	6909	0.311	2.13
21	3	40	400	75	1126	0.027	4156	0.173	4360	22201	0.637	3.68
21	3	40	400	150	1130	0.027	4172	0.173	4353	12790	0.443	2.56
21	3	40	400	300	1134	0.027	4175	0.172	2117	8085	0.316	1.84
21	3	40	500	75	1124	0.027	4561	0.194	5101	27603	0.721	3.72
21	3	40	500	150	1129	0.027	4560	0.193	5090	15421	0.514	2.66
21	3	40	500	300	1133	0.027	4567	0.192	4680	9329	0.369	1.92
21	3	60	300	75	1397	0.027	3711	0.133		18255		
21	3	60	300	150	1401	0.027	3727	0.133		11197		
21	3	60	300	300	1402	0.027	3726	0.133	1343	7668	2.527	19.00
21	3	60	400	75	1443	0.028	4225	0.156	346	22961	5.388	34.54
21	3	60	400	150	1401	0.027	4291	0.158	1529	13550	3.944	24.96
21	3	60	400	300	1402	0.027	4298	0.158	1633	8845	3.431	21.72
21	3	60	500	75	1499	0.027	5753	0.190	5220	27666	2.203	11.59
21	3	60	500	150	1399	0.027	4604	0.177	1504	15903	4.040	22.82
21	3	60	500	300	1402	0.027	4717	0.177		10021		
21	4	25	300	75	1196	0.031	4231	0.172	4292	23045	0.495	2.88
21	4	25	300	150	1201	0.031	4181	0.166	4247	13568	0.348	2.10

21	4	25	300	300	1207	0.031	4180	0.165	4021	8596	0.257	1.56
21	4	25	400	75	1196	0.031	4954	0.200	5308	27406	0.566	2.83
21	4	25	400	150	1198	0.031	4945	0.200	5234	15329	0.425	2.13
21	4	25	400	300	1204	0.031	4939	0.199	5017	9290	0.308	1.55
21	4	25	500	75	1196	0.031	5484	0.224	6328	30751	0.621	2.77
21	4	25	500	150	1197	0.031	5459	0.224	6220	16711	0.485	2.17
21	4	25	500	300	1202	0.031	5462	0.224	6002	9692	0.364	1.63
21	4	40	300	75	1233	0.027	4369	0.154	4494	24923	0.531	3.45
21	4	40	300	150	1237	0.027	4370	0.153	4402	14790	0.366	2.39
21	4	40	300	300	1240	0.027	4370	0.152	1943	9723	0.265	1.74
21	4	40	400	75	1231	0.027	5098	0.182	5518	28386	0.611	3.36
21	4	40	400	150	1235	0.027	5099	0.181	5434	16308	0.436	2.41
21	4	40	400	300	1239	0.027	5102	0.180	5020	10269	0.312	1.73
21	4	40	500	75	1229	0.027	5631	0.204	6544	29879	0.675	3.31
21	4	40	500	150	1234	0.027	5648	0.204	6439	16807	0.510	2.50
21	4	40	500	300	1238	0.027	5654	0.203	6133	10270	0.365	1.80
21	4	60	300	75	1510	0.027	4472	0.142	2733	23471	2.635	18.56
21	4	60	300	150	1515	0.027	4477	0.141	2397	14413	4.011	28.45
21	4	60	300	300	1515	0.027	4477	0.141	4628	9884	0.362	2.57
21	4	60	400	75	1505	0.027	5201	0.168	3558	29510	4.860	28.93
21	4	60	400	150	1514	0.027	5230	0.167	5688	17433	1.515	9.07
21	4	60	400	300	1515	0.027	5239	0.167	5766	11394	0.433	2.59
21	4	60	500	75	1499	0.027	5753	0.190	4335	29927	2.884	15.18
21	4	60	500	150	1513	0.027	5769	0.187	6312	17308	1.240	6.63
21	4	60	500	300	1515	0.027	5793	0.187	5941	10999	1.593	8.52